CONTRACT NAS8-21101

MCR-68-87 4
Copy No.

USE OF DYNAMIC SCALE MODELS TO DETERMINE LAUNCH VEHICLE CHARACTERISTICS

FINAL REPORT

VOLUME I
ANALYTICAL INVESTIGATION

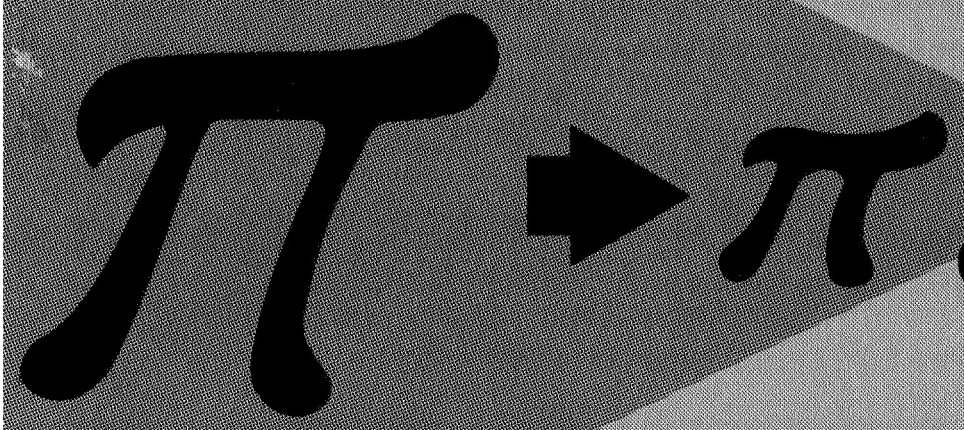

AUGUST 1969

prepared for NATIONAL AERONAUTICS AND SPACE ADMINISTRATION
GEORGE C. MARSHALL SPACE FLIGHT CENTER
HUNTSVILLE, ALABAMA 35812

MARTIN MARIETTA CORPORATION

MCR-68-87

CONTRACT NAS8-21101

USE OF DYNAMIC SCALE MODELS TO DETERMINE LAUNCH VEHICLE CHARACTERISTICS

FINAL REPORT

VOLUME I. ANALYTICAL INVESTIGATION

August 1969

Authors

I. J. Jaszlics

A. C. Park

Approved

George Morosow
Program Manager

MARTIN MARIETTA CORPORATION
DENVER DIVISION

FOREWORD

This volume presents the results of an analytical study performed from May 18, 1967 through May 17, 1968 on the use of dynamic scale models to determine launch vehicle characteristics. The investigation was conducted by the Denver Division of the Martin Marietta Corporation, Denver, Colorado, for the National Aeronautics and Space Administration, George C. Marshall Space flight Center, Huntsville, Alabama, under Contract No. NAS8-21101. Mr. L. Kiefling was the principal representative for the contracting office.

Mr. George Morosow was the Program Manager for the Denver Division and all work was performed under the direction of Mr. Morosow and Mr. Ivan J. Jaszlics, Principal Investigator. Significant contributions were provided by C. C. Feng, R. C. Reuter, Jr. and J. N. Singh. The report was critically reviewed by Professor L. G. Tulin of the University of Colorado.

Results of an experimental study to confirm some of the analytical results presented herein are provided in Volume II.

ABSTRACT

The purpose of this study was to develop modeling techniques that can be used for launch vehicle and space structure dynamic simulation when the parameters which define similarity between prototype and model cannot, due to physical or manufacturing limitations, be fully satisfied. In practice, all but the largest models have to make compromises in structural simulation and even very large models, using direct replica scaling, cannot duplicate all essential parameters.

During the study it became obvious that there is need for a comprehensive summary of the scaling techniques applicable to the design of launch vehicle and space structure models. This report, provides that summary; describes general model scaling methods; developes basic similarity laws for various structures including liquid propellants and shell structures. A survey of material and manufacturing limitations and a summary of the economic aspects of model construction and testing is included.

CONTENTS

ILLUSTRATIONS

TABLES

SUMMARY

Results of an analytical study on the use of dynamic scale models to determine launch vehicle characteristics are presented. The report is written in a way that permits its use as a general guide for launch vehicle model scaling and design.

The dimensional analysis methods required to establish dynamic model scaling parameters are developed in matrix form and used to summarize the scaling laws applicable to launch vehicle structures. Scaling laws are presented for beam-like and shell-like structures. Visco-elastic effects and coupled structural-liquid slosh effects are considered. The scaling laws applicable to the simulation of liquid propellant dynamic phenomena are presented. Some special distorted modeling techniques for shells are developed and the necessity of an experimental program to confirm these techniques is emphasized.

A limited discussion of the scaling requirements for space structures is presented and the relations for thermal scaling and scaling of gravity-gradient induced forces are summarized. A test configuration to simulate the gravity-gradient is discussed. A detailed theoretical and experimental program to investigate these and other modeling techniques applicable to large space structures is recommended.

A summary of the economic aspects of dynamic model design and construction and a review of past and present launch vehicle dynamic models are included.

1. INTRODUCTION

The first decade of space exploration was characterized by the continual increase in launch vehicle and payload dimensions and, with this increase, structural frequencies were reduced. Fundamental bending frequencies of first generation vehicles were on the order of 10 Hz; Titan and Saturn class vehicles have fundamental bending frequencies, during the boost phase, of 1 to 2 Hz. The degree of dynamic interaction between structural vibrations, propellant slosh and vehicle control systems increased considerably.

All present generation launch vehicle structures are designed, at least in part, by the dynamic loading conditions that arise during the pre-launch or during the boost phase. These conditions include loads due to ground winds, lift-off loads, dynamic loads generated by wind shear or atmospheric turbulence, transonic buffet loads, staging loads, upper stage engine ignition loads and engine shutdown transient loads.

The complete evaluation of these loads is only possible through combined analytical and test efforts. While analysis can predict the fundamental frequency of most conventional launch vehicle structures with approximately 3% to 8% accuracy, the risk involved in using only analytical methods, especially if the structure is complex, is so great that experimental verification is required. The analytical methods available for prediction of transonic buffet loads and ground wind-induced loads are of questionable accuracy at the present time: the use of test results in conjunction with analytical studies is of the greatest importance in predicting these aeroelastic loads.

Analytically determined vibration modes of launch vehicle structures have been verified with full-scale vibration surveys performed in a manner similar to that developed for aircraft. With the increase in overall dimensions, this approach has become more and more expensive. Current major United States launch vehicles range from approximately 120 feet to 320 feet and the suspension of these vehicles to simulate the free-free end conditions of flight is, in itself, a major task. The simulation of configuration changes and various propellant conditions present additional severe restrictions. The replacement of the full-scale vibration survey with an equivalent dynamic scale model test, can offer multi-million dollar savings in materials, manufacturing time and total test program time.

One of the first major launch vehicle programs in the United States where the full-scale vibration survey was replaced by a

model test was the Titan III program funded by the U. S. Air Force. Several Saturn class dynamic models have since been examined, and it is probable that most, if not all, of the large launch vehicles of the future will be vibration tested by the use of dynamic scale models. Recent research performed at the Langley Research Center of the National Aeronautics and Space Administration indicates the definite feasibility and accuracy of this approach.

Model testing is utilized exclusively for aeroelastic tests but model size is restricted by available wind tunnels.

The purpose of this study is to develop modeling techniques that can be used for launch vehicle and space structure dynamic simulation when the parameters which define similarity between prototype and model cannot, due to physical or manufacturing limitations, be fully satisfied. In practice, all but the largest models have to make compromises in structural simulation and even very large models, using direct replica scaling, cannot duplicate all essential parameters.

During the study it became obvious that there is need for a comprehensive summary of the scaling techniques applicable to the design of launch vehicle and space structure models. This report, provides that summary; describes general model scaling methods; developes basic similarity laws for various structures including liquid propellants and shell structures. A survey of material and manufacturing limitations and a summary of the economic aspects of model construction and testing is included.

2. REVIEW OF THE STATE OF THE ART

From the number of problems which have been solved using scale modeling techniques, the potential and application of this useful method are obvious. Static and dynamic models are being used to study structural response of space vehicles ranging from transportation occurring during ground handling to docking maneuvers in orbit to lunar and planetary landing.

A colloquim on the use of models and scaling in shock and vibration sponsored by the ASME in 1963 treated recent developments. These included wave simulation, aerospace vehicles, materials and elastic and plastic response to transient loading. A symposium on aeroelastic and dynamic modeling technology was sponsored in 1963 by the Air Force Flight Dynamics Laboratory of the Research and Technology Division, Air Force Systems Command in association with the Dynamics and Aeroelasticity panel of the Aerospace Industries Association. This meeting included papers on such topics as transonic buffeting, ground winds, dissimilar materials, thermal scaling, support systems and excitation techniques, fuel slosh, fatigue, photoelastic techniques, plus applications to space vehicles and aircraft.

All of the work on dynamic response of space vehicles is aimed at answering the same question: What are the dynamic stresses which we must design the vehicle to withstand? The current scale modeling technology for studying the various types of dynamic response is oriented toward those aspects for which analytical models are inadequate. The degree of reliance on the results of scale-model tests often depends on the willingness of the responsible engineer to rely on the results of analysis. This "willingness" is a function of schedule, available funds, past experience on the problem at hand, program penalties incurred if he believes analysis and program penalties incurred if analysis is wrong.

The philosophy of the scale-model test to be run also depends on this "willingness". By natural cause and effect, a large amount of money can be spent to solve a very serious problem (e.g., the wind-induced oscillations of the Saturn V vehicle or the POGO oscillations of the Titan II-Gemini). In this context "solve" means "make sure that the mission does not fail". The associated requirement on the scale-model test is that, it must

fill the gap between the lack of confidence in analysis and the "solution of the problem". Obviously, the range of requirements is extremely broad. All scale model tests have one thing in common, however, everyone of them is run to provide the "missing information" required to "solve the problem." Since the available knowledge of the problem area and the confidence in the results of analysis are usually closely correlated, the degree of similitude which is required in the scale-model test increases as the analytical model deteriorates.

Three general types of models have been used for predicting dynamic response of space vehicles. One type is the obvious geometrically scaled model made of the same material as the prototype. The second is again geometrically scaled but of a different material; and the third is a distorted model whereby one or more of the similitude requirements is not preserved. The first type of model has been used successfully for tests to determine static and dynamic stresses, displacements, and strains. However, the extremely light weight structure of aerospace vehicles sometimes makes geometric scaling impossible. For example, the tank wall thickness on one launch vehicle is only 0.005 inch full scale. On a 10% scale model geometric scaling would require a wall thickness of 0.0005 inch.

Scale models to predict dynamic response, therefore, often require departure from geometric scaling and the use of the different materials for model and prototype.

The structural response problem (static, dynamic, rigid body, vibrational, buckling, linear, nonlinear, elastic, plastic) can be formulated in terms of the geometry of the structure (dimensions), material properties of the structure (linear modulus, nonlinear modulus, damping, strain rate effects, density, Poisson's ratio), and forcing function applied to the structure (point loads, and/or pressure as functions of time). Four basic physical dimensions describe all of the above. Dimensional analysis formulates the problem of gaining full scale information from models in terms of the similitude requirements which when satisfied will result in reliable scaling laws.

It should be noted that the validity of a scale model test is measured by whether it provides the information required to solve the problem. The improvements in the state-of-the-art for scale-model tests can thus be accomplished in either of two ways:

(1) Development of more sophisticated methods of building scale models and improving the simulation of the environments; or

(2) Improvement of the methods of analysis and understanding of the physics of the problem, particularly in those areas which cause the most trouble in the design of scale-model tests.

Dynamic models of launch vehicles have had widespread application to two major areas: vibration surveys of the natural modes of oscillation and aeroelastic loads and stability testing.

The most common method of dynamic model design and construction is direct geometric scaling using similar materials for model and prototype (replica scaling). All prototype dimensions are scaled directly through the model-to-prototype characteristic length scale factor, $n = \ell_m/\ell_p$, and prototype materials are used in model construction.

In the design of launch vehicle dynamic models it is often necessary, due primarily to material or manufacturing limitations (Chapter 9), to employ limited distorted geometric scaling and/or dissimilar materials. Limited distorted geometric scaling deviates from replica scaling in that the characteristic length scale factor is not maintained throughout the entire structure. Small scale models may require extensive use of these techniques to provide the required stiffness distributions and to ensure that the several model components are strong enough to withstand handling and assembly loads. In addition, distorted geometric scaling is almost a necessity for the design of aeroelastic models where the scale factor is dictated by the wind tunnel imposed limitations on model size. The requirement of matching aerodynamic and structural scaling parameters at these small scale factors may dictate the use of dissimilar materials.

Total geometric distortion is dictated when very large structures are to be simulated. In these cases the model may not even resemble the prototype but the overall dynamic characteristics are retained.

2.1 Vibration Survey Models

Some of the most significant vibration survey models have been associated with research programs performed at the Langley Research Center (LRC) of the National Aeronautics and Space Administration. Two models of the Apollo/Saturn V vehicle were constructed; one at 1/40-scale (Fig. 2.1) and the other at 1/10-scale (Fig. 2.2). The 1/40-scale model did not use direct geometric scaling and, in some areas, dissimilar materials were used. The main load carrying

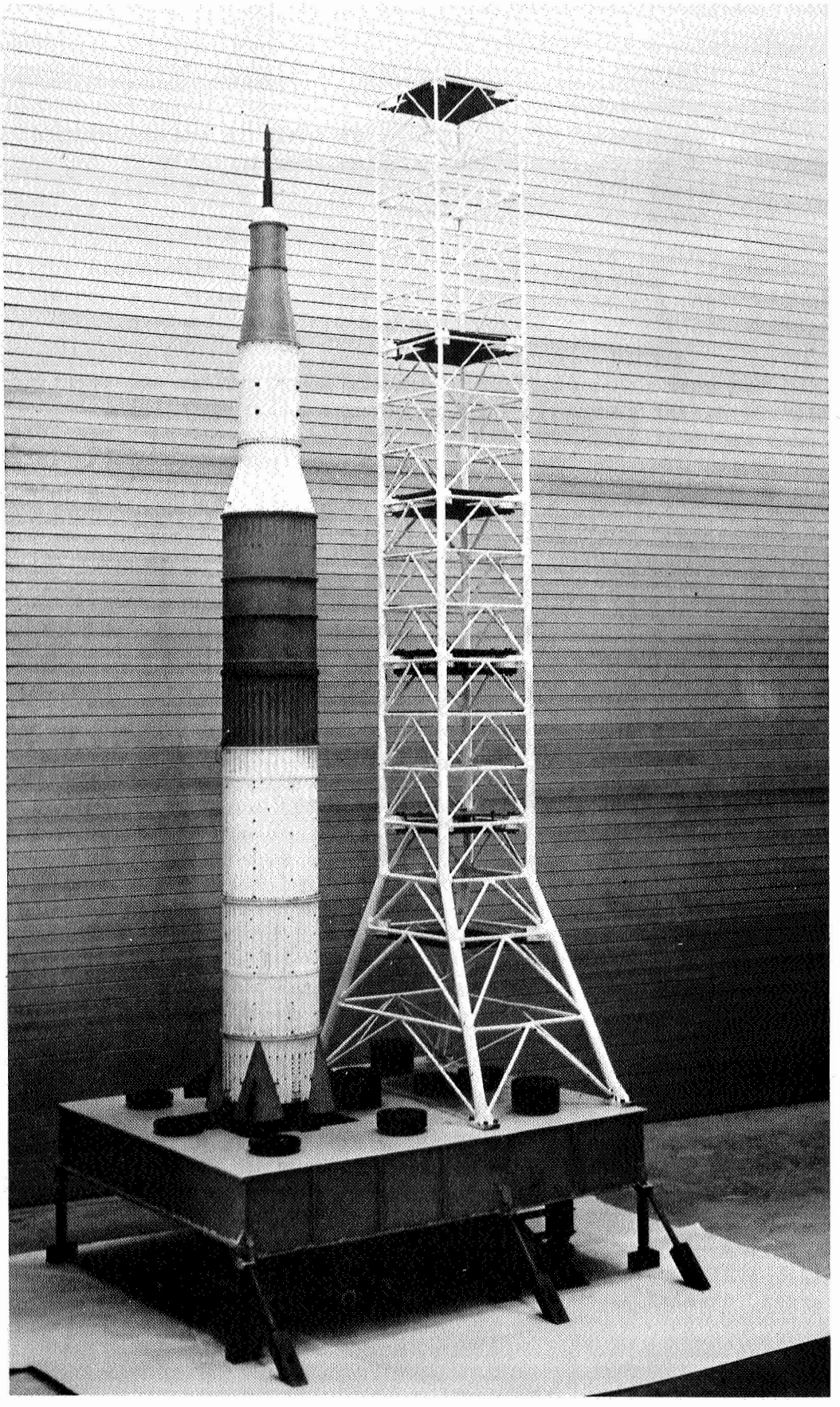

Figure 2.1 Saturn V 1/40-Scale Model

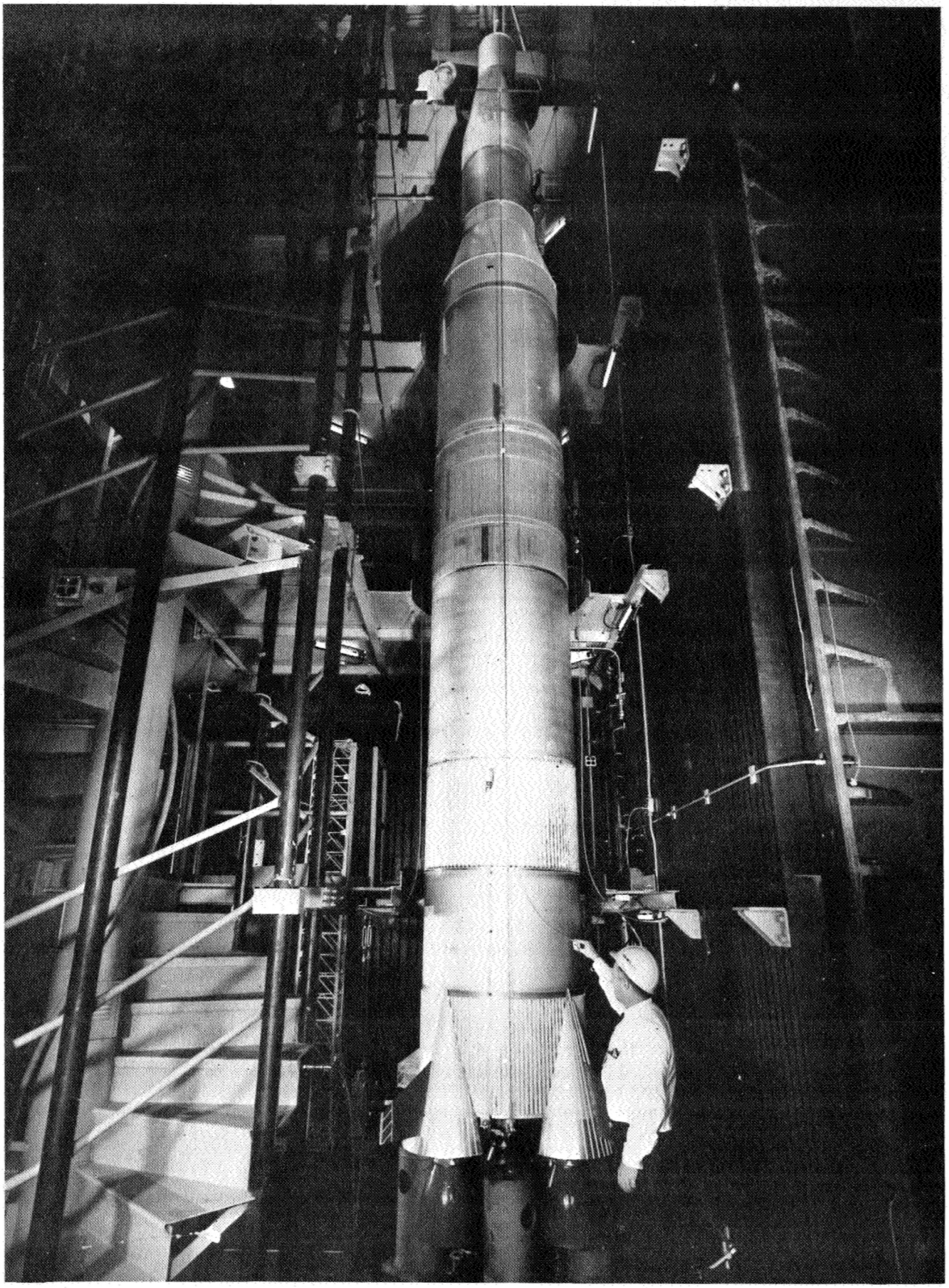

Figure 2.2 Saturn V 1/10-Scale Model

structure of the 1/10-scale model booster stages was represented by direct geometric scaling using similar materials but direct scaling was not employed for the payload and launch escape system. Good agreement (Ref 2.1) between experimental and analytical lateral bending frequencies (Fig. 2.3a) and vibration modes (Fig. 2.3b) was obtained. A summary discussion of this model program is presented in Reference 2.1.

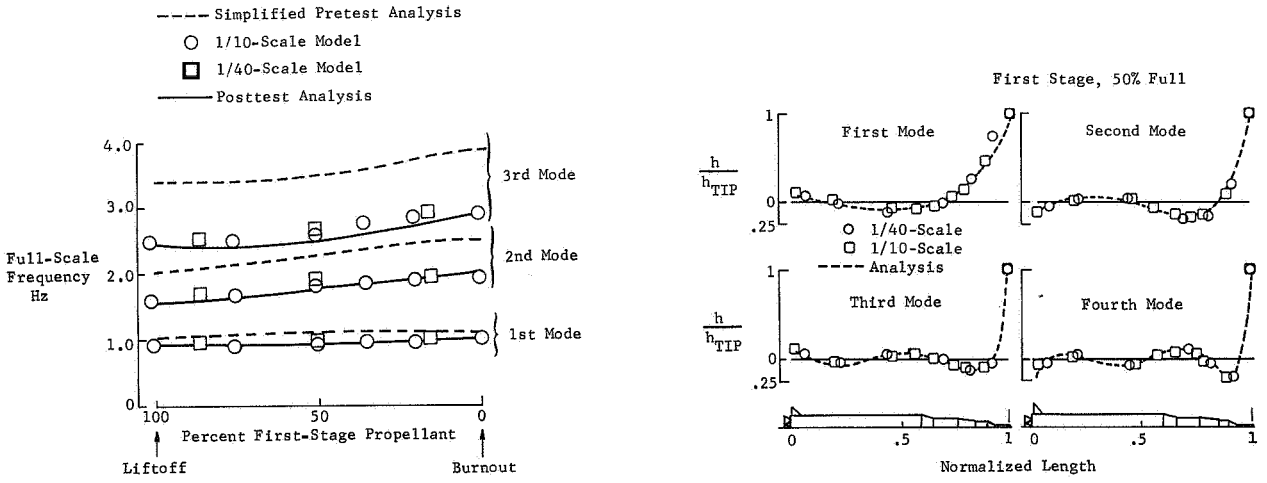

a) Lateral Bending Frequencies

b) Lateral Vibration Modes

Figure 2.3 Lateral Vibration Characteristics, Saturn V Dynamic Models

In addition to these models a 1/5-scale model of the Saturn I launch vehicle (Fig. 2.4) was constructed using direct replica scaling.

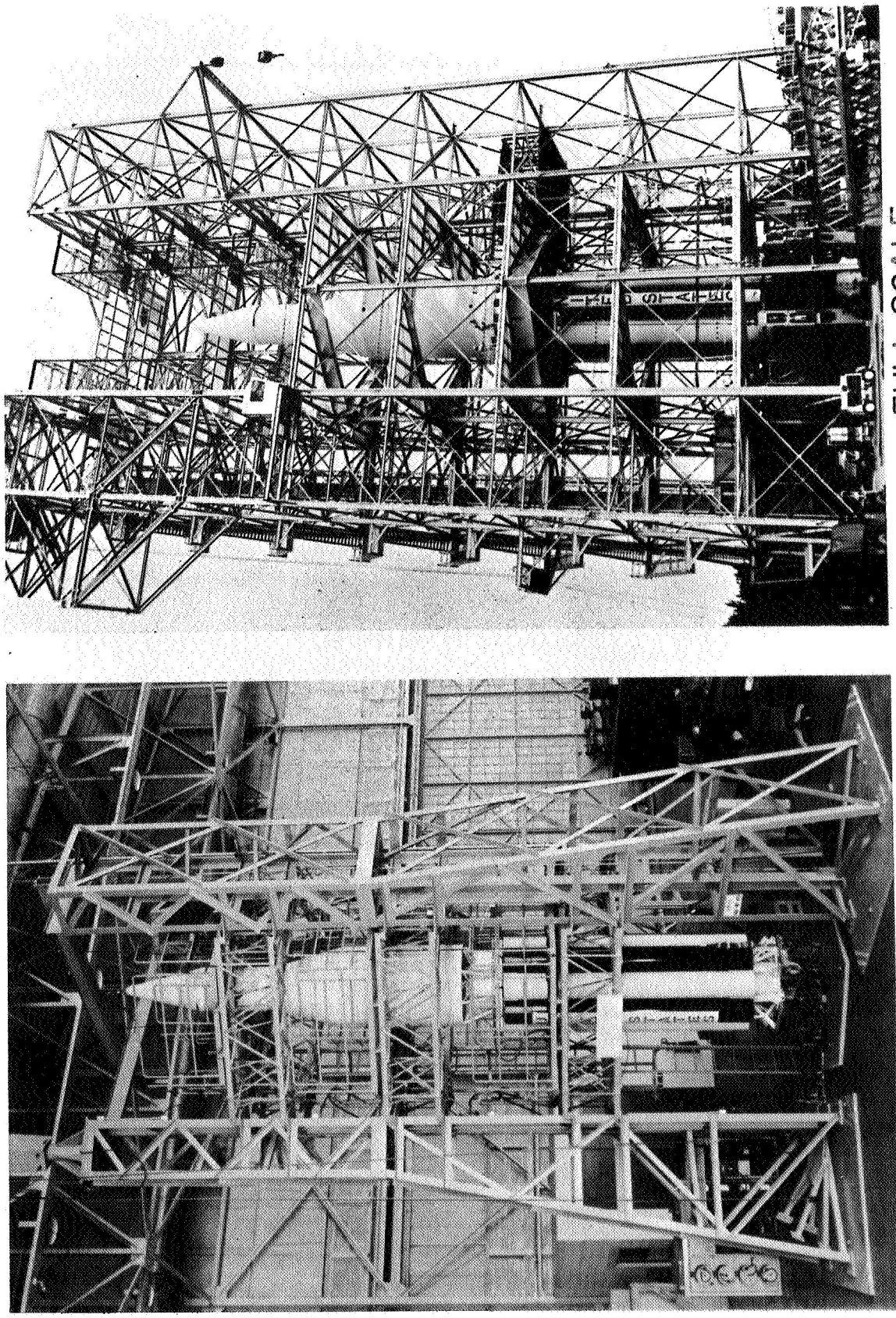

Figure 2.4 Saturn I Vibration Test Vehicles

Vibration test results for this model are compared with the results of a full-scale Saturn I vibration survey in Reference 2.2. First bending and cluster mode shapes and frequencies for the model and full-scale vehicle are presented in Figure 2.5.

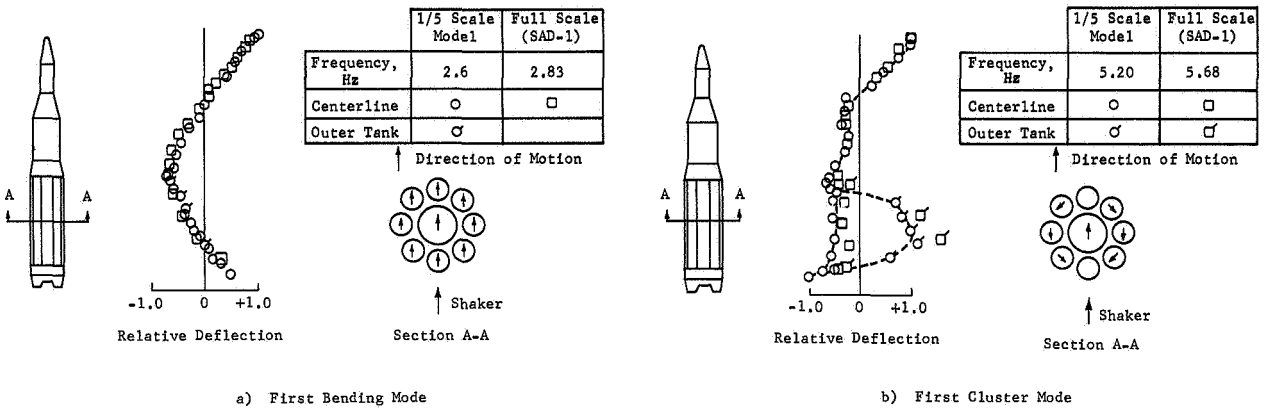

Figure 2.5 Fundamental Modes at Maximum Dynamic Pressure-Weight, Saturn I

Other launch vehicles that have undergone extensive analysis through the use of a dynamic scale model are the Titan IIIA and Titan IIIC. A complete ground vibration survey was performed at the Langley Research Center. The Titan IIIC model, in the test stand, is shown in Figure 2.6.

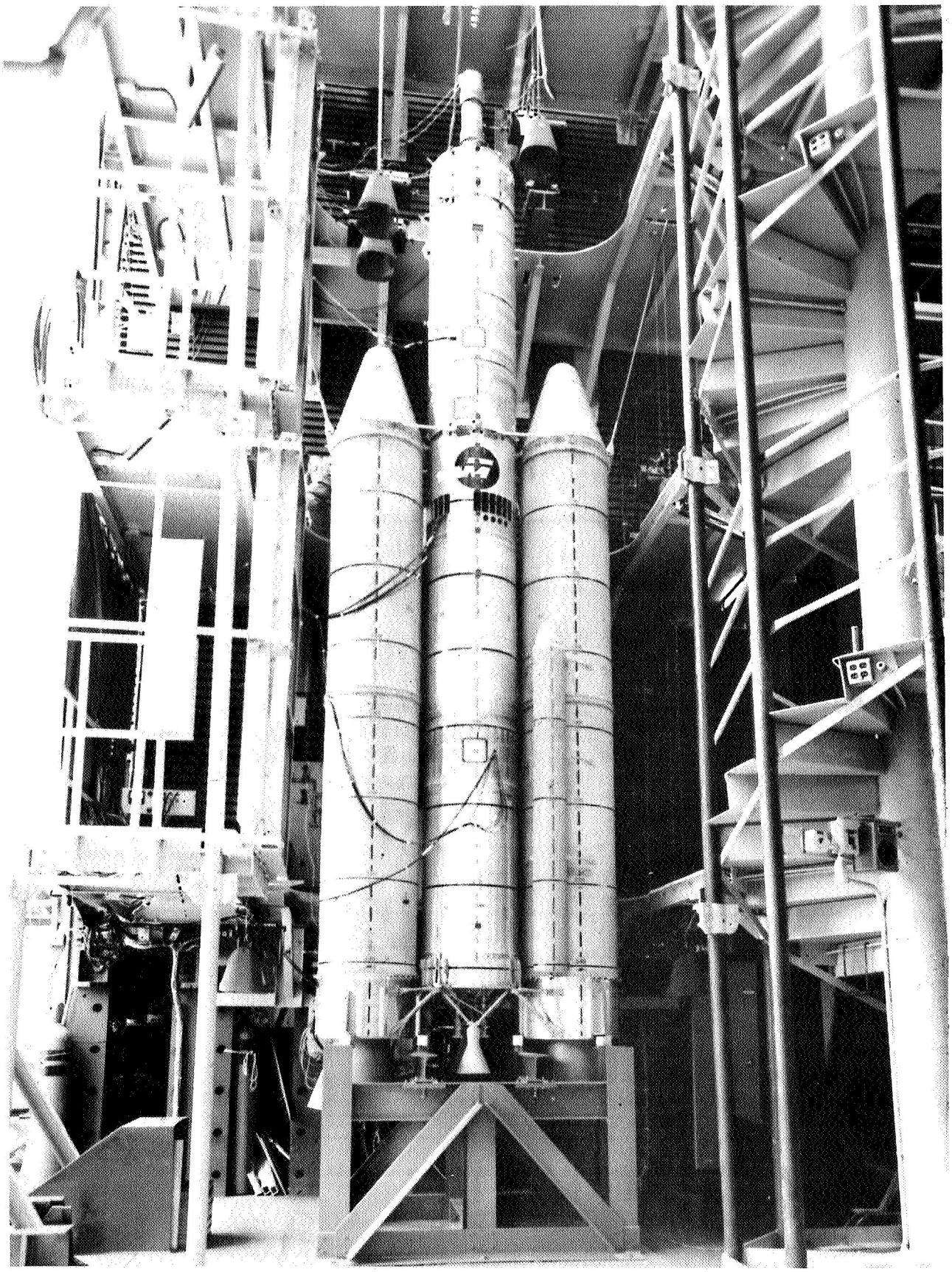

Figure 2.6 Titan III 1/5-Scale Model

The model utilized direct geometric scaling with similar materials (replica scaling) and full-scale manufacturing techniques except that some deviations were allowed in the Transtage structure. The model was used to replace the usual full-scale vibration survey. A discussion of this test program is found in Reference 2.3. Comparison of representative model vibration modes is shown in Figure 2.7. Comparison of representative model frequencies is presented in Table 2.1.

Table 2.1 Frequency Comparison, Titan IIIA and Titan IIIC 1/5-Scale Models

Mode	Titan IIIA, Lift-Off 5000 lb. Payload		Titan IIIC, Lift-Off 26,000 lb. Payload	
	Anal., Hz.	Expt., Hz.	Anal., Hz.	Expt., Hz.
1st pitch	11.7	11.7	5.9	6.0
2nd pitch	23.9	23.6	13.7	12.7
3rd pitch	30.7	32.0	18.2	20.3

Results of a statistical study conducted to establish the tolerances associated with the dynamic characteristics of the Titan IIIC are presented in References 2.13 and 2.14. Modal frequency tolerances for a 99% confidence level, are presented in Table 2.2.

Table 2.2 Modal Frequency Tolerance, Titan III C

Plane	Time of Flight, Sec	Values of Tolerances in %		
		Mode 1	Mode 2	Mode 3
Pitch	0	3.6	7.3	14.7
Pitch	105	3.1	5.3	10.6
Yaw	0	4.0	7.5	19.0
Yaw	105	3.4	5.6	13.0

Note that at modes as low as the third, a tolerance varying from 10% to 19% is determined.

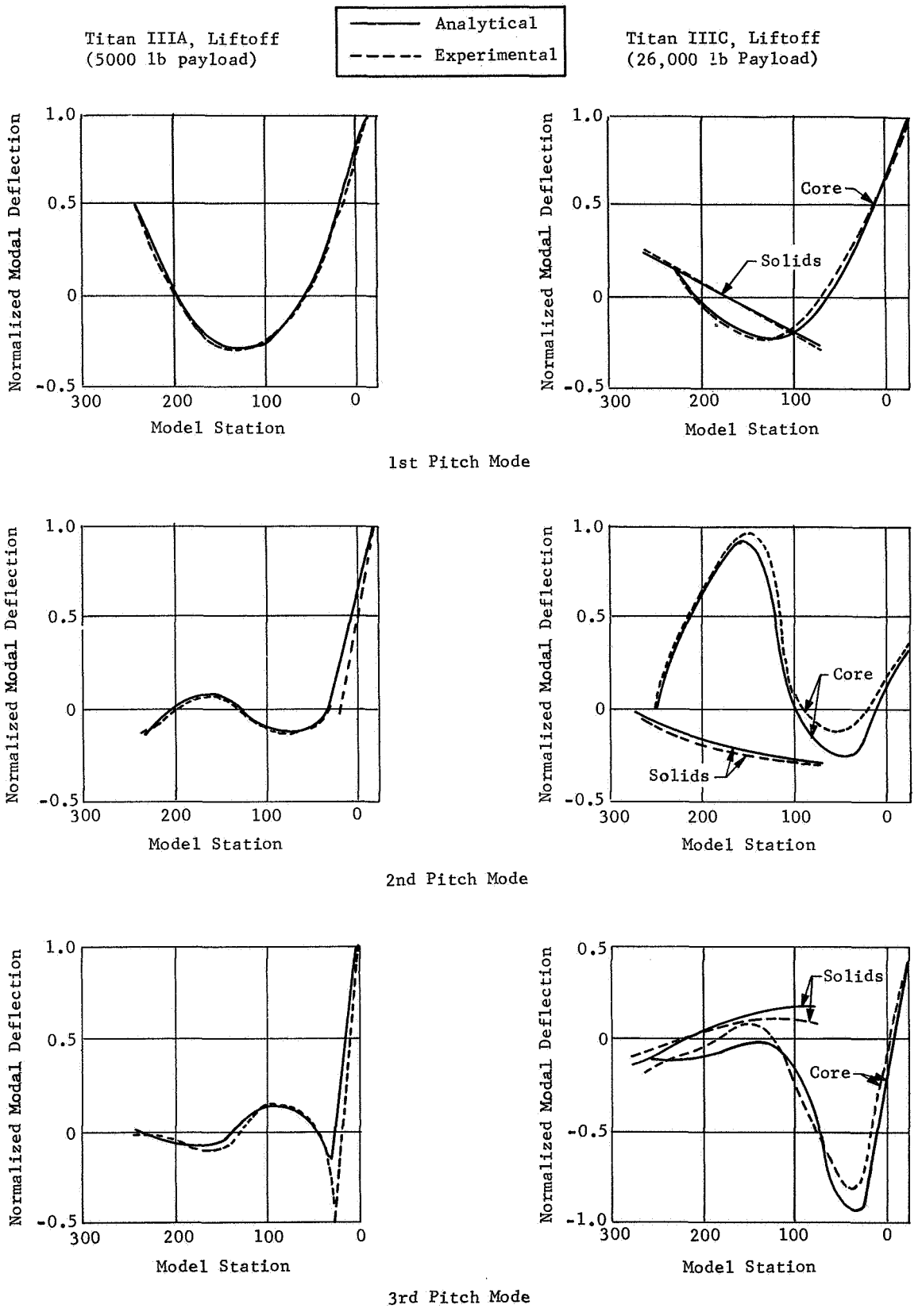

Figure 2.7 Mode Shapes, Titan IIIA and IIIC 1/5-Scale Models

Modal displacement and slope tolerances for the same configuration are presented in Table 2.3.

Table 2.3 Modal Displacement and Slope Tolerance, Titan III C

Description of Group		Values of Tolerances in % Mode 1	Mode 2	Mode 3
All payloads, all flight times pitch and yaw planes	ϕ	6	21	28
	θ	36	50	45
All payloads, all flight times pitch plane	ϕ	7	12	13
	θ	47	20	12
All payloads, all flight times yaw plane	ϕ	6	29	121
	θ	25	99	141
5,000 lb payload, all flight times pitch and yaw planes	ϕ	3	10	9
	θ	21	37	36
26,000 lb payload, all flight times pitch and yaw planes	ϕ	7	51	356
	θ	48	31	39
45,000 lb payload, all flight times pitch and yaw planes	ϕ	11	50	227
	θ	54	147	37
All payloads, flight time = 0 sec. pitch and yaw planes	ϕ	8	34	19
	θ	35	47	80
All payloads, flight time = 53 sec. pitch and yaw planes	ϕ	7	18	20
	θ	25	46	17
All payloads, flight time = 105 sec. pitch and yaw planes	ϕ	2	14	36
	θ	38	35	10

Note 1. ϕ = modal displacement, θ = modal slope
2. Payload weights are full scale values.

These tolerances represent average values of tolerances evaluated at individual sensor locations.

An analytical technique that can be used to improve the quality of experimental vibration modes was developed in conjunction with the Titan III Transtage test. Several modes with very little frequency separation resulted due to the complexity of the structure. These experimental modes were used as "assumed" modes for a vibration analysis and the coupled Transtage mass matrix was determined under the assumption that only inertial coupling exists. The uncoupled modes, computed by the vibration analysis, were then used as the Transtage modes for all further analyses. The uncoupled modes differed only slightly from the test modes but these differences were sufficient to provide modal orthogonality with respect to the mass matrix.

Modal damping data (Ref. 2.14) obtained during the Titan IIIA and Titan IIIC 1/5-scale model test are presented in Figure 2.8.

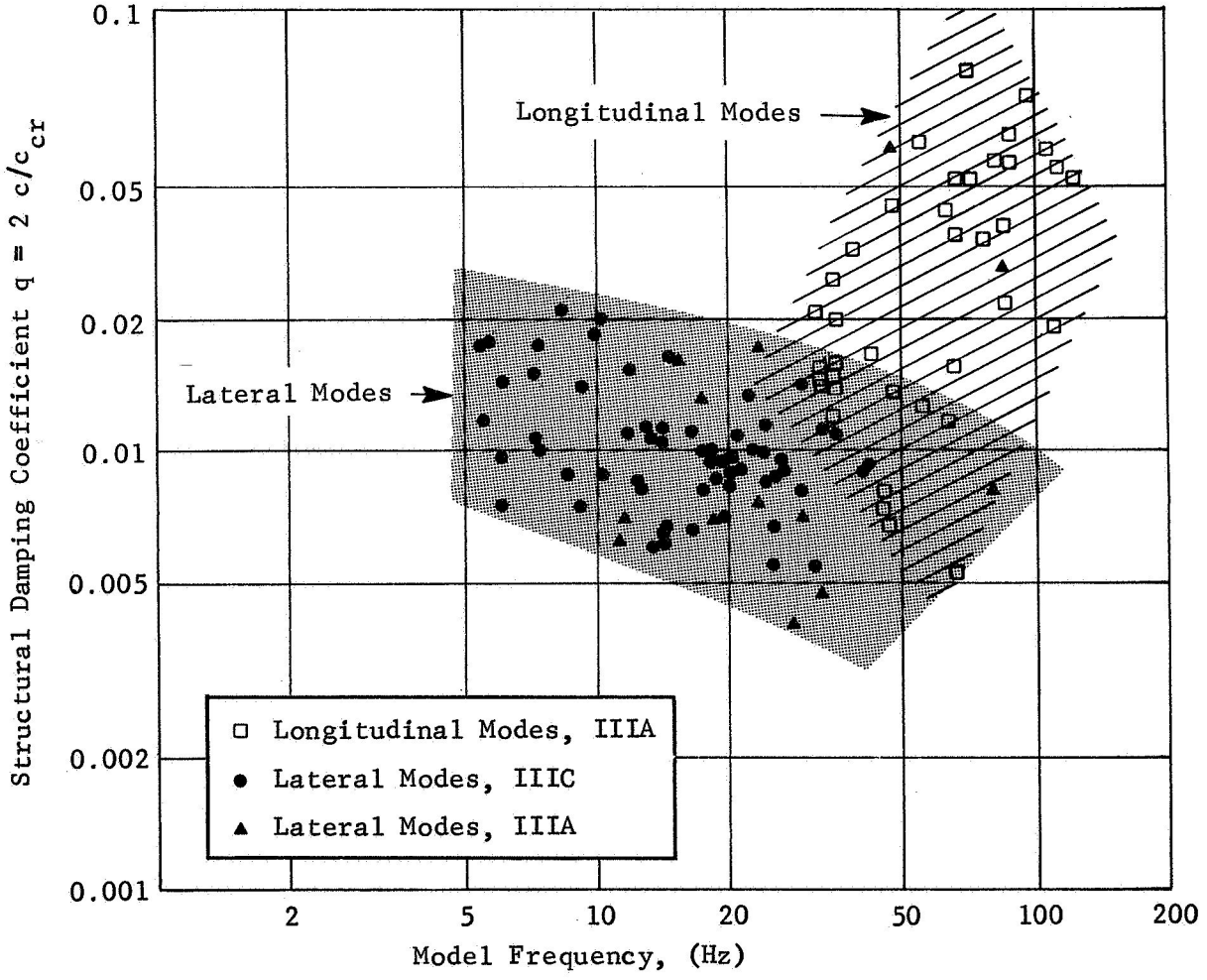

Figure 2.8 Modal Damping Data, Titan IIIA and Titan IIIC 1/5-Scale Models

2.2 Aeroelastic Models

Aeroelastic models of launch vehicles have been primarily constructed to investigate the response, and imposed loads, of vehicles subjected to ground winds and to random transonic buffet excitation.

2.2.1 Buffet Models

Available wind tunnels impose a size restriction on transonic buffet models and typical models are restricted to lengths of 10 feet to 16 feet. Figure 2.10 shows a 7% scale aeroelastic buffet model of the Titan III vehicle with various payloads. This model was scaled in accordance with the scale factors dictated by direct geometric scaling using similar materials but was not constructed with replica scaling. Only the simulation of bending modes was necessary to determine buffet response. The bending and shear stiffnesses were simulated with a machined metal tube of smaller diameter and higher wall thickness than a directly scaled replica. The model is shown in Figure 2.9. A basket-like machined pattern of cut-outs provided the proper ratio of bending to shear stiffness.

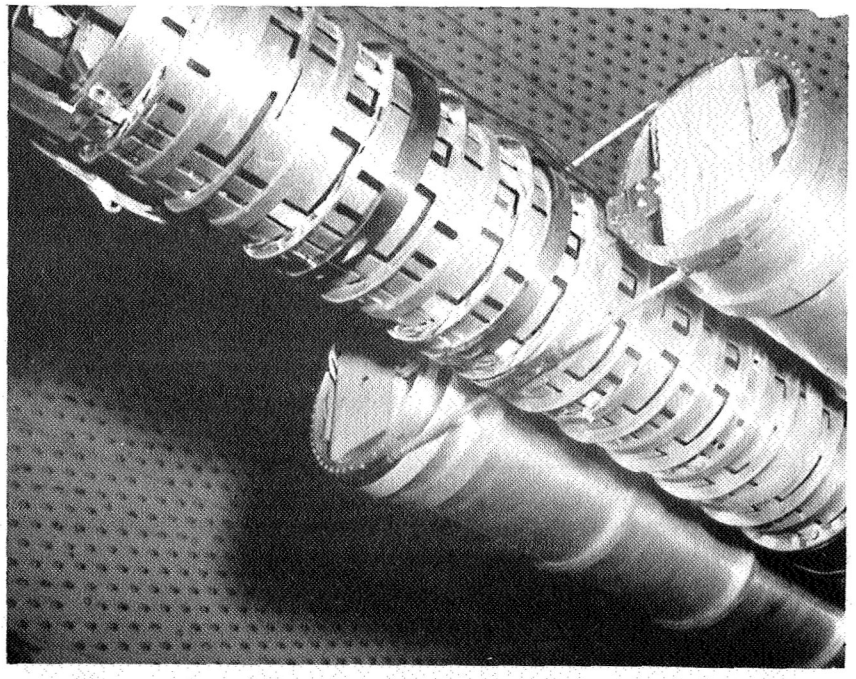

Figure 2.9 Titan III 7% Buffet Model Construction

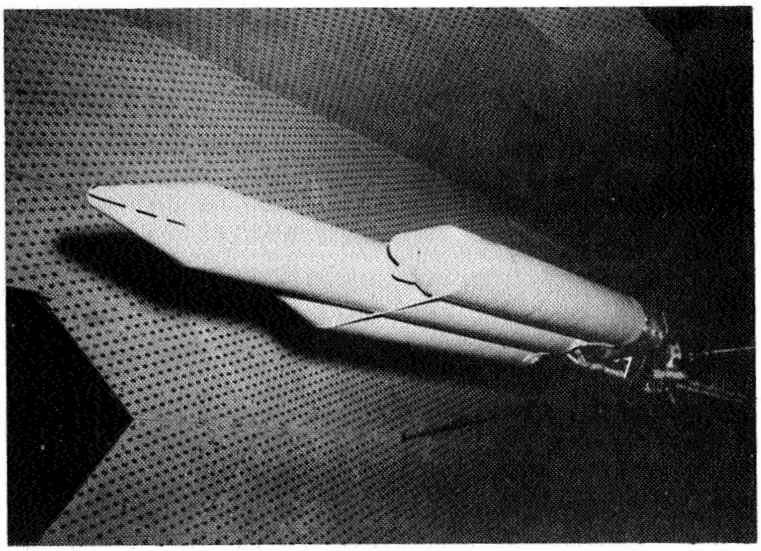

A. 7% Scale Buffet Model

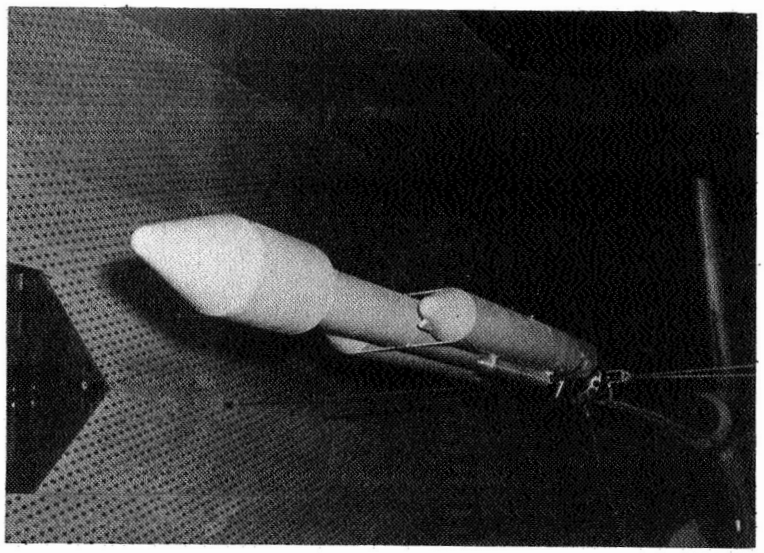

B. 180-in. Bulbous Payload

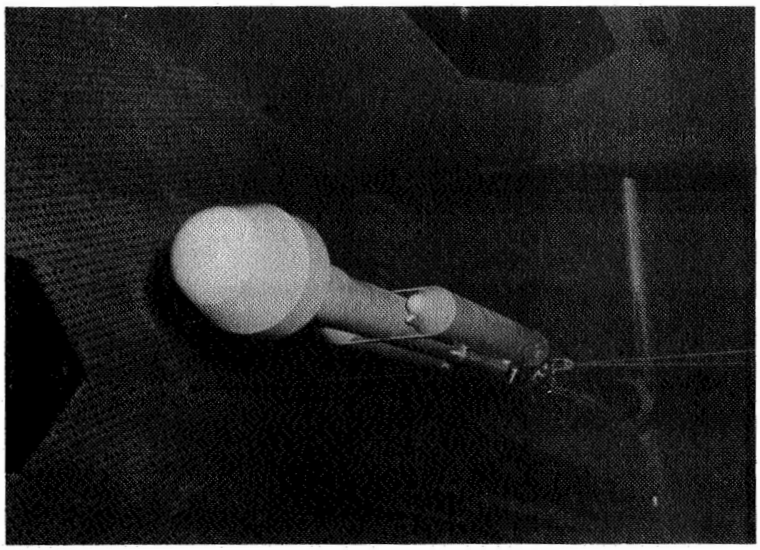

C. 260-in. Bulbous Payload

Figure 2.10 Titan III Aeroelastic Buffet Model

The more important scaling parameters (Ref 2.4) of this Titan III model are summarized in Table 2.4. The subscripts m and p refer to model and prototype, respectively.

Table 2.4 Scaling Parameters, Titan III 7% Buffet Model

Variable	Scaling Relation
Length	$\ell_m/\ell_p = 0.07 = n$
Total Mass	$M_m/M_p = (0.07)^3$
Velocity	$V_m/V_p = 1$
Frequency	$\omega_m/\omega_p = 1/0.07$

The test operating medium and conditions were such that the relations between the non-dimensional parameters Strouhal Number ($\omega\ell/V$) and Reynolds Number ($\rho V\ell/\mu$) were

$$S_m/S_p = (\omega_m/\omega_p)(\ell_m/\ell_p)(V_p/V_m) = 1$$

$$Re_m/Re_p = (\rho_m/\rho_p)(V_m/V_p)(\ell_m/\ell_p)(\mu_p/\mu_m) = n$$

A complete discussion of the model and test can be found in Reference 2.4. Comparison between model and scaled full-scale bending frequencies is shown in Table 2.5.

Table 2.5 Bending Frequencies, Titan IIIC

	Pitch, Hz.		Yaw, Hz.	
	Model	Full-Scale (scaled)	Model	Full-Scale (scaled)
1st Bending	24.3	23.2	23.3	20.5
2nd Bending	40.0	40.3	49.1	39.7
3rd Bending	76.8	71.8	150.2	79.7

Typical test results are presented in Figure 2.11.

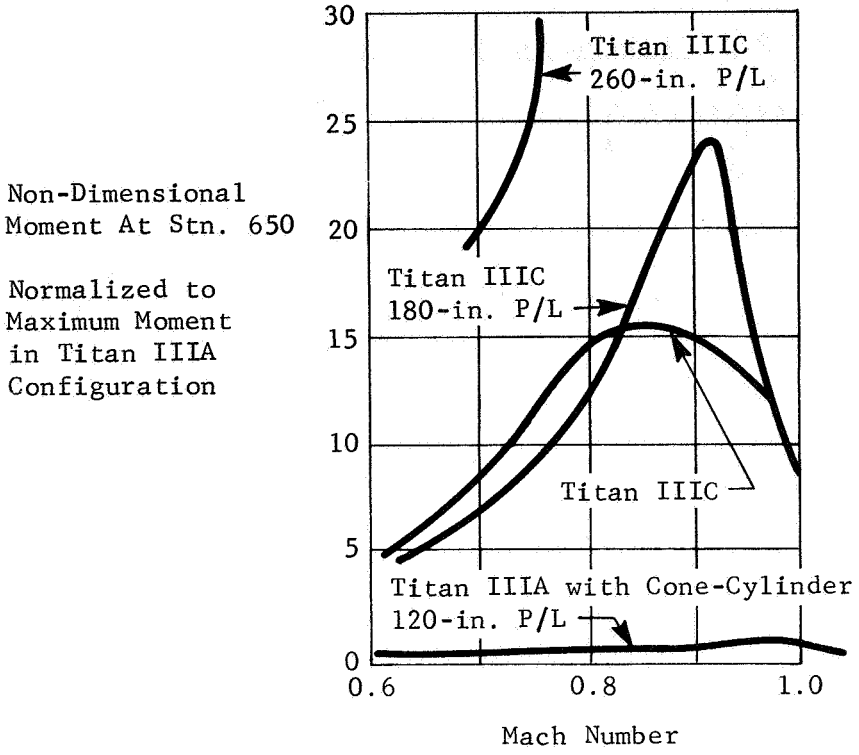

Figure 2.11 Normalized rms Oscillatory Core Bending Moment, Titan III Model

Aeroelastic models of the Saturn I launch vehicle have been built at 2% and 8% scale using dynamically similar construction. Complete structural replica scaling was not attempted. Test results for these models are presented in References 2.5 and 2.6. The 2% model was used primarily for the measurement of aerodynamic damping but it can be regarded as being characteristic of present-day buffet models.

The scaling approach used to transform model test results into usable full-scale values is developed in Reference 2.7. This document also presents test results for a simple buffet model (with two payload shapes) characteristic of single-body launch vehicles. References 2.8 through 2.10 present recent test results obtained during an extension to the Titan III buffet test program. Several configurations and payloads are considered.

2.2.2 Wind-Induced Oscillation Models

Several launch vehicle models have been built to predict dynamic loads induced by ground winds. Ground wind induced oscillations are associated with periodic vortex shedding on the vehicle and umbilical tower. Simulation, or at least resonable approximation, of the full-scale Reynolds Number is an important requirement and usually necessitates testing in media other than air (e.g., Freon). Proper simulation of the test gas-model density ratio then requires higher values of model mass than are dictated by direct density scaling.

One of the most significant ground wind models was the 7.5% aeroelastic Titan IIIA model and launch tower shown in Figure 2.12. The model was mounted on a turntable to permit variation of the relative wind direction.

As it was desirable to match full-scale Reynolds Numbers as closely as possible, the model was tested (using Freon 12 as the test medium) in the Langley Research Center 16 foot variable pressure tunnel. This use of Freon as the test medium imposed certain restrictions. The imposed density and viscosity ratios were

$$\rho_m/\rho_p = 3.7 \text{ and } \mu_m/\mu_p = 0.757.$$

Even with Freon it was impossible to match full scale Reynolds Numbers using practical materials for model construction without violating mass or stiffness scaling parameters. The test Reynolds Numbers were 0.45 of the full-scale values. Some other important scaling parameters for this Titan III model are presented in Table 2.6

Table 2.6 Scaling Parameters, Titan III 7.5% Aeroelastic Wind-Induced Oscillations Model

Variable	Scaling Relation
Length	$\ell_m/\ell_p = 0.075 = n$
Velocity	$V_m/V_p = 1.228$
Frequency	$\omega_m/\omega_p = 16.37$
Dynamic Pressure	$q_m/q_p = 5.576$
Density	$\rho_m/\rho_p = 3.7$

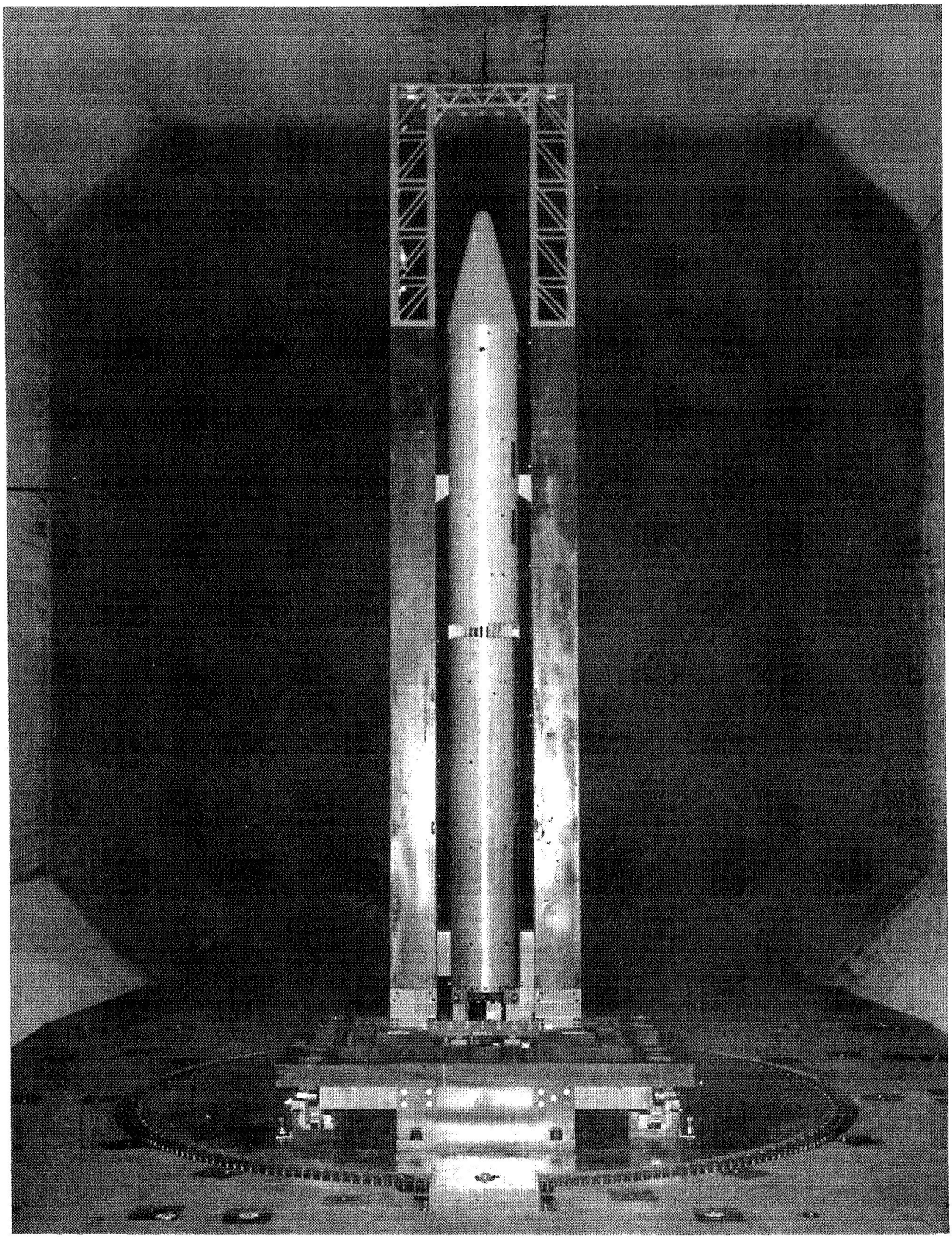

Figure 2.12 Titan IIIA 7.5% Aeroelastic Model with Umbilical Mast

Note that the Strouhal Number ($\omega\ell/V$) was scaled exactly. The mass ratio was

$$M_m/M_p = (\ell_m/\ell_p)^3(\rho_m/\rho_p) = 1.55 \times 10^{-3}.$$

These scaling parameters, with the exception of the Reynolds and Mach Numbers, represent a correct set for aeroelastic scaling. The test Mach Numbers did not equal the full-scale Mach Number but this discrepancy was shown to be negligible through calibration tests in which the Reynolds and Strouhal Numbers were held constant while the Mach Number was varied.

A summary discussion of this test program is presented in Reference 2.4 and a complete report is to be found in Reference 2.11. Response of the vehicle or umbilical structure (if affected by vortex shedding) is primarily a function of the Strouhal Number. Figure 2.13, taken from this reference, shows the dimensionless acceleration power spectral density measured for typical Titan III payloads and umbilical mast configurations.

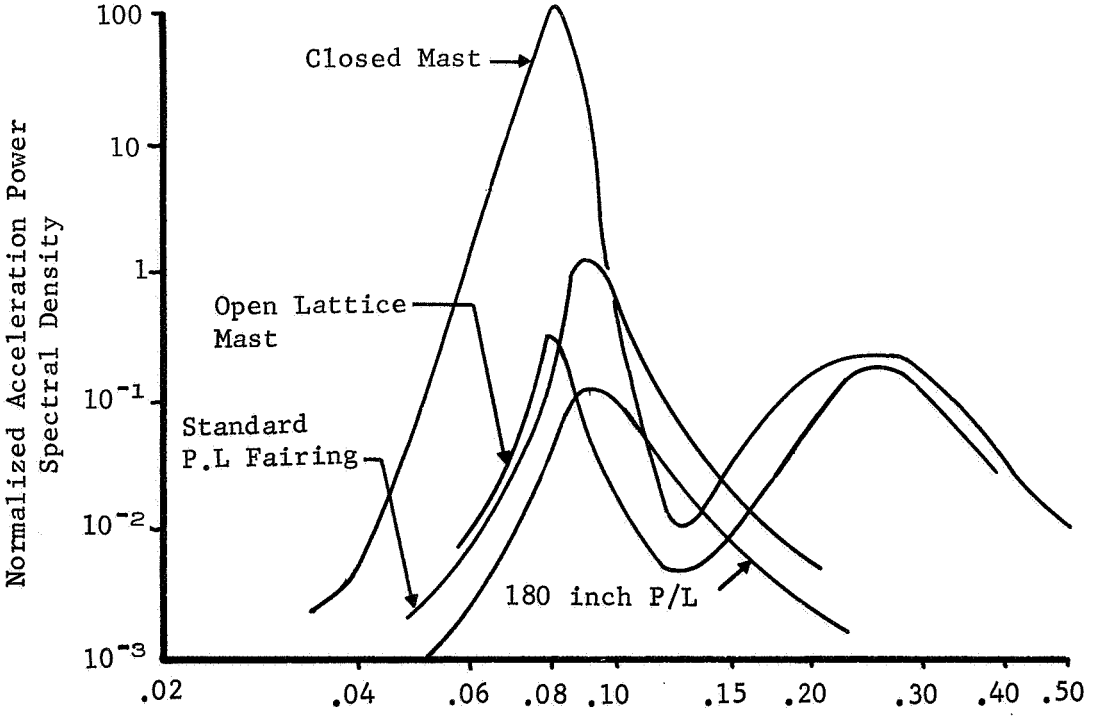

Figure 2.13 Normalized Distribution, Titan III Wind-Induced Oscillations Model

Figure 2.14 gives an indication of the effect of relative wind direction on the dynamic bending moment response of the Titan III umbilical mast at the Strouhal Number of maximum dynamic response.

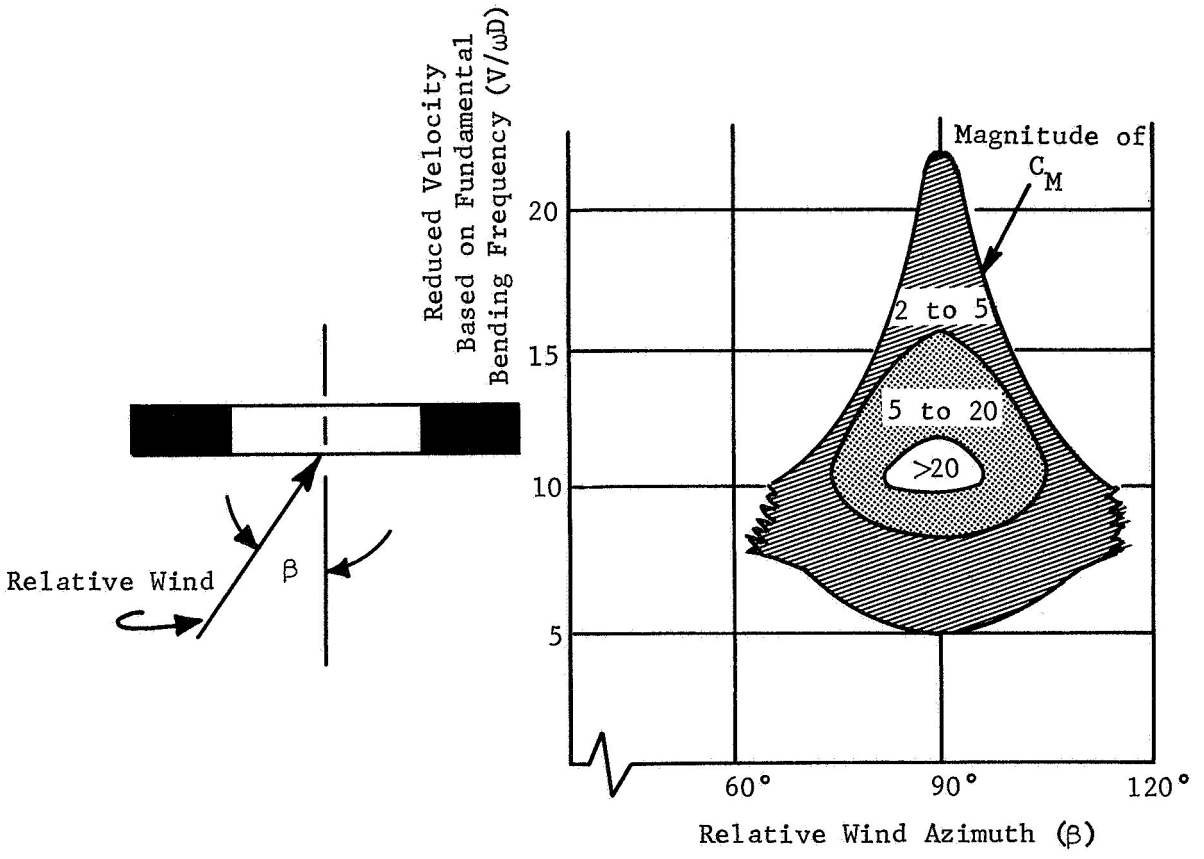

Figure 2.14 Contours of Constant Dynamic Moment Coefficient, Titan III 7.5% WIO Model

The dynamic bending moment coefficients used in this chart were determined from the relationship

$$C_{M_{dyn}} = M_{dyn}/qLR$$

where M_{dyn} = measured dynamic bending moment, FL

q = tunnel dynamic pressure, F/L^2

L = length of mast, L

and

$$R = \int_0^L \phi(x)W(x)dx$$

where x is the mast coordinate. The function $\phi(x)$ represents the normalized first bending mode shape (which accounted for practically all of the response) and W(x) is the width of the mast perpendicular to the wind direction. The parameter D (Figure 2.14) used in computing the reduced velocity (inverse Strouhal Number) is the width of the tip of the mast.

Other aeroelastic models designed to investigate the effects of ground winds (Fig. 2.15) have included a 3%-scale Saturn V model, a 15%-scale model of the Scout vehicle and a 20%-scale Jupiter vehicle. The use of the Langley Research Center 16-foot variable density transonic tunnel permitted close simulation of the full-scale Reynolds Number except for the Saturn model. In this case the model was tested at approximately one-third of the full-scale Reynolds Number (Ref 2.2).

The maximum lateral oscillatory bending moment as a function of the inverse Strouhal Number (Ref 2.2) for the 3%-scale Saturn V model is shown in Figure 2.16. A large response over a limited range of inverse Strouhal Number is indicated for the lowest damping case. This peak is seen to vanish as damping is increased.

A summary of publications dealing with the effects of ground winds on launch vehicles will be found in Reference 2.12.

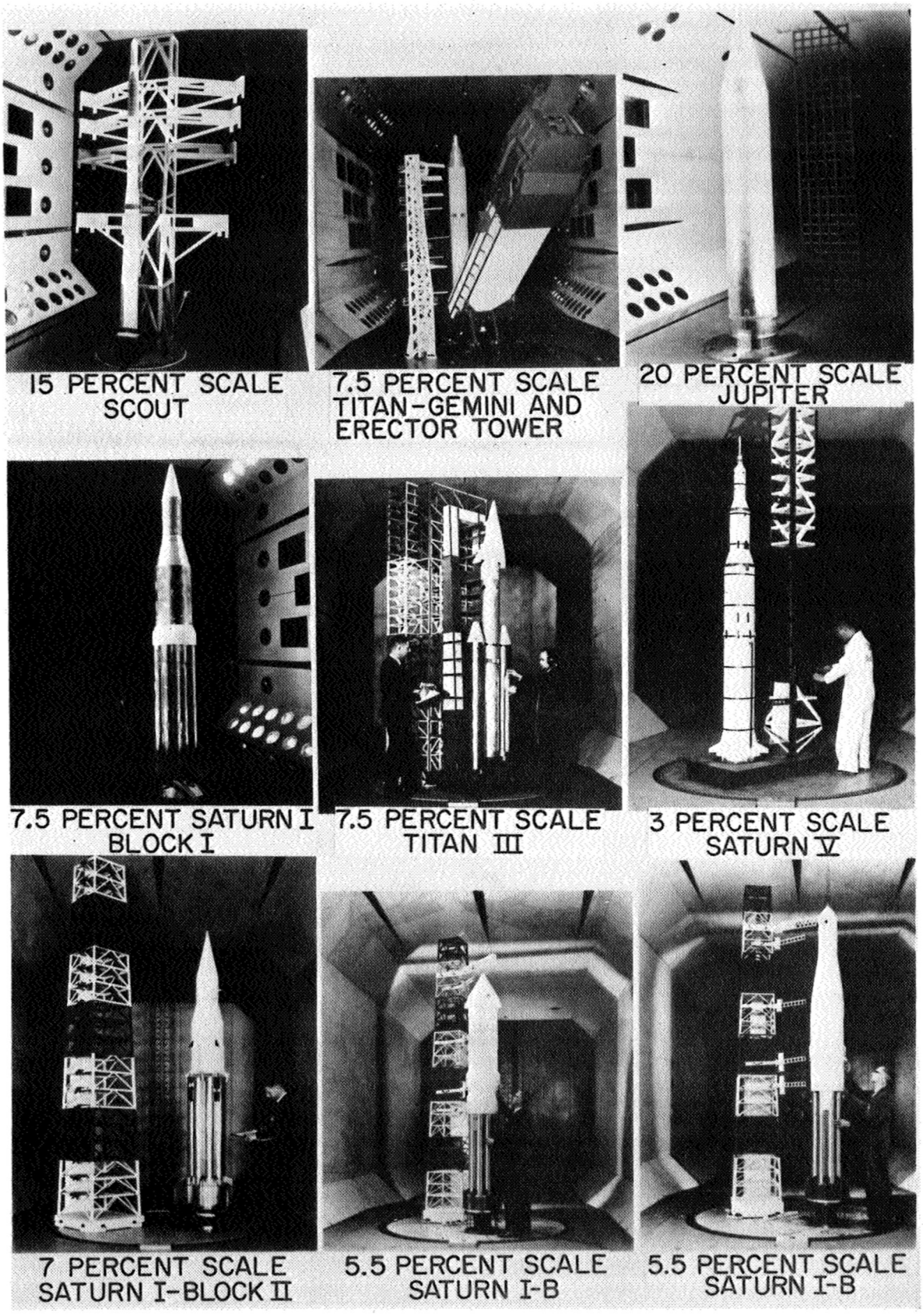

Figure 2.15 Aeroelastic Models, Recent Wind-Induced Oscillations Research

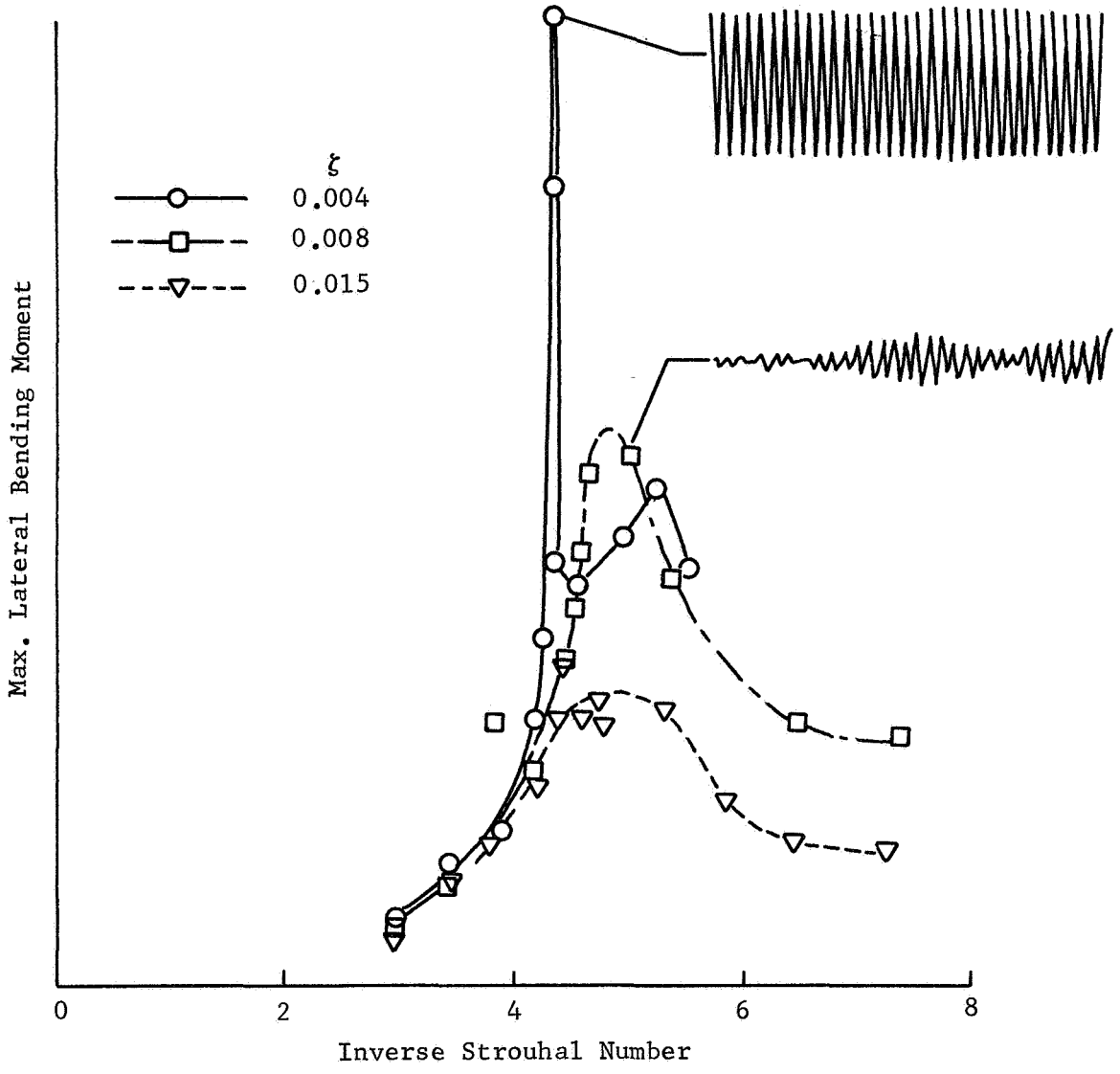

Figure 2.16 Effect of Damping, 3% Saturn V Model

3. DYNAMIC MODEL SCALING PHILOSOPHY

The basic requirement governing the design of any dynamic model is that of similitude between the model and the full-scale structure (or phenomenon) which is to be simulated. This requirement must be satisified for any of the time-dependent physical processes or characteristics that are of interest to the experimenter. The analytical tool generally used to develop the similitude laws governing model design is dimensional analysis. The development of this method (Ref 3.1, 3.2, 3.3, and 3.4) is attributed to Buckingham and Rayleigh. Dimensional analysis is based upon the hypothesis that the solution of a physical problem is expressible in the form of a dimensionally homogeneous equation written in terms of the variables affecting the problem. Once these variables are specified, a group of dimensionless scaling parameters can be derived. Similitude is achieved when the scaling parameters are identical for both the model and the prototype.

3.1 Scaling Laws for Structural Vibrations of Launch Vehicles

The prediction of the vibrational characteristics of launch vehicles through the use of scale models is based upon the assumption that both model and prototype are governed by the same physical laws. From these physical laws can be established the modeling laws which mathematically relate the corresponding characteristics of the two systems. The non-dimensional form of the system governing equations must be the same for both model and prototype.

In general, structural models can be separated into three classes; the particular model choice is governed by the complexity of the prototype structure, the type of exciting forces and the frequency range to be investigated. A graphical representation of the classes is shown in **Figure** 3.1.

If the exciting frequencies are below the first few structural frequencies many of the details present in the prototype vehicle can be neglected, the structure can be represented by mass-spring-damper elements and, within this limited frequency range, the model will exhibit faithful dynamic similarity. As the exciting frequency spectrum increases a more complete geometrical similarity is required as the prototype vehicle no longer behaves as a single unit but rather becomes a multi-branched structure.

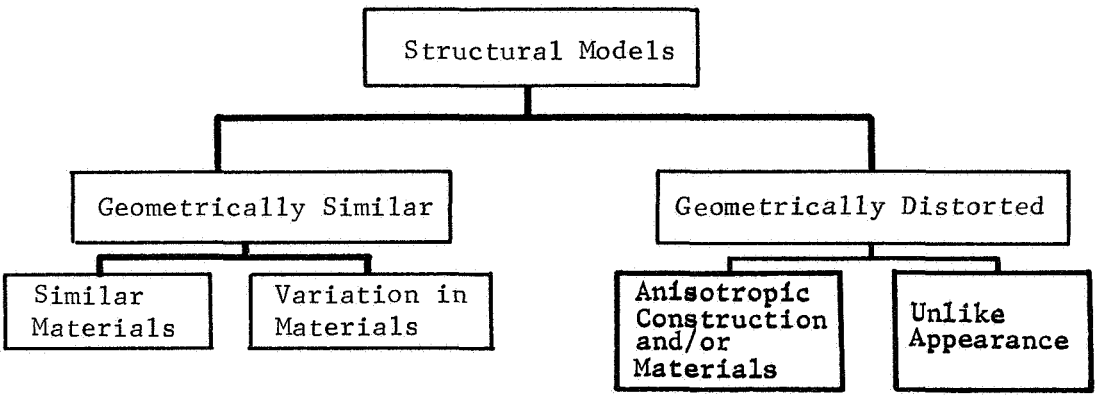

Figure 3.1 Dynamic Model Classes

The form of applied excitation also governs the choice of model. If the applied forces are approximately uniform over the surface, geometric scaling of skin panels is a reasonable approach. For propagating excitation (e.g., noise) it becomes necessary to accurately scale geometry, mass and stiffness characteristics.

There exist two methods of predicting the behavior of physical systems. One is by means of analysis or computer simulation whereby a mathematical model or an analog is created of the physical system in question. The second method is by tests on a prototype or a properly scaled model. Considering the model test, the problem is to identify the physical parameters which govern the phenomenon of interest, to cast them into groups of non-dimensional variables, to perform tests on properly scaled models, and to apply the results from these tests to prediction of the behavior of the prototype. Limitations exist for both systems. Assumptions made in the mathematical model may be too restrictive or inaccurate, thereby limiting the range of applicability. More complete mathematical models may be too complex for economical solutions. Scaled models may not be satisfactory if all the important variables are not identified and/or if proper similitude is not provided. The theory of dimensional analysis is based on the Buckingham Pi theorem from which scaling laws are evolved.

The measure of physical phenomena can be expressed in units of the independent quantities of mass, length, time, and temperature either singly or in multiple combinations.* Assume a physical phenomenon y depends on several independent variables, x_1, x_2 . . . x_n in some unknown manner. If all the independent variables are known, it is possible to predict the outcome y for a given set x_1, x_2, . . . x_n by means of a properly scaled model test, even if the functional relationship between y and its independent variables in unknown.

The following theory underlies the derivation of the scaling laws. The functional relationship between y and all the variables on which it depends can be expressed in general as

$$y = f(x_1, x_2, \ldots x_n) \tag{1}$$

If the exact nature of the function f were known, then this would be the mathematical expression of the physical law expressing the dependence of y on x_1, x_2, . . . x_n. This physical law is independent of the units used in the measurement, and applies just as well to the model as it does to the prototype. Using the subscripts m to apply to the model and p to apply to the prototype, we have the relationships

$$\begin{aligned} y_m &= f(x_{1m}, x_{2m}, \ldots x_{nm}) \\ y_p &= f(x_{1p}, x_{2p}, \ldots x_{np}) \end{aligned} \tag{2}$$

Since the variables in a physical problem can be expressed in terms of the four basic dimensions of mass, length, time, and temperature, then the n + 1 variables (y , x_1, x_2, . . . x_n) can be combined into (n + 1)-4 = n-3 dimensionless groups.

Remembering that the physical law is the same for model and prototype, Equation 2 can then be rewritten

$$\begin{aligned} \pi_{1m} &= F(\pi_{2m}, \pi_{3m}, \ldots \pi(n-3)m) \\ \pi_{1p} &= F(\pi_{2p}, \pi_{3p}, \ldots \pi(n-3)p) \end{aligned} \tag{3}$$

where the dimensionless groups π_{1m}, π_{1p}, contain the dependent variable y, and the other dimensionless groups contain the independent variables. If the model is so constructed that the similitude requirements

*Electrical and magnetic phenomena require additional units.

$$\begin{aligned} \pi_{2m} &= \pi_{2p} \\ &\cdot \quad\quad \cdot \\ &\cdot \quad\quad \cdot \\ &\cdot \quad\quad \cdot \\ \pi(n-3)m &= \pi(n-3)p \end{aligned} \tag{4}$$

are satisfied, then it must follow from Equation 3 that the scaling law for the dependent variable is

$$\pi_{1m} = \pi_{1p} \tag{5}$$

Since y_m (contained in π_{1m}) can be measured from the model test, the dimensionless quantity $\pi_{1p} = \pi_{1m}$ can therefore be determined experimentally.

Thus knowing π_{1p}, the numerical value of the physical quantity y_p contained in π_{1p} can be calculated. Equation 5 thus gives the desired scale factor for the dependent variable y_p.

With four basic dimensions in the problem (mass, length, time, and temperature), four scale factors may be chosen arbitrarily to suit test requirements. The remaining scale factors will then be expressed in terms of one or more of these four.

In general, if all the variables on which a particular phenomenon depends are known, dimensional analysis will give the desired scaling law for the dependent variable and all the similitude requirements necessary to ensure its theoretical validity. However, two important practical difficulties usually must be overcome to develop a workable scaling law. The first difficulty is the practical impossibility of satisfying all the similitude requirements that are theoretically necessary (Eq. 4). An approximately correct scaling law, however, can still be obtained. Only by experimentation can the importance of the similitude requirements that are necessarily neglected, be determined. In any case, empirical corrections to the scaling law can usually be developed. For example, if a particular similitude requirement, $\pi_{km} = \pi_{kp}$, proves to be important, and yet cannot be satisfied, the difficulty can be overcome by determining experimentally how π_1 varies with π_k, keeping all other π terms constant.

The second difficulty is that a complete knowledge of all the variables may not exist. Thus, the unsatisfied similitude requirement for each unknown variable may cause deviations from the scaling law.

The study of the modeling parameters is applicable to the determination of lateral vibrations of aerospace vehicles, vehicle stages, and orbiting space structures such as antennas, mirrors and space stations. The application of scaling techniques has been used to study a wide variety of mechanics problems. The work in this study investigates, in a quantitative manner, some applications of unconventional modeling techniques. The purpose of this approach is to identify and to evaluate those techniques that can be used on structures and structural problems that do not lend themselves to the more common modeling techniques.

The formulation of a problem in dynamics response requires synthesis of three related parts. These are

1. Geometry of the structure and its components.

2. Mechanical properties of the material and characteristics of joining techniques used in the structure.

3. Loads and environment of the structure.

Dimensional analysis is used to identify the numerical values of scaled indepdendent variables (geometry and materials properties) required to provide complete similitude for lateral vibrations of space vehicle. Requirements of model geometry and model material cannot be satisfied using conventional modeling techniques. It is the intent of this study to determine the values of materials properties (such as density and modulus) required for the preservation of lateral vibration similitude. The limits imposed on model size are identified by the availability and economy of unusual techniques.

A study of the convenience of the four arbitrary scale factors can be undertaken to identify which combinations are most convenient for the particular aspect of the problem being modeled. One requirement for the set of properties (independent variables) chosen is that the basic dimensions of M, L. T, and θ must be obtainable by combinations of those properties. A very common choice is as follows:

Symbol	Property	Dimension	Scale Factor
ℓ	Length	L	$\frac{\ell_m}{\ell_p} = \frac{L_m}{L_p} = n_1$
ρ	Mass Density	ML^{-3}	$\frac{\rho_m}{\rho_p} = \frac{M_m L_m^{-3}}{M_p L_p^{-3}} = n_2$

Symbol	Property	Dimension	Scale Factor
v	Velocity	LT^{-1}	$\frac{v_m}{v_p} = \frac{L_m T_m^{-1}}{L_p T_p^{-1}} = n_3$
θ	Temperature	^oR	$\frac{\theta_m}{\theta_p} = \frac{^oR_m}{^oR_p} = n_4$

Once chosen, these factors must be used for scaling on all of the aspects of the given problem:

Instead of the list given above, any set of independent variables which contains all four of the basic dimensions can be chosen. For example, one can choose a pressure variable instead of mass density since ρv^2 has units of pressure. In the end, however, the similitude requirements for all the other independent variables and the scaling laws for the dependent variables are expressed in terms of the four scale factors n_1, n_2, n_3, and n_4 which have been chosen. Thus, this choice determines the specific difficulties which will be encountered in building the scale-model. A particular difficulty can be exchanged for a less-formidable difficulty by altering the choice of arbitrary scale factors.

Candidate fabrication techniques for metal models are: electroplating copper or mickel on a wax mandrel (a system used for very thin shell specimens for buckling experiments); vacuum deposition of thin films on lost wax and chem-milling (currently used on aluminum and titanium aerospace structures).

Application of nonmetallic materials (plastics, fiberglass composites, and sandwich composites) for models are possible. It is important to identify those materials which can provide appreciable variation in other properties such as modulus and density and still maintain the required geometric similitude.

Producing models of materials different from the prototype generally means a difference in material paramters (E, ρ, and ν). For example, let us consider the following similitude requirement.

$$\frac{\rho_m \ell_m^2}{E_m t_m^2} = \frac{\rho_p \ell_p^2}{E_p t_p^2}$$

Assume that all times for model and prototype are required to be the same for a 10% model. We then have

$$1 = \frac{E_p}{E_m} \times \frac{\rho_m}{\rho_p} \times \frac{1}{100}$$

Obviously, this cannot be satisfied using the same material for the prototype and model. If a broad choice of material is available, we can choose for the model

$$E_m = \frac{E_p}{10} \text{ , a very flexible material}$$

$$\rho_m = 10\rho_p \text{ , a very dense material}$$

A phenomenon that can be important in modeling using plastics is the presence of viscoelastic behavior. If the model material exhibits a strain-rate effect during vibration studies, but the prototype material does not, then the modeling laws must account for this violation of the similitude requirements.

Requirements for adequate scaling of joint details (including friction, roughness, prestress, and internal forces of fasteners) is a formidable task. The need to make small-scale exact replicas of structural joints results from the lack of an analytical or empirical model of the dynamic behavior of these joints.

3.2 Basic Dimensions for Scaling Analysis

For the several classes of problems to be considered, we will first establish three arbitrary scale factors from which we can isolate mass (or force), length, and time. Although the primary interest is dynamic scaling, we shall not neglect the static problem. The procedure is to build the dynamic problem from the static and to have forced vibrations related to free vibrations.

To indicate many of the terms that should be considered in structural scaling, Table 3-1 is presented in dimensional form. Both the engineering dimensions of force (F), length (L), and time (T) are given as well as the basic dimensions of mass (M), length (L), and time (T). Converting from one system to the other we use for the definition of force mass times acceleration or symbolically

$$F = MLT^{-2}$$

Table 3.1 Physical Quantities and Dimensions

Quantity	Symbol	Engineering Units		Basic Units
Length (Any linear dimension)	ℓ	in.	L	L
Radius	R	in.	L	L
Thickness	h	in.	L	L
Displacement	w	in.	L	L
Dynamic Response Amplitude	x	in.	L	L
Area	A	$in.^2$	L^2	L^2
Volume	V	$in.^3$	L^3	L^3
Moment of Inertia	I	$in.^4$	L^4	L^4
Polar Moment	J	$in.^4$	L^4	L^4
Force	P	lb.	F	MLT^{-2}
Moment	M	in. lb.	FL	ML^2T^{-2}
Pressure	q	lb/in^2	FL^{-2}	$ML^{-1}T^{-2}$
Stress	σ	lb/in^2	FL^{-2}	$ML^{-1}T^{-2}$
Modulus of Elasticity	E	lb/in^2	FL^{-2}	$ML^{-1}T^{-2}$
Shear Modulus	G	lb/in^2	FL^{-2}	$ML^{-1}T^{-2}$
Unit Mass Density	ρ	$lb.sec^2/in^4$	$FL^{-4}T^2$	ML^{-3}
Unit Weight Density	γ	lb/in^3	FL^{-3}	$ML^{-2}T^{-2}$
Velocity	v	in/sec	LT^{-1}	LT^{-1}
Acceleration	a	in/sec^2	LT^{-2}	LT^{-2}
Gravity constant	g	in/sec^2	LT^{-2}	LT^{-2}
Time	t	sec	T	T
Frequency	ω	1/sec	T^{-1}	T^{-1}
Beam Extension Rigidity	AE	lb	F	MLT^{-2}
Beam Bending Rigidity	EI	in^2lb	FL^2	ML^3T^{-2}
Beam Torsion Rigidity	GJ	in^2lb	FL^2	ML^3T^{-2}
Beam Shear Rigidity	kAG	lb	F	MLT^{-2}
Shell Extension Rigidity	K	lb/in	FL^{-1}	MT^{-2}
Shell Flexural Rigidity	D	in. lb.	FL	ML^2T^{-2}
Poisson Ratio	ν	--	--	--
Wave Number	n	--	--	--
Coordinate Angle	ϕ	--	--	--

Arbitrary Scale Factor, n_i i = 1, 2, . . .
Dimensionless Quantity, π_i i = 1, 2, . . .
Subscript m (model)
Subscript p (prototype)

Several classes of problems become apparent when considering launch vehicle structures. They may be separated into beam-type and shell-type structures, free vibrations or forced vibrations, with liquid or solid propellants, various boundary conditions and several gravity-type loadings. Some of the previous general discussions regarding π terms and arbitrary scale factors are considered in more detail for several kinds of structures, loadings and responses.

To isolate the basic dimensions using arbitrary scale factors n_1, n_2 and n_3 we will establish, the scaling ratios of F, L, and T for model and prototype. The usual arbitrary scale factor is the length factor and will be designated n_1 so that

$$n_1 = \frac{\ell_m}{\ell_p} = \frac{L_m}{L_p}$$

This can be written for the model quantity containing L_m as

$$L_m = n_1 L_p \tag{6}$$

Using the ratio of modulus of elasticity as another arbitrary scale factor we have

$$n_2 = \frac{E_m}{E_p} = \frac{F_m L_m^{-2}}{F_p L_p^{-2}}$$

From Equation 6 for n_1 this can be expressed as

$$n_2 = \frac{F_m}{F_p} n_1^{-2}$$

and solving for the model force

$$F_m = n_1^2 n_2 F_p \tag{7}$$

To incorporate the time scale factor the third arbitrary scale factor will be ratio of mass densities so that

$$n_3 = \frac{\rho_m}{\rho_p} = \frac{F_m L_m^{-4} T_m^2}{F_p L_p^{-4} T_p^2}$$

By using Equations 6 and 7 we can express n_3 as

$$n_3 = (n_1^2 n_2)(n_1^{-4}) \frac{T_m^2}{T_p^2}$$

and solving for T_m we have

$$T_m = n_1 n_2^{-1/2} n_3^{1/2} T_p \tag{8}$$

Based on the previous discussion of π terms it is now possible to scale several kinds of problems, and to design properties into the model depending on the quantity to be measured. It is important to note that independent variables are scaled, dependent variables measured, and this measured value can be correlated to the prototype by the scaling laws. Important pieces of information available from the π terms include the ranges of physical values that must be provided or may be impossible to satisfy.

3.2.1. Static Beam, Scaled Geometrically

For the static problem either stress or deflection are the usual dependent variables of interest. We can isolate the important independent parameters and write the following:

$$u = f(P, \rho g, M, \ell, E, \nu) \tag{9a}$$

$$\sigma = g(P, \rho g, M, \ell, E, \nu) \tag{9b}$$

Dependent π terms

$$\pi_1 = \frac{u}{\ell}$$

$$\pi_2 = \frac{\sigma}{E}$$

Independent π terms

$$\pi_3 = \frac{P}{E\ell^2}$$

$$\pi_4 = \rho g \frac{\ell}{E}$$

$$\pi_5 = \frac{M}{E\ell^3}$$

$$\pi_6 = \frac{\nu_m}{\nu_p} = 1$$

Applying the scaling laws $\pi_{im} = \pi_{ip}$

Model dimensions from the π terms in terms of arbitrary factors become for the dependent variables

$$u_m = u_p \frac{m}{p} = n_1 u_p \tag{10a}$$

$$\sigma_m = \sigma_p \frac{E_m}{E_p} = n_2 \sigma_p \tag{10b}$$

and for the independent variables

$$P_m = \frac{E_m}{E_p} \frac{\ell_m^2}{\ell_p^2} P_p = n_1^2 n_2 P_p \tag{11a}$$

$$\rho_m g_m = \frac{E_m}{E_p} \frac{\ell_p}{\ell_m} \rho_p g_p = n_1^{-1} n_2 \rho_p g_p \tag{11b}$$

$$M_m = \frac{E_m}{E_p} \frac{\ell_m^3}{\ell_p^3} M_p = n_1^3 n_2 M_p \tag{11c}$$

$$\nu_m = \nu_p \tag{11d}$$

Model deflections scale directly as the length scale factor and stresses as the modulus scale factor providing the other quantities are properly scaled.

If the weight of the structure is not important then π_4 can be neglected. If, however, the structural weight is important similitude requires that π_4 be satisfied.

3.2.2 Static Beam, Not Scaled Geometrically

If for some purpose of convenience the model does not faithfully reproduce the prototype in a geometric way then other

properties need to be specified and scaled. Geometric scaling automatically provides similitude for the additional terms involving properties of areas.

$$u = f(P, \rho g, M, \ell, E, \nu, EI, GJ, kAG) \tag{10a}$$

$$\sigma = g(P, \rho g, M, \ell, E, \nu, EI, GJ, KAG) \tag{10b}$$

Dependent π terms are

$$\pi_1 = \frac{u}{\ell}$$

$$\pi_2 = \frac{\sigma}{E}$$

Independent π terms become

$$\pi_3 = \frac{P}{E\ell^2}$$

$$\pi_4 = \rho g \frac{\ell}{E}$$

$$\pi_5 = \frac{M}{E\ell^3}$$

$$\pi_6 = \frac{\nu_m}{\nu_p} = 1$$

$$\pi_7 = \frac{EI}{P\ell^2}$$

$$\pi_8 = \frac{GJ}{P\ell^2}$$

$$\pi_9 = \frac{kAG}{P}$$

For $\pi_m = \pi_p$ and applying this to the above π terms we can scale model quantities for the dependent variables from Equation 10a and 10b

$$u_m = n_1 u_p$$

$$\sigma_m = n_2 \sigma_p$$

and for the dependent variables using Equations 11a through 11d and including π_7, π_8 and π_9 we have for the model

$$P_m = n_1^2 n_2 P_p$$

$$\rho_m g_m = n_1^{-1} n_2 \rho_p g_p$$

$$M_m = n_1^3 n_2 M_p$$

$$\nu_m = \nu_p$$

$$E_m I_m = \frac{P_m}{P_p} \frac{\ell_m^2}{\ell_p^2} E_p I_p = n_1^4 n_2 E_p I_p \qquad (12a)$$

$$G_m J_m = \frac{P_m}{P_p} \frac{\ell_m^2}{\ell_p^2} G_p J_p = n_1^4 n_2 G_p J_p \qquad (12b)$$

$$k_m A_m G_m = \frac{P_m}{P_p} k_p A_p G_p = n_1^2 n_2 k_p A_p G_p \qquad (12c)$$

Quantities from the geometrically scaled model are retained. In addition the bending, torsional, and shear rigidities are included to ensure their proper scaling. If, however, one or more of these additional terms is not considered important, depending on the loading condition, then that scaling can be disregarded.

3.2.3 Free Vibrations, Geometrically Scaled Beam

Another class of problems involving beams and beam-like structures is free vibrations. Many launch vehicle structures are large beams of circular cross section. Boundary conditions, and loads change on the beam from prior to launch, to liftoff, to staging, etc.

The usual depedent variable for free vibrations are the natural frequencies ω. If, however, stress or displacement are also required, the previous treatments given by Equations 10a

and 10b apply, providing the important similitude requirements have been met. For free vibrations of a beam subjected to a load (loads) P and with unit mass density ρ the important independent variables can be expressed as

$$\omega = f(P, \rho g, \ell, E, \nu)$$

The dependent π term for the natural frequency ω is given by

$$\pi_1 = \omega \ell \sqrt{\frac{\rho}{E}}$$

In a manner similar to the static problem the other π terms become

$$\pi_2 = \frac{P}{E\ell^2}$$

$$\pi_3 = \rho g \frac{\ell}{E}$$

$$\pi_4 = \frac{\nu_m}{\nu_p} = 1$$

Making $\pi_m = \pi_p$ for dynamic similitude we find the frequency for the model as

$$\omega_m = \frac{\ell_p}{\ell_m} \sqrt{\frac{E_m}{E_p} \frac{\rho_p}{\rho_m}} \omega_p$$

$$\omega_m = n_1^{-1} n_2^{1/2} n_3^{-1/2} \omega_p \qquad (13)$$

This result is to be expected after examining Equation 8 for model time T_m. The frequency has the dimensions of T^{-1} (referring to Table 3-1) and obviously Equation 13 is the reciprocal of Equation 8. When modeling with identical materials $n_2 = 1$, $n_3 = 1$ then the well known expression for model and prototype frequency relationship $(1/n_1)$ is apparent from Equation 13. However, as shown for the independent variables given below, when the mass of the structure compared to the applied load (loads) P is large and must be scaled then similitude is violated when $n_2 = 1$ and model and prototype are of the same material.

For the independent variables from Equation 11

$$P_m = n_1^2 \, n_2 \, P_p$$

$$\rho_m g_m = n_1^{-1} \, n_2 \, \rho_p g_p$$

$$\nu_m = \nu_p$$

If the external load (loads) P are significantly greater than the weight of the beam then scaling the model loads by n_1^2 x prototype load (and $n_2 = 1$) then model and prototype can be of the same material and frequencies scale as given. It is theorectically possible, by examining Equation 13 to select any frequency ratio that appears convenient. The n_1 term is the length factor and can be manipulated rather easily. Both n_2 and n_3 refer to the material properties of a modeling substance. Manipulations such as centrifuges, composite materials, additional masses are some of the devices used to modify these arbitrary scale factors.

3.2.4 Free Vibrations, Beam Not Scaled Geometrically

By using the three additional terms introduced for beams not scaled geometrically and by using the procedure outlined above this class of problem can also be scaled.

3.2.5 Forced Vibrations, Geometrically Scaled Beam

For forced vibrations the dependent quantity of interest is generally the amplitude of vibration. Both stress and displacement have been discussed and modeling for these quantities has been established. We will use the hat symbol to denote the forcing frequency as $\hat{\omega}$ and the peak value (sinusoidal excitation) of the forcing function as $\hat{P}$. Other symbols refer to quantities defined in Table 3-1.

$$x = f(P, \rho g, \ell, E, \nu, \hat{\omega}, \hat{P})$$

If dynamic similitude is provided then the dependent variable x can be nondimensionalized as

$$\pi_1 = \frac{x}{\ell}$$

To ensure dynamic similitude the independent variables when made nondimensional the corresponding terms must be made numerically equal. These variables are given by

$$\pi_2 = \frac{P}{E\ell^2}$$

$$\pi_3 = \rho g \frac{\ell}{E}$$

$$\pi_4 = \frac{\nu_m}{\nu_p} = 1$$

$$\pi_5 = \hat{\omega}\ell \frac{\rho}{E}$$

$$\pi_6 = \frac{\hat{P}}{E\ell^2}$$

Previously developed equations permit us to write directly for the dependent variable, the amplitude of vibration

$$x_m = n_1 x_p$$

For the several independent terms

$$P_m = n_1^{\ 2}\ n_2\ P_p$$

$$\rho_m g_m = n_1^{\ -1}\ n_2\ \rho_p g_p$$

$$\nu_m = \nu_p$$

$$\hat{\omega}_m = n_1^{\ -1}\ n_2^{\ 1/2}\ n_3^{\ -1/2}\ \hat{\omega}_p \qquad (14a)$$

$$\hat{P}_m = n_1^{\ 2}\ n_2\ \hat{P}_p \qquad (14b)$$

To scale the amplitude of the response by the length scale factor the model must be vibrated as given by $\hat{\omega}_m$ with a peak force of $\hat{P}_m$. If the applied model load (loads) meets the requirement of P_m and the weight of the structure is not significant then similar materials for model and prototype provide well defined scaling. If however, there are no loads, then π_3 must be satisfied and the term $\rho_m g_m$ becomes important.

3.2.6 Forced Vibrations, Beam Not Scaled Geometrically

As discussed in 3.2.4, no new techniques or terms are required. Those rigidities not automatically satisfied by geometric scaling (bending, torsion, and shear) are scaled with the n_1 and n_2 terms to appropriate powers as developed by Equations 12a to 12c.

3.3 Matrix Approach to Compatible Scaling Parameters

A generalized matrix approach to dimensional analysis can be used to develop scaling laws for vibrations of launch vehicle structures. The technique is straightforward and reduces the problem to one of matrix algebra.

In principle, a physical problem will involve a functional relationship among n variables necessary to describe the phenomonon. For example

$$V_n = f\ (V_1, V_2, \ldots, V_{n-1}), \tag{15}$$

or equivalently,

$$g(V_1, V_2, \ldots, V_n) = 0 \tag{16}$$

Dimensional analysis presupposes the form of Equation 16 to be that of a product of the pertinent variables, exponentiated in accordance with their unknown contribution to the product. Theoretically, there are n functional relations of the type shown in Equation 15 (or 16). However, all n of these relations will not be independent as will be shown. Further, if Equation 16 is dimensionally homogeneous (that is, it does not depend on the fundamental units of measurement) it can be reduced to a relation among a complete set of dimensionless products, or scaling parameters, π_j,

$$F(\pi_1, \pi_2, \ldots, \pi_N) = 0 \tag{17}$$

In essence, this is a statement of Buckingham's Theorem (Ref 3.5). When a force, length, time system of measurement is used, the size, N, of a complete set of dimensionless products is equal to the number, n, of necessary variables minus the number, d, of fundamental dimensions (Ref 3.6). Thus, there are N independent relations of the form of Equation 16. Equation 17 does not imply that the functional relationship is known, but merely that one exists. Calculation of the dimensionless products, π_j, is accomplished through dimensional analysis. However, the functional relationship, F, among these products must lie within the realm of experimentation. Whatever the form of Equation 17, it must be satisfied by both the model and the prototype.

A dimensionless product can be expressed in the form

$$\pi_j = \prod_{i=1}^{n} V_i^{q_{ij}}, \quad j = 1, 2, \ldots, N \tag{18}$$

A dimensional equation (one expressed in terms of fundamental dimensions only) can be obtained from Equation 18 if each variable V_i, is expressed in terms of its fundamental dimensions. For example, if the acceleration of gravity is the n^{th} variable, then $V_n^* = LT^{-2}$ where the * indicates dimensionality.

Let

$$V_i^* = \prod_{k=1}^{d} D_k^{P_{ki}} \tag{19}$$

where D_k is the k^{th} fundamental dimension. The exponents, q_{ij}, can be determined if Equation 15 (or 16) is expressed in product form

$$K \prod_{i=1}^{n} V_i^{C_i} = 1 \tag{20}$$

where K is some constant.

This is equivalent to the j^{th} dimensionless product of Equation 4, where C_i is the j^{th} column of q_{ij}.

Substitution of Equation 19 into a dimensional form of Equation 20 yields

$$\prod_{i=1}^{n} \left[\prod_{k=1}^{d} D_k^{P_{ki}} \right]^{C_i} = 1 \tag{21}$$

In order for Equation 21 to be satisfied, all exponents must vanish. Therefore,

$$[P_{ki}] \{C_i\} = 0. \tag{22}$$

Equation 22 represents d linear, homogeneous equations in n unknowns. For a well formulated analysis the rank of $[P_{ki}]$ will be d, so that (n-d) = N independent solutions exist. This is consistent with the number of dimensionless products in a complete set (see Equation 17). Equation 22 can be solved by several techniques of matrix algebra, one of which is outlined as follows:

1) Remove N columns of [P] by post-multiplication with an (n x d) transformation matrix $[Z_1]$, forming a (d x d) matrix $[P_1]$,

$$[P_1] = [P] [Z_1] \tag{23}$$

where $[Z_1]$ must be chosen so as not to render $[P_1]$ singular. The remaining columns of [P] then form a (d x N) matrix $[P_2]$ so that

$$[P_2] = [P]\ [Z_2] \tag{24}$$

where $[Z_2]$ is an (n x N) transformation matrix.

2) Let [Q] be an arbitrary (N x N) matrix whose columns are mutually orthogonal (such as the (N x N) identity matrix). Then [Q] represents an arbitrary choice of the N independent q_{ij}'s of Equation 18, forming N linearly independent vectors. A matrix equation analogous to Equation 22 can be written for the exponents of the N dimensionless parameters

$$[P_1]\ [U] + [P_2]\ [Q] = 0 \tag{25}$$

where the vectors of [U] are the unknown q_{ij}'s. Therefore, since $[P_1]$ is non-singular,

$$[U] = -[P_1]^{-1}\ [P_2]\ [Q]. \tag{26}$$

3) The exponents of the pertinent physical variables, V_i, can be determined by assembling the [U] and [Q] matrices according to

$$[q_{ij}] = [Z_1]\ [U] + [Z_2]\ [Q]. \tag{27}$$

4) With the solution of Equation 27, a complete set of N dimensionless scaling parameters is determined.

3.3.1 Example of Scaling Parameter Derivation

Consider the vibration of a slender beam with bending and shear stiffness. The functional relationship between the physical variables is

$$\omega = f(m, \ell, AG, EI)$$

or

$$f(m, \ell, AG, EI, \omega) = 0$$

where ω = natural frequency, 1/T

m = mass/unit length, FT^2/L^2

ℓ = length, L

AG = shear stiffness, F

EI = bending stiffness, FL^2

and

n = 5 (pertinent variables)

d = 3 (fundamental dimensions)

N = 2 (size of complete set of dimensionless products).

1) The n physical variables can be expressed in terms of the d basic dimensions (F, L, T) through the (d x n) matrix P

$$[P] = \begin{array}{c} \\ F \\ L \\ T \end{array} \begin{array}{c} \begin{array}{ccccc} m & \ell & AG & EI & \omega \end{array} \\ \begin{bmatrix} 1 & 0 & 1 & 1 & 0 \\ -2 & 1 & 0 & 2 & 0 \\ 2 & 0 & 0 & 0 & -1 \end{bmatrix} \end{array}$$

The (n x d) matrix Z_1, and the (n x N) matrix Z_2 can be arbitrarily selected to be

$$[Z_1] = \begin{bmatrix} 1 & 0 & 0 \\ 0 & 1 & 0 \\ 0 & 0 & 1 \\ 0 & 0 & 0 \\ 0 & 0 & 0 \end{bmatrix} \qquad [Z_2] = \begin{bmatrix} 0 & 0 \\ 0 & 0 \\ 0 & 0 \\ 1 & 0 \\ 0 & 1 \end{bmatrix}$$

The (d x d) matrix P_1 and the (d x N) matrix P_2 are

$$[P_1] = [P][Z_1] = \begin{bmatrix} 1 & 0 & 1 & 1 & 0 \\ -2 & 1 & 0 & 2 & 0 \\ 2 & 0 & 0 & 0 & -1 \end{bmatrix} \begin{bmatrix} 1 & 0 & 0 \\ 0 & 1 & 0 \\ 0 & 0 & 1 \\ 0 & 0 & 0 \\ 0 & 0 & 0 \end{bmatrix} = \begin{bmatrix} 1 & 0 & 1 \\ -2 & 1 & 0 \\ 2 & 0 & 0 \end{bmatrix}$$

and

$$[P_2] = [P][Z_2] = \begin{bmatrix} 1 & 0 & 1 & 1 & 0 \\ -2 & 1 & 0 & 2 & 0 \\ 2 & 0 & 0 & 0 & -1 \end{bmatrix} \begin{bmatrix} 0 & 0 \\ 0 & 0 \\ 0 & 0 \\ 1 & 0 \\ 0 & 1 \end{bmatrix} = \begin{bmatrix} 1 & 0 \\ 2 & 0 \\ 0 & -1 \end{bmatrix}$$

2) If the (N x N) matrix Q is defined to be

$$[Q] = \begin{bmatrix} 1 & 0 \\ 0 & 1 \end{bmatrix},$$

the (d x N) matrix U is

$$[U] = -[P_1^{-1}]\,[P_2]\,[Q]$$

$$= \begin{bmatrix} 0 & 0 & -\frac{1}{2} \\ 0 & -1 & -1 \\ -1 & 0 & \frac{1}{2} \end{bmatrix} \begin{bmatrix} 1 & 0 \\ 2 & 0 \\ 0 & -1 \end{bmatrix} \begin{bmatrix} 1 & 0 \\ 0 & 1 \end{bmatrix} = \begin{bmatrix} 0 & \frac{1}{2} \\ -2 & 1 \\ -1 & -\frac{1}{2} \end{bmatrix}$$

3) The exponents are therefore

$$[q_{ij}] = [Z_1]\,[U] + [Z_2]\,[Q]$$

$$= \begin{bmatrix} 1 & 0 & 0 \\ 0 & 1 & 0 \\ 0 & 0 & 1 \\ 0 & 0 & 0 \\ 0 & 0 & 0 \end{bmatrix} \begin{bmatrix} 0 & \frac{1}{2} \\ -2 & 1 \\ -1 & -\frac{1}{2} \end{bmatrix} + \begin{bmatrix} 0 & 0 \\ 0 & 0 \\ 0 & 0 \\ 1 & 0 \\ 0 & 1 \end{bmatrix} \begin{bmatrix} 1 & 0 \\ 0 & 1 \end{bmatrix}$$

$$[q_{ij}] = \begin{bmatrix} 0 & \frac{1}{2} \\ -2 & 1 \\ -1 & -\frac{1}{2} \\ 0 & 0 \\ 0 & 0 \end{bmatrix} + \begin{bmatrix} 0 & 0 \\ 0 & 0 \\ 0 & 0 \\ 1 & 0 \\ 0 & 1 \end{bmatrix} = \begin{matrix} \\ m \\ \ell \\ AG \\ EI \\ \omega \end{matrix} \begin{matrix} \begin{matrix} \pi_1 & \pi_2 \end{matrix} \\ \begin{bmatrix} 0 & \frac{1}{2} \\ -2 & 1 \\ -1 & -\frac{1}{2} \\ 1 & 0 \\ 0 & 1 \end{bmatrix} \end{matrix}$$

4) The N = 2 dimensionless scaling parameters are determined from the vectors of q_{ij} as follows

$\pi_1 = EI/AG\ell^2$, $\pi_2 = m^{1/2}\,\ell\omega/(AG)^{1/2}$ or $\pi_2' = m\ell^2\omega^2/AG$.

π_1 and π_2 comprise the complete set of dimensionless scaling parameters and any other parameter can be obtained from them. For example

$$\pi_2^* = \frac{\pi_2'}{\pi_1} = \frac{m\ell^4\omega^2}{EI}$$

4. VIBRATIONS OF BEAM-LIKE STRUCTURES

Launch vehicles or certain portions of them, can be represented as beam structures. The modal characteristics are determined from the bending, torsional, shear, and longitudinal stiffnesses. Response is governed by the mass distributions, and the applied loads. Each of these quantities can be a function of position along the longitudinal axis.

Four classes of vibration problems are considered for dynamic scaling. The are identified as: (1) Free vibrations, no external loads; (2) Free vibrations, large external loads; (3) Forced vibrations, no external loads; (4) Forced vibrations large external loads. Notations, symbols, and arbitrary scale factors from Section 3 are retained. For convenience we repeat the arbitrary scale factors and the resulting similitude requirements for force (F), length (L), and time (T). Subscripts m and p represent model and prototype respectively.

$$n_1 = \frac{\ell_m}{\ell_p} \tag{1a}$$

$$n_2 = \frac{E_m}{E_p} \tag{1b}$$

$$n_3 = \frac{\rho_m}{\rho_p} \tag{1c}$$

After manipulating the dimensions of ℓ, E, and ρ we have for model requirements in terms of prototype dimensions from Equation 1.

$$L_m = n_1 L_p \tag{2a}$$

$$F_m = n_1^2 n_2 F_p \tag{2b}$$

$$T_m = n_1 n_2^{-1/2} n_3^{1/2} T_p \tag{2c}$$

Any of the physical properties of interest has one or more of these dimensions raised to some power.

4.1 Free Vibrations, No External Loads

It is assumed that beam rigidities are representative of cylindrical shells exhibiting beam-like behavior. End conditions for the model must be identical to those for the prototype.

For the free vibration problem the dependent variable of interest is the frequency of vibration of the several mode shapes. Without external loads the frequency can be shown to depend on several independent factors such that

$$\omega = f(\rho g,\ \ell,\ E,\ EI,\ GJ,\ kAG) \tag{3}$$

Frequency ω can be written nondimensionally as

$$\pi_1 = \omega\ell \sqrt{\frac{\rho}{E}}$$

From which we can write

$$\omega_m = n_1^{-1}\ n_2^{1/2}\ n_3^{-1/2}\omega_p \tag{4}$$

For this relationship to be valid the following model terms must be scaled using preselected values of n_1, n_2 and n_3.

$$\rho_m g_m = n_1^{-1}\ n_2\ \rho_p g_p \tag{5a}$$

$$E_m I_m = n_1^{4}\ n_2\ E_p\ I_p \tag{5b}$$

$$G_m J_m = n_1^{4}\ n_2\ G_p\ J_p \tag{5c}$$

$$k_m A_m G_m = n_1^{2}\ n_2\ k_p A_p G_p \tag{5d}$$

The most difficult modeling requirement to meet is given in Equation 5a. For $g_m = g_p$, both model and prototype in the same gravity field, the mass density ratio requirement is shown in Fig. 4.1. The three lines show the effect of changing modulus. The upper line is a model material twice as stiff as the prototype, the middle line is the same modulus for model and prototype and the lower line is a model material 1/2 as stiff as the prototype. As the model becomes relatively smaller the model material must become increasingly more dense.

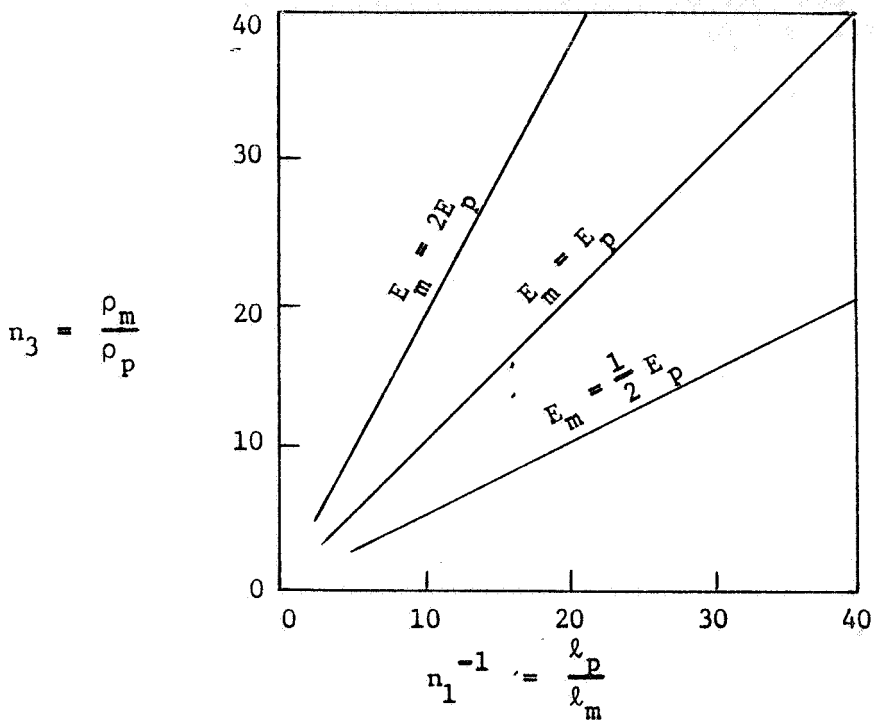

Fig. 4.1 Model Density Requirements as a Function Scale Factor for $g_m = g_p$

By solving for n_1 in Equation 5a and substituting in Equation 4 the model frequency becomes

$$\omega_m = n_2^{-1/2} \, n_3^{1/2} \, \frac{g_m}{g_p} \, \omega_p, \text{ for } n_1 = n_2 n_3^{-1} \frac{g_m}{g_p} \qquad (6)$$

If model and prototype are made of the same material and tested in the same g field, Equation 6 gives $\omega_m = \omega_p$; however, from Equation 4 for the same material

$$\omega_m = n_1^{-1} \, \omega_p.$$

To satisfy both requirements, it is apparent that $n_1 = 1$ and the model becomes exactly the same as the prototype.

For structures carrying no external loads or small external loads, one of the means of providing a different g environment

(for $n_1 < 1$ $g_m > g_p$) is the use of a centrifuge. Model and prototype can then be modeled of the same material and the frequency relation,

$$\omega_m = n_1^{-1} \omega_p \text{ can be used}$$

if

$$g_m = n_1^{-1} g_p.$$

Another means of achieving the proper mass effect is to attach to the model additional material and not use centrifugal force. Added material must not provide rigidities that are not scaled or accounted for.

When transverse bending modes are being studied, then Equation 5b defines that rigidity requirement for the model. Torsional vibrations require the model condition given in Equation 5c. If large deformations are expected, or if the structure is short with respect to its depth, Equation 5d must be satisfied for the model to provide accurate dynamic response.

Free lateral vibrations of beams can be found from the partial differential equations of the form

$$EI \frac{\partial^4 x}{\partial \ell^4} = - \rho g \frac{\partial^2 x}{\partial t^2} \qquad (7)$$

Consideration of boundary conditions provides solutions for the response of a particular system. Exact geometric scaling provides the proper moment of inertia (I) and is accounted for by the scale factor n_1. Material properties of the beam are included in the modulus term E, and scaled by the factor n_2. Another property of the system is the unit mass density ρ and is included in the arbitrary scale factor n_3. A term that is not arbitrary is the gravity constant g. The other two terms of Equation 7 are partial derivatives of the dynamic displacement x, fourth order in the length direction, second order in time, and are included in the modeling laws.

4.2 Free Vibrations, Large External Loads

For many of the practical cases the mass of the structure is small compared to other loads imposed on that structure. These may come from several sources such as payload, propellants, winds, movement through the atmosphere, control forces, trajectory

profiles, and others. The imposed moments, shears, torques and axial loads must be properly scaled for reliable model representation of large scale launch vehicles.

Continuing in the manner previously established, the frequency of a beam-like structure with a relatively small beam mass is a function of the following external loads and beam properties.

$$\omega = f(P, M, \rho g, \ell, E, EI, GJ, kAG) \tag{8}$$

The relationship for model and prototype frequency is

$$\omega_m = n_1^{-1} n_2^{1/2} n_3^{-1/2} \omega_p \tag{4}$$

Model requirements for the independent terms are

$$P_m = n_1^2 n_2 P_p \tag{9a}$$

$$M_m = n_1^3 n_2 M_p \tag{9b}$$

$$\rho_m g_m = n_1^{-1} n_2 \rho_p g_p \tag{5a}$$

$$E_m I_m = n_1^4 n_2 E_p I_p \tag{5b}$$

$$G_m J_m = n_1^4 n_2 G_p J_p \tag{5c}$$

$$k_m A_m G_m = n_1^2 n_2 k_p A_p G_p \tag{5d}$$

The two vibration problems of one system with no external vibrating loads and another with large external loads is analogous to comparing a vibrating spring where in one case the spring only vibrates and the second case when the spring supports a large vibrating mass. In the first instance the inertial forces come from the vibrating spring and are important because they are the only inertial forces. In the second case when the mass is large compared to the spring mass the predominant inertial force is that of the mass. Scaling for this kind of load is accomplished using the similitude requirement of Equation 5a. Beam mass if sufficiently small is neglected and the supported mass oscillating in the same as the beam is scaled dynamically.

Transverse vibrations are modified by axial loads on beams. A loaded launch vehicle on the stand or an accelerating vehicle

undergoes axial loading, and the magnitude of the load changes the frequency of vibration. Scaling this load is accomplished using Equation 9a. The model force is the square of the length scale factor times the modulus ratio times the prototype load.

Another source of axial load, acting as a prestress, exists when launch vehicle tanks are pressurized. Lateral vibrational frequencies increase when longitudinal tension is applied to a beam and decrease when the beam is compressed. The tensile load from tensile prestress (pressure times cross sectional area) is scaled through the force term in Equation 9a.

Shear loads, applied transversely to the axis of the beam, are scaled by the same factors used for axial loads. Equation 9a expresses the similitude requirements for shearing forces.

Moments and torques are scaled by Equation 9b, the moment is applied in a plane containing the beam axis, and the torque in a plane normal to the axis. Whereas the force scale factor for the model is modified by the square of the length ratio the moment and/or torque on the model is a function of the length factor cubed times the modulus ratio.

Lateral vibrations are resisted by the stiffness term EI, scaled in Equation 5b. If this quantity is scaled and if the forces and masses that influence the response are properly scaled the free vibrations of the prototype structures can be found from the model from Equation 4. Torsional stiffness supplied by the GJ term provides the structural resistance to torsional vibrations, and the same frequency equation applies.

When the model is an exact replica of the prototype and made of the same material, stiffnesses EI, GJ, and kAG will be numerically correct and n_2 and n_3 will be equal to unity. Force quantities will be scaled by n_1^2, moment and torque by n_1^3 and inertial loads by n_1^{-1}.

4.3 Forced Vibrations, No External Loads

Beam structures not carrying masses, not subjected to axial loads, and being excited by time dependent forces can be dynamically modeled. Frequency becomes an independent variable, and is scaled according to the previously established similitude requirements. Additionally, the maximum values of the exciting force applied to the model must be modeled assuming the prototype force is repetitive and of some known magnitude.

For the beam only the variables important to its response under forced vibrations with amplitude or the dependent variables can be given in the form

$$x = f(\hat{\omega}, \hat{P}, g, \ell, E, EI, GJ, kAG) \tag{10}$$

The hat superscript over ω and P designate the frequency of the forcing function and the maximum value of the force. Any periodic, aperiodic, varying amplitude, or transient forcing system can be modeled if each of the frequency and load components of the complex system are scaled individually then combined and applied simultaneously to the model.

When complete similitude is achieved, the relationship between the response of the model and prototype is given by

$$x_m = n_1 x_p \tag{11}$$

Every component of the frequency spectrum of the forcing function imposed on the model is given by

$$\hat{\omega}_m = n_1^{-1} n_2^{1/2} n_3^{-1/2} \hat{\omega}_p, \tag{12a}$$

and the corresponding force applied to the model when scaled dynamically becomes

$$\hat{P}_m = n_1^{2} n_2 \hat{P}_p \tag{12b}$$

The $\rho_m g_m$ term for unloaded structures is given by Equation 5a and applies to the forced vibration problem with the same discussion found for the free vibration problem with the same discussion found for the free vibrations. Remaining variables in Equation 9 are again scaled as rigidity terms given by Equations 5a, 5b, and 5c.

4.4 Forced Vibrations, With External Loads

External loads, not part of the forcing function, on a vibrating structure are of two kinds; constant with time, acting as a prestress; and inertial loads varying as mass times acceleration. Prestress loads exist as pressures, or dead loads, or acceleration loads and remain constant or vary slowly with time. Inertial loads can be varying because of changing velocity (acceleration) or changing mass (as a rocket) or both.

The terms for forced vibrations of beams carrying external loads are given by

$$x = f(\hat{\omega}, \hat{P}, P, M, \rho g, \ell, E, EI, GJ, kAG) \tag{13}$$

Each of these terms has been previously scaled and no new similitude requirements are needed. However, for launch vehicles the external load P acting as a prestress either constant in time or varying time can be examined in greater detail. The definition of P comes from Newton's second law of motion so that

$$P = \frac{d}{dt} (\rho V v) \tag{14}$$

To help establish the dimensionality of these terms, we take each of them individually to show using basic MLT dimensions,

$$MLT^{-2} = \frac{1}{T} (ML^{-3})(L^3)(LT^{-1})$$

and obviously after simple manipulation we have

$$MLT^{-2} = MLT^{-2}$$

Therefore ρ is unit mass density of a given volume V, v is velocity, and the product of ρVv is changing with time. For dynamic similitude from Equation 9a

$$P_m = n_1^2 \, n_2 \, P_p$$

giving for the right hand side of Equation 14

$$\frac{d}{dt_m} (\rho_m V_m v_m) = n_1^2 \, n_2 \frac{d}{dt_p} (\rho_p V_p v_p) \tag{15}$$

The time rate of change of momentum for the prototype must follow Equation 15. If the mass remains constant then

$$\frac{d}{dt} (\rho V) = 0$$

and

$$\rho_m V_m \frac{dv_m}{dt_m} = n_1^2 n_2 \rho_p V_p \frac{dv_p}{dt_p} \tag{16}$$

And if we designate $\frac{dv}{dt}$ as acceleration a, then from Equation 16

$$\frac{a_m}{a_p} = n_1^2 n_2 \frac{\rho_p}{\rho_m} \frac{V_p}{V_m} = n_1^2 n_2 n_3^{-1} n_1^{-3}$$

or by combining terms the acceleration ratio becomes

$$\frac{a_m}{a_p} = n_1^{-1} n_2 n_3^{-1} \tag{17}$$

This is an expected result when considering just the vibrating beam. From Equation 5a

$$\rho_m g_m = n_1^{-1} n_2 \rho_p g_p$$

Treating the g terms as acceleration terms and dividing by ρ_m the results of Equation 17 are readily found from Equation 5a above.

If, however, the mass term is varying and the velocity remains constant, $\frac{dv}{dt} = 0$ then Equation 15 becomes

$$v_m \frac{d}{dt_m} (\rho_m V_m) = n_1^2 n_2 v_p \frac{d}{dt_p} (\rho_p V_p) \tag{18}$$

This describes the modeling for a system losing mass while maintining a constant velocity, and for launch vehicles this does not have much application.

Most useful form of the equation for external forces on a rocket due to change of momentum is given by Equation 15 and the modeling laws can be applied to it in many forms.

4.5 Loads From Fluids

From the study of fluid mechanics we obtain a list of variables describing the physical quantities of gases. Not considering, at this time, temperature effects the several variables are listed in Table 4.1 using the engineering units and basic units.

Table 4.1 Quantities and Dimensions for Fluids

Quantity	Symbol	Engineering Units	Basic Units
Force	P	F	MLT^{-2}
Length	ℓ	L	L
Velocity	v	LT^{-1}	LT^{-1}
Unit Mass Density	ρ	$FL^{-4}T^{2}$	ML^{-3}
Dynamic Coefficient of viscosity	μ	$FL^{-2}T$	$ML^{-1}T^{-1}$
Acceleration of Gravity	g	LT^{-2}	LT^{-2}
Speed of Sound	c	LT^{-1}	LT^{-1}
Surface Tension	σ*	FL^{-1}	MT^{-2}

Nondimensional numbers have been created by combining the quantities in Table 4.1. Similitude is achieved when the nondimensional number has the same numerical value for the model and the prototype. See Ref. 3.6 for further discussion.

For fluid simulation where viscosity is important the Reynolds' Number is scaled so that

$$\frac{v_m \ell_m \rho_m}{\mu_m} = \frac{v_p \ell_p \rho_p}{\mu_p} \tag{18}$$

Any combination of model velocity, length fluid density and kinematic viscosity that produces the same value as the prototype quantity satisfies this scaling requirement.

To scale the resulting forces from fluid flow such as drag force the pressure coefficient relates force P to density, velocity and length so that

$$\frac{P_m}{\rho_m v_m^2 \ell_m^2} = \frac{P_p}{\rho_p v_p^2 \ell_p^2} \tag{19}$$

Drag forces can be separated into two components, one due to viscosity (Reynolds' Number) and the other due to gravity. To

*Not to be confused with stress in Table 3.1.

scale for gravity the Froude Number requires that

$$\frac{v_m^2}{\ell_m g_m} = \frac{v_p^2}{\ell_p g_p} \tag{20}$$

When considering the effects of velocity in the sonic region or supersonic regime the Mach Number is given by

$$\frac{v_m}{c_m} = \frac{v_p}{c_p} \tag{21}$$

For those fluids or scaling situations where surface tension effects are important then Weber's Number defines a similitude requirement. To satisfy this requirement

$$\frac{\rho_m v_m^2 \ell_m}{\sigma_m} = \frac{\rho_p v_p^2 \ell_p}{\sigma_p} \tag{22}$$

Although arbitrary scale factors such as ℓ_m / ℓ_p have not been defined for this section they can be applied in the same manner as for structures. Some of the forces P were not defined in the previous sections. In a launch vehicle these loads can come from many sources. When they occur as a result of actions between a structure and a fluid then considering the three basic dimensions of mass, length and time and by consistently modeling so that an arbitrary but unique relation exists

$$L_m = n_1^a \, n_2^b \, n_3^c \, L_p$$

$$M_m = n_1^d \, n_2^e \, n_3^f \, M_p$$

$$T_m = n_1^g \, n_2^h \, n_3^i \, T_p$$

and applying it to all physical quantities the model will give information regarding the prototype.

4.6 Temperature Scaling

When the temperature, or the quantity of heat, becomes a consideration for a prototype structure then other modeling laws and dimensions are necessary. The mechanical equivalent of heat

and energy establishes that a quantity of heat has the dimensions of work FL in engineering units and ML^2T^{-2} in basic units. Another dimension, temperature θ, and other definitions are introduced to express these physical quantities. These are given in Table 4.2

Table 4.2 Quantities and Dimensions of Thermal Quantities

Quantity	Symbol	Engineering Units	Basic Units
Temperature	θ	θ	θ
Heat Transfer Coefficient	h	$FL^{-1}T^{-1}\theta^{-1}$	$MT^{-3}\theta^{-1}$
Coefficient of Thermal Conduction	k*	$FT^{-1}\theta^{-1}$	$MLT^{-3}\theta^{-1}$
Specific Heat	C	$L^2T^{-2}\theta^{-1}$	$L^2T^{-2}\theta^{-1}$
Coefficient of Thermal Exp.	β	θ^{-1}	θ^{-1}

Several scaling numbers have become associated with heat transfer in gases. By using terms identified in Table 4.1 in combination with the thermal quantities in Table 4.2 we have from Ref. 3.6

$$\text{Grashof's Number} = \frac{\beta\theta g \ell^3 \rho^2}{\mu^2} \tag{23}$$

$$\text{Nusselt's Number} = \frac{h\ell}{k} \tag{24}$$

$$\text{Praudtl's Number} = \frac{C\mu}{k} \tag{25}$$

$$\text{No Name} = \frac{k\theta}{\rho v^3 \ell} \tag{26}$$

Another dimension, temperature θ, is introduced and is treated the same as length, mass, or time. The technique of scaling established for mechanical systems is simply extended from three dimensions to four dimensions.

*k not to be confused with form factor k of kAG.

4.7 Nonlinear Effects of Structures

Materials that are used to construct real structures and model structures can and do exhibit nonlinear behaviors. Some of the nonlinearities are exhibited by elastic and plastic behavior, strain-rate sensititivity, damping characteristics, and other phenomena observable on a macroscopic scale or in a microscopic snese. Generally when displacements are small compared to the least dimension of a structure, when frequencies are low, and when thermal effects are negligible, the nonlinearities are not important.

For those cases where nonlinearities are important scaling is still possible if the nondimensionalized response of the materials used for model and prototype can be plotted as the same curve. For example, when the nondimensional stress strain curves for model and prototype are the same curves, then the deflections of the model will scale as the length scale ratio, the forces will be changed by the length scale ratio squared, and the moments will be affected as the length scale cubed.

The most important aspect of scaling is that a physical phenomena is not dependent on the numerical magnitude used to describe it. Physical laws when considered nondimensionally to relate model and prototype are the same physical laws and are not affected by size or dimension, all important physical quantities being considered.

5. SCALING OF SHELL STRUCTURES

Shells used for launch vehicle structures may be monocoque construction of isotropic materials, orthotropic construction of isotropic materials, orthotropic construction of composite materials, or anisotropic construction of composite materials. Scaling for shell structures will be limited to isotropic materials, e.g. aluminum, titanium, magnesium and either monocoque (no stiffening) or orthotropic (stiffeners, rings) construction. Composite material or sandwich construction will not be considered although the scaling requirements are based on the same principles used for isotropic materials.

Shell theory assumes the shell material to be an artificial substance with three moduli having infinite values and two Poisson ratios equal to zero. Using the coordinate system in Fig. 5.1 the several assumptions are given in Equation 1.

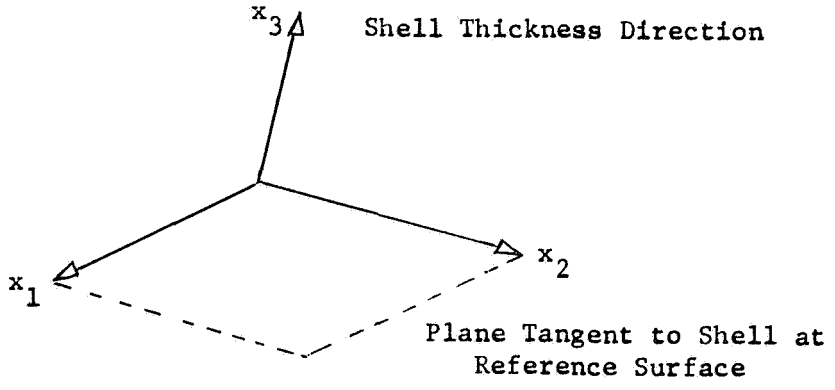

Fig. 5.1 Coordinate System for Shell Material

Using the directions identified in Fig. 5.1, the Hooke's law for shell materials takes the form

$$\sigma_{11} = E_1\varepsilon_1 + E_2\nu_{21}\varepsilon_2 \qquad (1)$$

$$\sigma_{22} = E_1\nu_{12}\varepsilon_1 + E_2\varepsilon_2$$

$$\sigma_{33} = 0$$

$$\tau_{23} = 0$$

$$\tau_{31} = 0$$

$$\tau_{12} = G_{12}\gamma_{12}$$

This form of Hooke's law arises from the assumptions that

$$E_3 = G_{13} = G_{23} \rightarrow \infty \qquad (2)$$

$$\nu_{13} = \nu_{23} = 0$$

$$\varepsilon_3 = \gamma_{31} = \gamma_{23} = 0$$

These assumed values occur from the several hypothesis made regarding shell behavior such as normals remaining normal, no changes in shell wall thickness, small displacements, and thin shells.

Although no material exists for which these assumptions are valid most materials used for shell construction approximate, sufficiently closely, this behavior. Model material for model shells made of materials other than used for the prototype may not be satisfactory if their properties are too different when compared to these assumptions. When approximating the shell as a beam with a hollow circular cross section, these considerations are unnecessary. When studying shell behavior these assumptions are required for tractable analytical solutions. Comparisons between experiment and theory are valid when both the test and the analysis use the same rules for material behavior.

5.1 Monocoque Shells

Dynamic scaling requires consideration of the three basic quantities of physical systems, mass, length, and time. These may be converted to the engineering units of force, length, and time. From previous developments (See Chapter 3) the three arbitrary scale factors will be chosen as

$$n_1 = \frac{\ell_m}{\ell_p} \qquad (3a)$$

$$n_2 = \frac{E_m}{E_p} \tag{3b}$$

$$n_3 = \frac{\rho_m}{\rho_p} \tag{3c}$$

From Equation 3 the engineering units of length (L), force (F), and time (T) are modeled by using

$$L_m = n_1 L_p \tag{4a}$$

$$F_m = n_1^2 \, n_2 \, F_p \tag{4b}$$

$$T_m = n_1 \, n_2^{1/2} \, n_3^{-1/2} \, T_p \tag{4c}$$

Free vibrations of shells are associated with a circular frequency ω, the dependent variable. Shell properties, material properties, and external loads are independent variables. Symbols and dimensions for these quantities are given in Table 3.1. A functional relationship can be written such that

$$\omega = f(R, \ell, h, \rho g, E, \nu, D, K, P, M, q) \tag{5}$$

A set of π terms for these variables can be established as shown below. The dependent variable ω is given by π_1 and the independent variables follow from π_2 on.

$$\pi_1 = \omega \ell \sqrt{\frac{\rho}{E}} \tag{6}$$

For the independent factors from Equation 5 and recalling that ℓ, E, and ρ have been chosen to define arbitrary scale factors given by Equations 3 the remaining terms are

$$\pi_2 = \frac{R}{\ell} \tag{7a}$$

$$\pi_3 = \frac{h}{R} \tag{7b}$$

$$\pi_4 = \rho g \frac{\ell}{E} \tag{7c}$$

$$\pi_5 = 1, \ \nu_m = \nu_p \tag{7d}$$

$$\pi_6 = \frac{D}{\rho g R^4} \tag{7e}$$

$$\pi_7 = \frac{K}{\rho g R^2} \tag{7f}$$

$$\pi_8 = \frac{P}{E \ell^2} \tag{7g}$$

$$\pi_9 = \frac{M}{E \ell^3} \tag{7h}$$

$$\pi_{10} = \frac{q}{E} \tag{7i}$$

Similitude requirements for Equations 7 to provide the equality of model and prototype π terms can be expressed as

$$\pi_{2m} = \pi_{2p} \tag{8}$$

$$\pi_{3m} = \pi_{3p}$$

$$\vdots \qquad \vdots$$

$$\pi_{10m} = \pi_{10p}$$

From the dimesnions of Table 3.1 and the relations expressed in Equations 4 the model dimensions become from Equations 7a and 7b

$$R_m = n_1 R_p \tag{9a}$$

$$h_m = n_1 h_p \tag{9b}$$

Model material properties and gravity requirements are found from Equations 7c and 7d

$$g_m = n_1^{-1}\, n_2\, n_3^{-1}\, g_p \qquad (9c)$$

$$\nu_m = \nu_p \qquad (9d)$$

Bending rigidity D and extensional rigidity K are scaled as follows

$$D_m = n_1^{3}\, n_2\, D_p \qquad (9e)$$

$$K_m = n_1\, n_2\, K_p \qquad (9f)$$

External loads, moments, and pressures and internal loads, moments, and pressures are scaled for the model from corresponding prototype quantities by

$$P_m = n_1^{2}\, n_2\, P_p \qquad (9g)$$

$$M_m = n_1^{3}\, n_2\, M_p \qquad (9h)$$

$$q_m = n_2\, q_p \qquad (9i)$$

Equations 9a to 9i provide a working set of model requirements to find the dynamic response of a shell structure. If Equation 9b model thickness is scaled, then Equations 9e and 9f are satisfied when modeling with similar materials. If the structure is unloaded or lightly loaded, its mass becomes important and π_4 (Eq. 9c) must be considered. Masses other than the structural mass that respond as the basic structure responds must also be scaled by making $\pi_{4m} = \pi_{4p}$.

Applied loads, shears, moments, torques and pressures are made correct for the model by considering the modeling requirements imposed by Equations 9g, 9h and 9i.

Nonlinearities known to exist in the prototype can be scaled into the model if the corresponding curves describing these nonlinearities, when drawn nondimensionally, are the same curve. An example of this is the elastic-plastic behavior shown by the stress-strain curve of a prototype material. If the nondimensional stress-strain curves for the modeling material and prototype material are the same curve then the model will respond in a scaled manner and will provide information about prototype response.

From π_1 of Equation 6 the dependent variable of interest becomes for the model a frequency realted to the prototype by

$$\omega_m = n_1^{-1} n_2^{1/2} n_3^{-1/2} \omega_p \tag{10}$$

For models made of the same material as the full scale structure ($n_2 = n_3 = 1$) the frequency relation is

$$\omega_m = n_1^{-1} \omega_p$$

For dissimilar materials the terms n_2 and n_3 for modulus and mass density affect the model response. Equation 10 applies only if the important modeling requirements outlined by Equation 9 are fulfilled.

5.2 Stiffened Shells

Many launch vehicles are made of stiffened shells with stringers running longitudinally. Combinations of rings and stringers are also used and in some cases rings alone may be used. Frequency response given by Equation 10 applies to the stiffened shell when all π terms are scaled by Equation 9. For replica modeling the rigidity terms K and D are properly scaled.

When replica modeling is not used, extensional and bending rigidities can be scaled. Expressions for these rigidities for stiffened shells are given in Table 5. When made nondimensional by π_6 and π_7 and made equal for model and prototype, then stiffnesses are scaled. Other variables must also be scaled as required.

In Table 5.1 subscripts x and ϕ refer to axial and circumferential directions respectively. Spacing of stiffening members is given by b_1 measured in the axial direction and b_2 measured circumferentially. Distance of the stiffener center of gravity from the reference surface (given by R) is given as dimension c. All other terms are as defined in Table 3.1.

Table 5.1 Stiffened Shell Rigidities

Rigidity	Engineering Dimensions	Stiffened Shells			Unstiffened Shells	
		Symbol	Ring and Stringer	Skin-Stringer	Symbol	Monocoque
Extensional	lb/in	K_ϕ	$\frac{Eh}{1-\nu^2} + \frac{EA_\phi}{b_1}$	$\frac{Eh}{1-\nu^2}$	K	$\frac{Eh}{1-\nu^2}$
	(FL^{-1})	K_x	$\frac{Eh}{1-\nu^2} + \frac{EA_x}{b_2}$	$\frac{Eh}{1-\nu^2} + \frac{EA_x}{b_2}$		
		K_ν	$\frac{Eh\nu}{1-\nu^2}$	$\frac{Eh\nu}{1-\nu^2}$		
		$K_{x\phi}$	$\frac{Eh}{2(1+\nu)}$	$\frac{Eh}{2(1+\nu)}$	Gh	$\frac{Eh}{2(1+\nu)}$
Bending	in-lb	D_ϕ	$\frac{Eh^3}{12(1-\nu^2)} + \frac{E(I_\phi + A_\phi c_\phi^2)}{b_1}$	$\frac{Eh^3}{12(1-\nu^2)}$	D	$\frac{Eh^3}{12(1-\nu^2)}$
	(FL)	D_x	$\frac{Eh^3}{12(1-\nu^2)} + E\frac{(I_x + A_x c_x^2)}{b_2}$	$\frac{Eh^3}{12(1-\nu^2)} + E\frac{(I_x + A_x c_x^2)}{b_2}$		
		D_ν	$\frac{Eh^3\nu}{12(1-\nu^2)}$	$\frac{Eh^3\nu}{12(1-\nu^2)}$		

Table 5.1 Stiffened Shell Rigidities (Continued)

Rigidity	Engineering Dimensions	Stiffened Shells			Unstiffened Shells	
		Symbol	Ring and Stringer	Skin-Stringer	Symbol	Monocoque
Bending	in-lb	$D_{\phi x}$	$\frac{Eh^3}{12(1+\nu)} + \frac{GJ_\phi}{B_1}$	$\frac{Eh^3}{12(1+\nu)}$		
	(FL)	$D_{x\phi}$	$\frac{Eh^3}{12(1+\nu)} + \frac{GJ_x}{b_2}$	$\frac{Eh^3}{12(1+\nu)} + \frac{GJ_x}{b_2}$		

6. SCALING OF LIQUID PROPELLANTS

The dynamic behavior of launch vehicle liquid propellants is of considerable interest. At lift-off the propellants may comprise as much as 90% of the vehicle mass. The free surface of these propellants has a strong tendency to undergo large amplitude motion due to excitations caused by the flight environment. Lateral accelerations arising from control surface deflections may contribute to these motions.

With the development of large launch vehicles it has become difficult to provide adequate separation of slosh frequencies, control system frequencies and vehicle elastic frequencies. Knowledge of the dynamic slosh characteristics, including the coupled slosh-structural characteristics (e.g., the well known POGO phenomonon) is of vital importance to loads and stability studies. An excellent treatment of the dynamic behavior of liquids in moving containers can be found in Reference 6.1.

Scale models can be used to study lateral sloshing, coupled elastic-liquid oscillations. viscosity effects, compressibility effects, cavitational and surface tension effects. Typically, any model is designed for the simulation of some (but not all) of these phenomena.

A general dimensional analysis of liquid sloshing phenomenon is developed (Section 6.1) for rigid and elastic tanks. Special limitations on several types of dynamic simulation of liquids are established (Section 6.2) and the results are presented in graphical form. These graphs may be used by the analyst to establish the overall simulation limitations if two or more liquid effects are considered simultaneously. The results of Section 6.2 are an extension of the results of Reference 6.1.

6.1 Simulation of Lateral Propellant Sloshing

The investigation of the sloshing motions of liquid propellants in partially filled tanks is of importance to a complete dynamic analysis. If the slosh frequency is considerably below the fundamental structural frequency, slosh modes will couple with the flight control system and may produce instability. Slosh frequencies approximately equal to structural frequencies may cause considerable elastic-slosh coupling. Correct simulation of these coupled modes is essential to accurate loads and stability studies.

Slosh modes can be suppressed to some extent through the use of mechanical devices (e.g., baffles as discussed in Ref 6.2). It is

important to evaluate these devices through analysis or test. A mathematical approach is often not feasible due to the complexity of the boundary conditions introduced by the suppressing devices. However, the investigation of the problem through the use of suitably designed model experiments (Ref 6.3 and 6.4) is feasible.

Simulation of slosh modes can be investigated for two general conditions: uncoupled and coupled with elastic modes. The uncoupled case can be considered when tank construction is such that the tank stiffness gives rise to structural frequencies which are not in close proximity to the lowest uncoupled slosh frequencies. On the other hand, there are many instances where the coupling of liquid modes and elastic tank modes becomes significant due to the proximity of the uncoupled natural frequencies.

The important bending frequencies of current launch vehicles are usually less than 5 Hz and, as the important liquid surface modes in cylindrical tanks also occur at low frequency, coupling between the respective modes is likely. One of the few investigators to have considered this phenomenon is Miles (Ref 6.5). This author developed the equations of motion for a circular cylindrical tank using a Lagrangian formulation and established the frequency equation in terms of uncoupled bending and sloshing frequencies and coupling coefficients. It was concluded that the liquid effects are only significant in those cases where the sloshing mass is a appreciable fraction of total mass. For typical launch vehicle structures the sloshing mass can be omitted from the calculation of bending frequencies and rigid-tank sloshing frequencies can be used in the determination of the tank bending characteristics. Results of an experimental investigation to confirm the analysis of Reference 6.5 are presented in Reference 6.6.

A considerable amount of investigation has been devoted to the coupling of propellant motions with elastic tank breathing vibrations (e.g., Ref 6.7 and 6.8). An extensive summary discussion of these efforts is presented in Reference 6.1.

6.1.1 Uncoupled Propellant Sloshing

The analysis of uncoupled lateral sloshing is based upon the following assumptions:

a. Constant longitudinal acceleration,

b. Sloshing arises from small amplitude excitations caused by either translational or rotational accelerations acting normal to the flight path,

c. Surface tension forces are negligible when compared to inertial and viscous forces,

d. Forces due to gas pressure are negligible,

e. Geometrical similarity between model and prototype.

Translational Excitation

A typical propellant tank subject to translational excitation is shown in Figure 6.1.

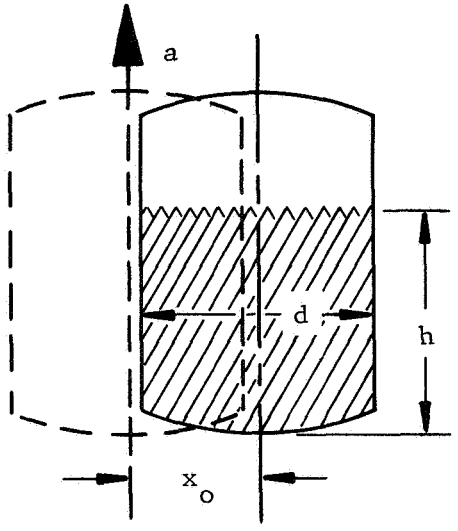

Figure 6.1 Translational Excitation of Propellant Tank

The resultant liquid force on the tank walls, expressed in functional form, is

$$R = f(a, \ell, \lambda, \mu, \tau, \rho)$$

where R = resultant liquid force on tank wall, F

a = longitudinal acceleration, L/T^2

ℓ = characteristic length, L

λ = any length (e.g., tank diameter (d), liquid depth (h), excitation amplitude (x_o)), L

μ = liquid viscosity, FT/L^2

ρ = liquid density, FT^2/L^4

τ = excitation period, T.

Application of the dimensional analysis techniques of Chapter 3 yields four scaling parameters. These parameters are

$$\pi_1 = R\tau^2/\rho\ell^4, \qquad \pi_2 = a\tau^2/\ell,$$

$$\pi_3 = \rho\ell^2/\mu\tau \quad \text{and} \quad \pi_4 = \lambda/\ell.$$

The π_2 term is equivalent to the Froude Number and the π_3 term is equivalent to the Reynolds Number. Complete dimensional similarity is dictated by π_4 where the parameter λ may be replaced by any desired physical dimension.

If the analysis is developed using the resulting liquid pressure P as the dependent variable, the π_1 term becomes

$$\pi_1 = P\tau^2/\rho\ell^2$$

which is a form of the Euler Number. The other non-dimensional terms are unchanged.

Rotational Excitation

The analysis is similar to that for translational excitation. The accelerations are determined by the location of the rotational axis and the amplitude of excitation.

The functional relationship becomes

$$M = f(a, \ell, \lambda, \mu, \rho, \tau, \theta_o)$$

where M = moment due to liquid pressure, F/L

λ = any length (including location of rotational axis (b)), L

θ_o = excitation amplitude,

and the other variables are as defined previously.

The five non-dimensional scaling relations are

$$\pi_1 = M\tau^2/\rho\ell^3, \qquad \pi_2 = a\tau^2/\ell, \qquad \pi_3 = \rho\ell^2/\mu\tau,$$

$$\pi_4 = \lambda/\ell \qquad \text{and} \qquad \pi_5 = \theta_o.$$

As previously, π_2 is equivalent to the Froude Number and π_3 is equivalent to the Reynolds Number. Dimensional similarity is dictated by π_4. Similarity of excitation amplitude follows from π_5.

The scaling relations for translational and rotational excitation can be examined for two conditions:

a. Viscosity Neglected

If viscous fluid forces are assumed to be negligible, the π_3 term becomes insignificant and the non-dimensional scaling relationship developed previously can be expressed as

$$\lambda_m/\lambda_p = \ell_m/\ell_p = n,$$

$$a_m/a_p = n(\tau_p/\tau_m)^2,$$

$$R_m/R_p = n^3(\rho_m/\rho_p)(a_m/a_p),$$

$$P_m/P_p = n(\rho_m/\rho_p)(a_m/a_p),$$

$$M_m/M_p = n^2(\rho_m/\rho_p)(a_m/a_p),$$

$$\text{and} \qquad \theta_{o_m} = \theta_{o_p}$$

where the subscripts m and p refer to model and prototype, respectively.

The first relation defines the geometric scale factor. The second indicates that any prototype acceleration can be simulated in a 1-g test environment through a time scale adjustment. The model-to-prototype frequency ratio, established by π_2, is

$$\omega_m/\omega_p = [(a_m/a_p)/n]^{1/2}.$$

The expressions for force, pressure and moment indicate that the prototype fluid relations can be established following selection of the model fluid.

b. Viscosity Included

The scaling relations are identical to those presented above. In addition, the π_3 term must be satisfied. This relation can be written as

$$n = (\nu_m/\nu_p)^{2/3}(a_p/a_m)^{1/3}$$

where $\nu = \mu/\rho$ is the liquid kinematic viscosity, L^2/T.

This expression indicates that the length scale factor, n, is affected by both the density and viscosity of the model fluid. In order to investigate prototype accelerations at scale factors different from unity, the modeling liquid must have different properties than the prototype liquid.

6.1.2 Elastically Coupled Propellant Sloshing

The analysis of elastically coupled propellant sloshing is based upon the assumptions (a) through (e) of Section 6.1.1 but the complexity of the problem is magnified as the elastic structural tank properties must now be considered. The resultant liquid force acting on the tank walls, expressed as a function of the independent variables, is

$$R = f(a, \ell, \lambda, \nu, \nu', \nu_b', GJ, K_x, B_{xy}, B_z, EI, \tau)$$

where R = resultant liquid force on tank wall, F

a = longitudinal acceleration, L/T^2

ℓ = characteristic length, L

λ = any length (e.g., tank diameter (d), liquid depth (h), excitation amplitude (x_o)), L

ν = liquid kinematic viscosity, L^2/T

ν' = Poisson's ratio,

ν_b' = Poisson's ratio for bending,

GJ = tank torsional stiffness, FL^2

K_x = tank extensional stiffness, F/L

B_{xy} = tank in-plane shear stiffness, F/L

B_z = tank transverse shear stiffness, F/L

EI = tank bending stiffness, FL^2

τ = excitation period, T.

The non-dimensional scaling parameters, developed in accordance with the techniques established in Chapter 3, are

$$\pi_1 = R\nu^2 \tau^2/\ell^2 EI, \qquad \pi_2 = a\tau^2/\ell, \qquad \pi_3 = \lambda/\ell,$$

$$\pi_4 = K_x \ell^3/EI, \qquad \pi_5 = \nu\tau/\ell^2, \qquad \pi_6 = \nu',$$

$$\pi_7 = \nu_b', \qquad \pi_8 = GJ/EI, \qquad \pi_9 = B_z/K_x,$$

$$\text{and} \quad \pi_{10} = B_{xy}/K_x.$$

Note that π_2, π_3 and π_6 are similar to the scaling terms derived for uncoupled propellant sloshing.

These scaling relations can be examined for two conditions:

a. Viscosity Neglected

If viscous fluid forces are assumed to be negligible the scaling relations which are dependent upon the length scale factor become

$$\lambda_m/\lambda_p = \ell_m/\ell_p = n,$$

$$a_m/a_p = n(\tau_p/\tau_m)^2,$$

and $$(K_x/EI)_m/(K_x/EI)_p = 1/n^3.$$

The first of these defines the model-to-prototype scale factor. The second indicates that any prototype acceleration can be simulated with an appropriate time scale. The frequency ratio, established by this expression is

$$\omega_m/\omega_p = [(a_m/a_p)/n]^{1/2}.$$

Other scaling relationships, derived from π_4, π_8, π_9 and π_{10}, are

$$(B_{xy}/EI)_m/(B_{xy}/EI)_p = 1/n^3,$$

$$(B_z/EI)_m/(B_z/EI)_p = 1/n^3,$$

$$(K_x/GJ)_m/(K_x/GJ)_p = 1/n^3.$$

The similarity requirements imposed by these other scaling equalities may be difficult to maintain when small scale models are fabricated. The inaccuracy of scaled skin thicknessess, due primarily to tolerance limitations, may cause significant deviations in these parameters.

b. Viscosity Included

Additional scaling relationships arise if viscous fluid forces are considered. The expression developed from π_5 is

$$n = (\nu_m/\nu_p)^{2/3} (a_p/a_m)^{1/3},$$

which is identical to the scaling relationship of Section 6.1.1. The expression for fluid forces,

$$R_m/R_p = [(EI)_m/(EI)_p]/n^2,$$

is established by π_1 and the above relation.

6.2 General Limitations on Liquid Scaling

Density simulation or the scaling of slosh effects in a rigid, uncoupled tank (Section 6.1.1) presents no difficulties. Scaling of liquid propellants to other conditions may impose limitations on physically feasible models. Typical scaling requirements include gravitational-viscosity scaling, gravitational-compressibility scaling, gravitational-cavitation scaling and gravitational-surface tension scaling.

The non-dimensional scaling relations for each of the above cases can be established through examination of the functional relationship

$$f(\Delta P,\ \ell,\ a,\ \nu,\ c,\ \rho,\ r,\ \sigma/g,\ \theta) = 0$$

where $\Delta P = P_{gas} - P_{vapor}$ (P_{gas} = gas pressure above liquid, P_{vapor} = vapor pressure of liquid), F/L^2

ℓ = characteristic length, L

a = longitudinal tank acceleration, L/T^2

ν = liquid kinematic viscosity, L^2/T

c = velocity of sound in liquid, L/T

ρ = liquid density, FT^2/L^4

r = radius of meniscus in equivalent capillary tube, L

σ = liquid gas surface tension, F/L

g = acceleration of gravity, L/T^2

θ = contact angle between liquid and tank wall.

It is assumed that the solid-liquid and solid-gas interface effects are negligible.

Application of the dimensional analysis techniques of Chapter 3 yields six scaling parameters. These parameters are

$$\pi_1 = \ell^3 a/\nu^2, \qquad \pi_2 = c^2/a\ell, \qquad \pi_3 = \Delta P/\rho a\ell,$$

$$\pi_4 = r/\ell, \qquad \pi_5 = \rho g r^2/\sigma \quad \text{and} \quad \pi_6 = \theta.$$

The scaling requirements imposed by these parameters and the limitations on scaling of liquids in a rigid tank are discussed in Sections 6.2.1 through 6.2.5. Gravitational-density scaling of liquids in elastic tanks is discussed in Section 6.2.6.

6.2.1 Gravitational-Viscosity Scaling

The significant scaling parameter for gravitational-viscosity simulation is

$$\pi_1 = \ell^3 a/\nu^2.$$

A bar chart which compares the kinematic viscosities of typical propellents and possible model liquids is presented in Figure 6.2. The kinematic viscosities are shown for the temperature ranges which may be experienced during launch vehicle boost flight.

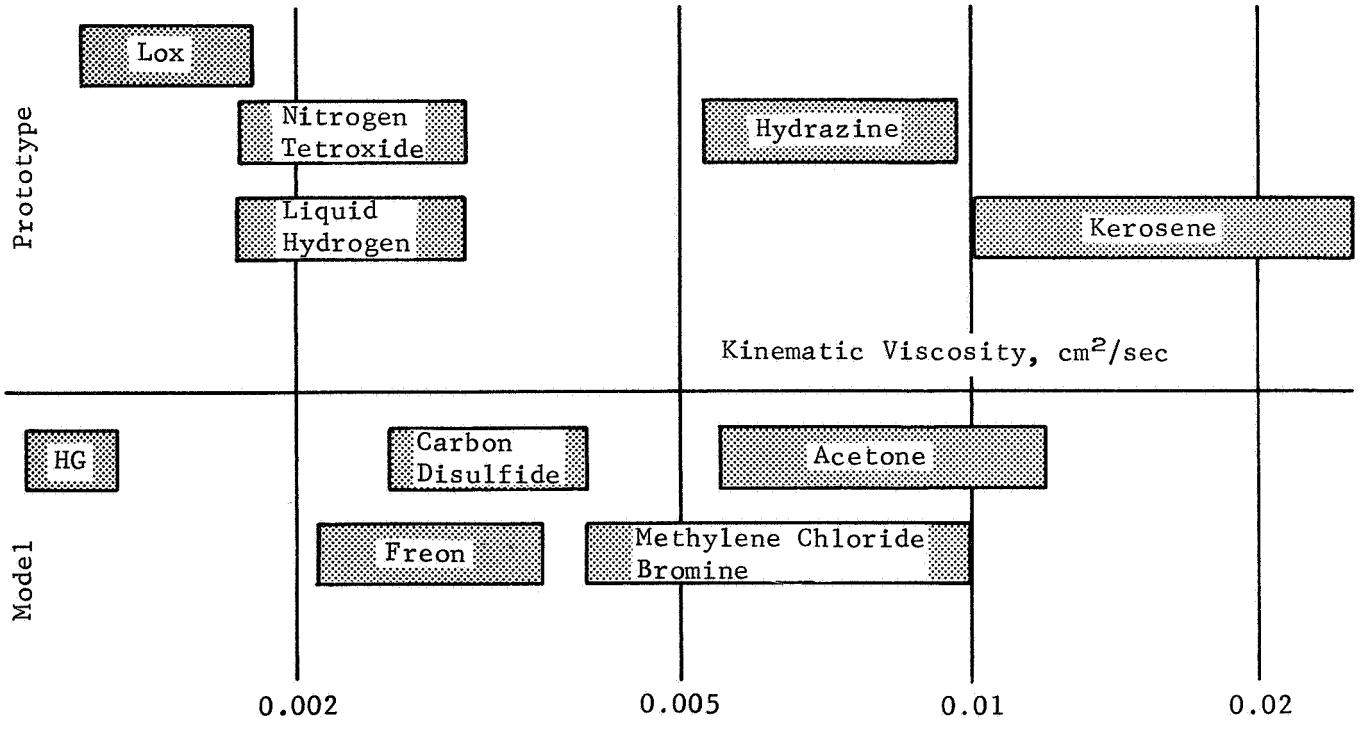

Figure 6.2 Kinematic Viscosity, Typical Missile Propellant and Model Liquids (Based on Fig. 5.4 and 5.5, Ref 6.1)

The required model-to-prototype scaling can be established from π_1. This scaling is

$$\ell_m{}^3 a_m / \nu_m{}^2 = \ell_p{}^3 a_p / \nu_p{}^2$$

or

$$\nu_r = (n^3 a_r)^{1/2}$$

where $\nu_r = \nu_m / \nu_p$, $n = \ell_m / \ell_p$, $a_r = a_m / a_p$

and the subscripts m and p refer to model and prototype, respectively.

The relation between the these parameters is presented in Figure 6.3.

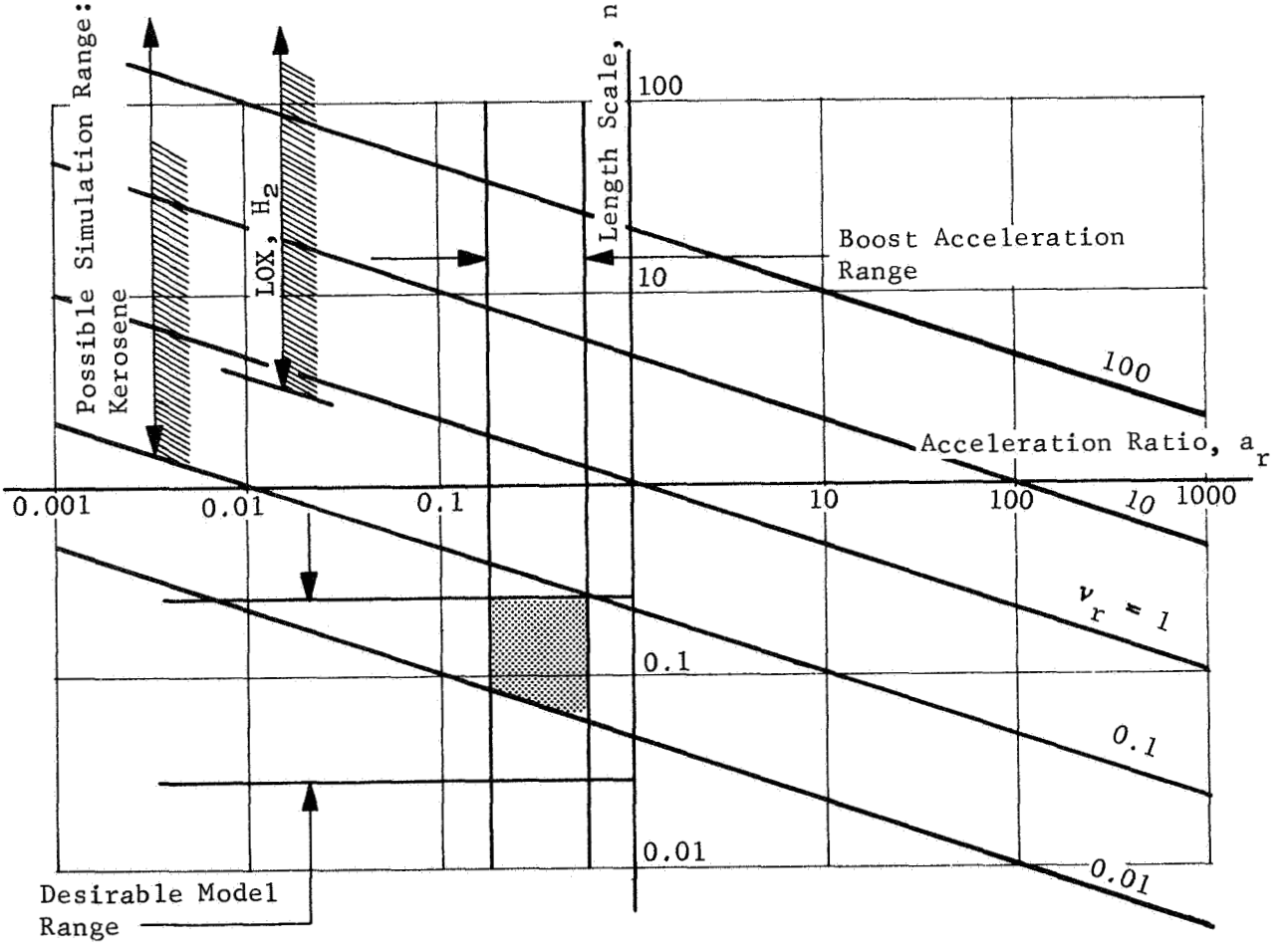

Figure 6.3 Simulation Chart: Gravitational-Viscosity Scaling (Based on Fig. 5.6, Ref 6.1)

The difficulty which arises if gravitational-viscosity simulation of cryogenic propellants is attempted becomes evident. The kinematic viscosity ratio must be approximately equal to or greater than unity which makes it virtually impossible to preserve the required scaling parameters, for typical boost acceleration ranges, with model scale factors less than unity.

6.2.2 Gravitational-Compressibility Scaling

The controlling scaling parameter for gravitational-compressibility scaling is

$$\pi_2 = c^2/a\ell.$$

The required model-to-prototype scaling condition, established by π_2, is

$$c_m^2/a_m\ell_m = c_p^2/a_p\ell_p$$

or

$$c_r = (na_r)^{1/2}$$

where $c_r = c_m/c_p$.

The relation between these three parameters is presented in Figure 6.4. As typical values of the sonic velocity ratio will lie in the range $1/4 < c_r < 4$, gravitational-compressibility propellant scaling for typical boost acceleration ranges is possible for a limited range of desirable model scale factors. The simulation of nitrogen tetroxide or LOX is difficult (at desirable scale factors) as the sonic velocity ratio, assuming the use of a common modeling liquid, will not be much less than unity.

6.2.3 Gravitational-Cavitation Scaling

The scaling parameter for gravitational-cavitation scaling is

$$\pi_3 = \Delta P/\rho a\ell.$$

This scaling requirement can be satisfied, for any length scale and prototype liquid, by adjusting the gas pressure (assuming that the absolute gas pressure is not determined by any other scaling parameter). The ratio $\Delta P/\rho$, for typical model liquids and an assumed model gas pressure of one atmosphere, will lie between 0.6 and 1.4. The required model-to-prototype scaling condition, established by π_3, is

$$(\Delta P/\rho)_m / a_m \ell_m = (\Delta P/\rho)_p / a_p \ell_p$$

or $$(\Delta P/\rho)_r = n a_r$$

where $$(\Delta P/\rho)_r = (\Delta P/\rho)_m / (\Delta P/\rho)_p .$$

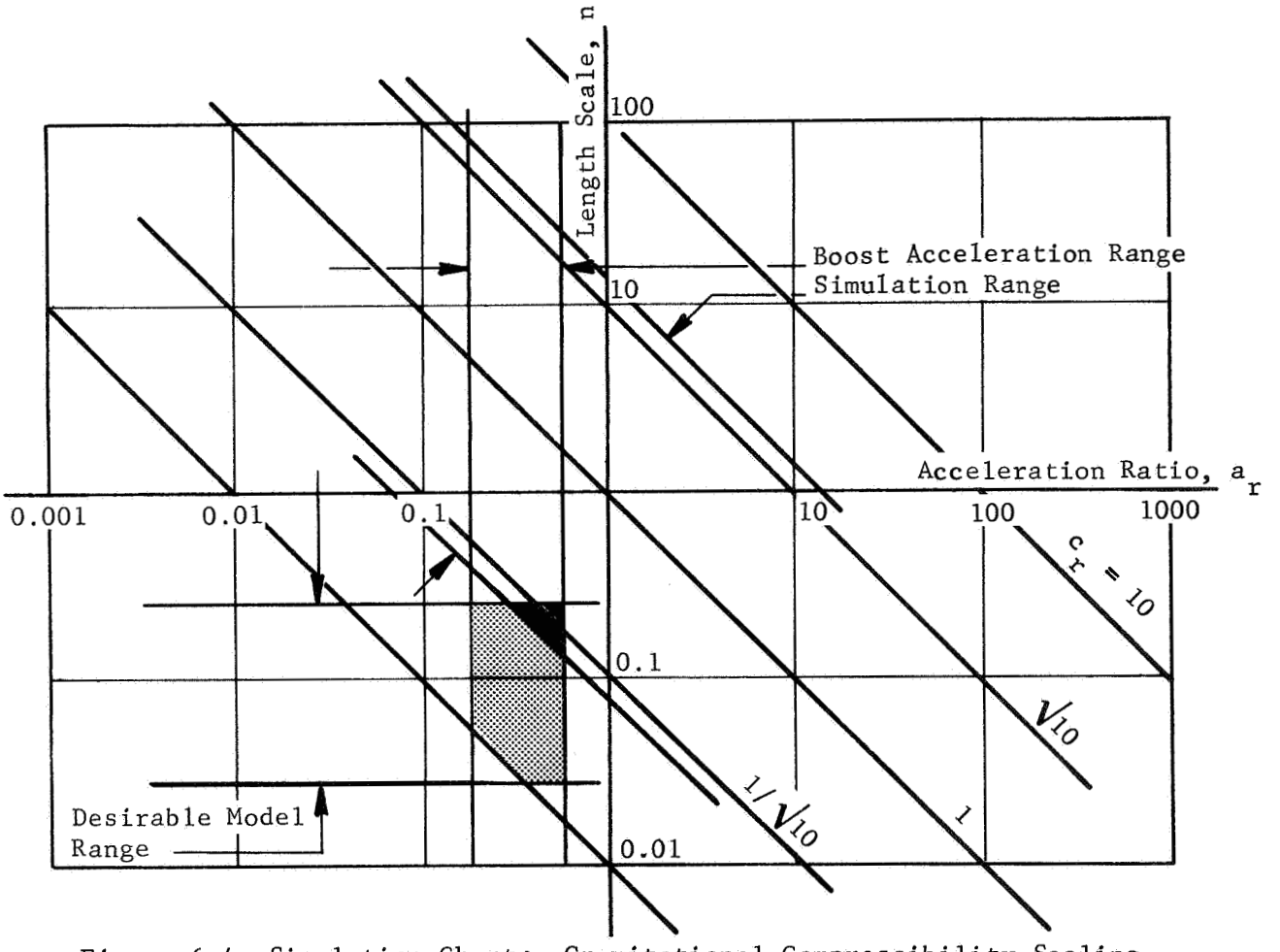

Figure 6.4 Simulation Chart: Gravitational-Compressibility Scaling
(Based on Fig. 5.7, Ref 6.1)

The relation between these three parameters is presented in Figure 6.5.

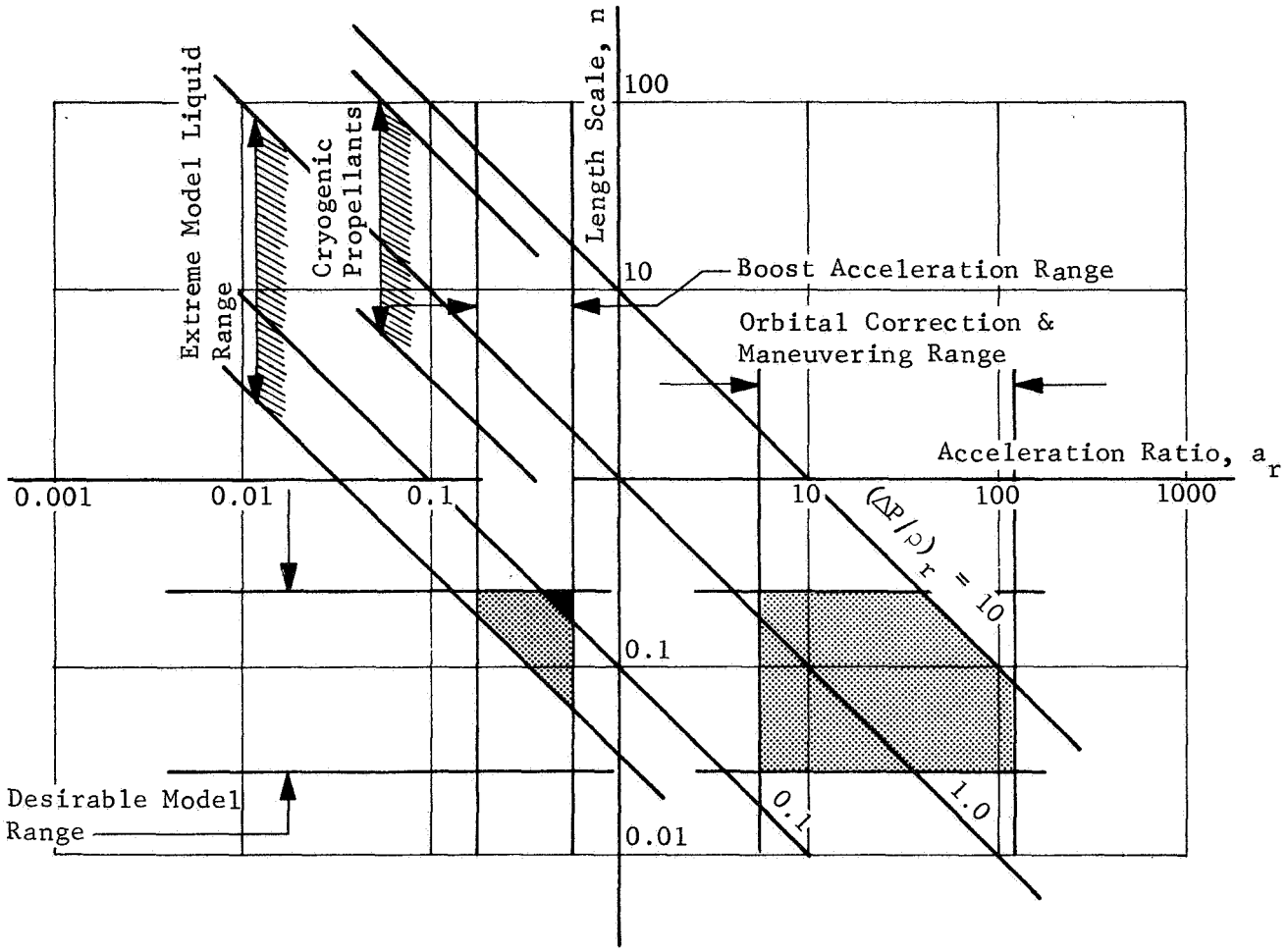

Figure 6.5 Simulation Chart: Gravitational-Cavitation Scaling (Based on Fig. 5.9, Ref 6.1)

Simulation (at atmospheric pressure) of a cryogenic prototype fluid or a fluid with a very high vapor pressure does not appear to be feasible for convenient model scale factors. Boost acceleration

simulation will require model gas pressures to be reduced below atmospheric. Gravitational-cavitation effects in a low-g environment can be simulated with small scale models and atmospheric gas pressures.

6.2.4 Gravitational-Surface Tension Scaling

Gravitational-surface tension scaling is controlled π_4, π_5 and π_6 of Section 6.2. π_5, a variation of the Bond Number, can be combined with π_4 to yield

$$\pi_5^* = \rho g \ell^2/\sigma.$$

The required model-to-prototype scaling, expressed in terms of the kinematic surface tension, $\phi = \sigma/\rho$, is,

$$g_m \ell_m^2/\phi_m = g_p \ell_p^2/\phi_p$$

or

$$\phi_r = n^2 a_r$$

where $\phi_r = \phi_m/\phi_p$ and $g_m/g_p = a_m/a_p = a_r$.

The relation between these parameters is presented in Figure 6.6. Velues of ϕ_r, for typical prototype propellants (e.g., kerosene, LOX) and model fluids will lie between 0.1 and 10. It is obvious that surface tension scaling with desirable size models at small acceleration ratios is not feasible. The simulation of low gravity surface tension effects is possible with small scale models in a 1-g test environment.

The scaling relation imposed by π_6,

$$\theta_m = \theta_p,$$

is probably insignificant for dynamic simulation as the contact angle influences interface area variations in the energy equations as cos θ. Nevertheless, this requirement eliminates the possibility of simulating a wetting fluid with a non-wetting fluid and vice versa.

The discussion of Sections 6.2.1 through 6.2.4 has been restricted to the simulation of inertial effects with any of four of the more important liquid effects. The results of these sections may be used concurrently if the analyst wishes to consider the simultaneous simulation of several of these effects.

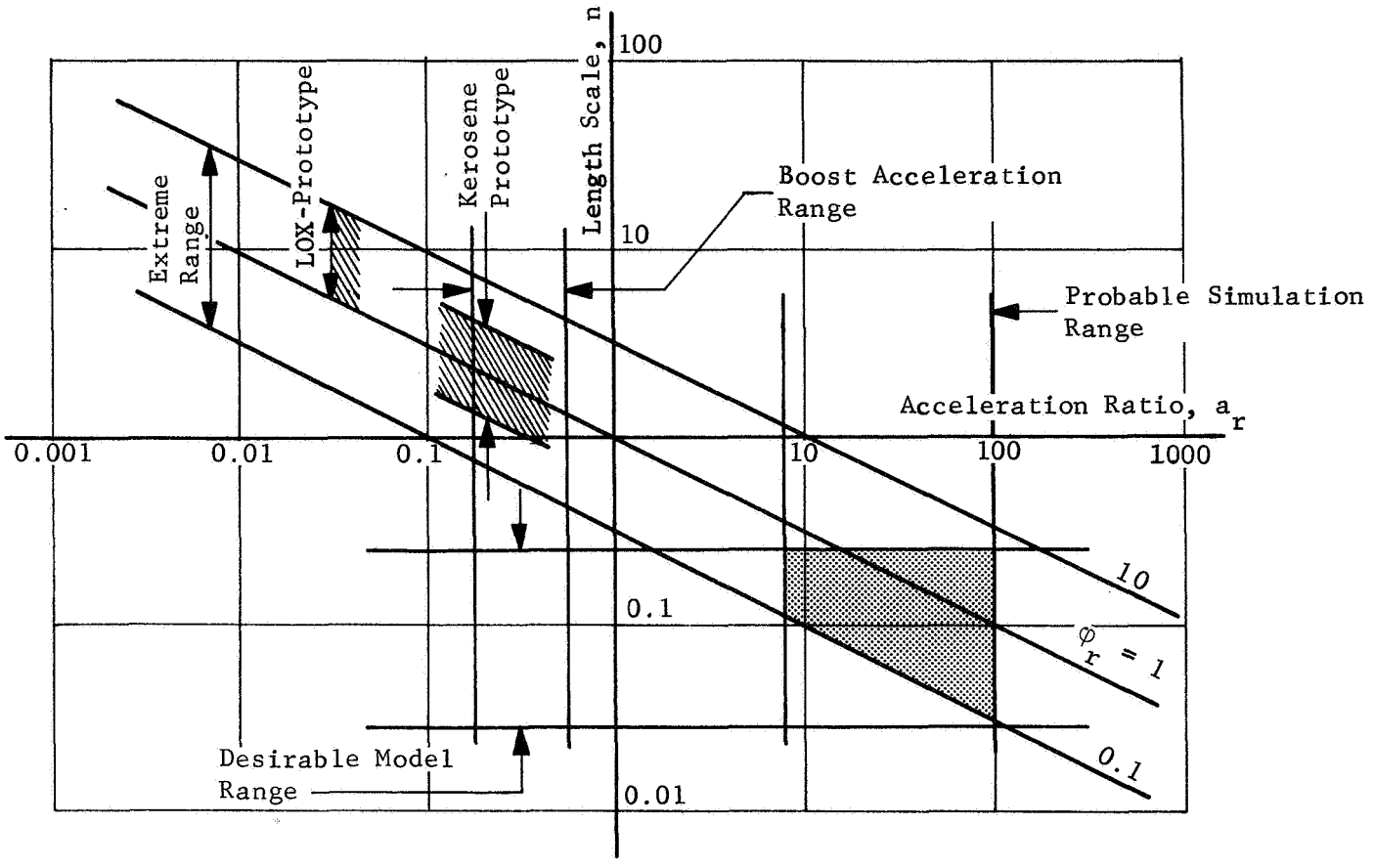

Figure 6.6 Simulation Chart: Gravitational-Surface Tension Scaling (Based on Fig. 5.10, Ref 6.1)

6.2.5 Relative Importance of Capillary and Gravitational Effects

The dynamic characteristics of a gas-liquid system may be influenced by several forces (e.g., viscous forces, capillary forces, body forces) but often all but one of these forces can be regarded as

negligible. The hydrodynamic behavior of the system can be separated into approximate regimes through examination of several dimensionless parameters.

The Weber Number, $We = \rho V^2 \ell/\sigma$, defines an estimate of the ratio of inertial to capillary forces. This parameter appears (in a slightly different form) in Section 6.2.4 as the non-dimensional scaling relation π_5*. Note that for We much greater than unity the capillary forces are insignificant. For We much less than unity the opposite is true.

The Froude Number, $Fr = V^2/g\ell$, relates the inertial forces to the body forces. It is evident that body forces play an important role in the fluid dynamics for values of Fr much less than unity.

The regimes defined by the Weber Number, Froude Number and Bond Number (Bo = We/Fr) are indicated in Figure 6.7 taken from Reference 6.1.

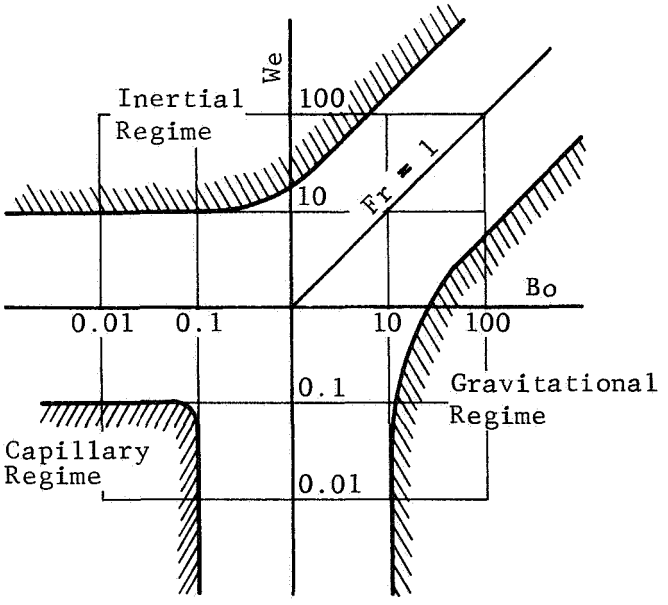

Figure 6.7 Hydrodynamic Regimes (See Fig. 11.5, Ref 6.1)

This figure gives no indication of the relative importance of viscous effects and the effect of these forces must be established separately.

An order-of-magnitude estimate of the time required for liquid reorientation following the transition between two hydrostatic regimes can be obtained through examination of the "characteristic response time." An analysis which develops expressions for these times is presented in Section 11.4 of Reference 6.1. The characteristics times are determined to be

$$t = (\ell/g)^{1/2} \quad \text{for the gravity dominated regime}$$

and

$$t = (\rho\ell^3/\sigma)^{1/2} \quad \text{for the capillary dominated regime.}$$

Figure 6.8 indicates characteristic response times for the various hydrostatic regimes.

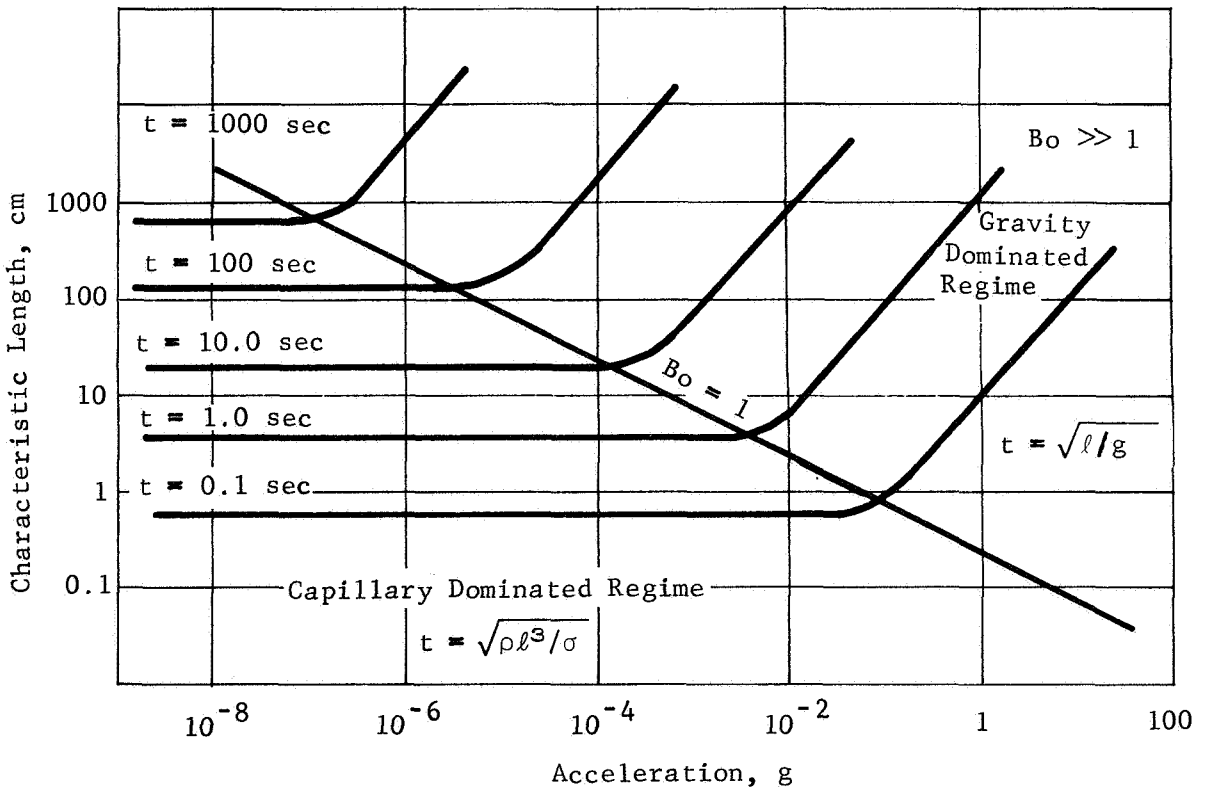

Figure 6.8 Characteristic Response Times (Based on Fig. 11.6, Ref 6.1)

6.2.6 Elastic-Gravitational-Density Scaling

The simulation of an elastic launch vehicle structure containing a sloshing liquid has been developed in Chapter 4 where it was assumed that significant coupling exists between the slosh modes and the beam-like structural modes. The controlling scaling parameters, established in Chapter 4, are

$$\pi_1 = m\ell^4\omega^2/EI, \quad \pi_2 = \ell\omega^2/a \quad \text{and} \quad \pi_3 = \rho\ell^2/m$$

where m = mass/unit length, FT^2/L^2

ℓ = characteristic length, L

ω = frequency, $1/T$

EI = beam stiffness, FL^2

a = acceleration, L/T^2

ρ = liquid density, FT^2/L^4

and geometrical structural similarity is required.

The acceleration ratio, using the subscript r to denote model-to-prototype ratios, is

$$a_r = (EI)_r/m_r n^3$$

where $n = \ell_r = \ell_m/\ell_p$. The mass ratio, due to the assumption that the ratio of sloshing to non-sloshing masses be identical for model and prototype, is

$$m_r = \rho_r n^2$$

and the acceleration ratio then becomes

$$a_r = (EI)_r/\rho_r n^5$$

Replica scaling requires geometric similarity and idential materials. This implies that $E_r = 1$, $I_r = n^4$ and $\rho_r = 1$ so that the acceleration ratio becomes

$$a_r = 1/n$$

which clearly indicates the impossibility of modeling the boost acceleration phase with small scale replica models. However, the possibility of using dissimilar materials must not be precluded although tank geometric similarity is always required to preserve adequate slosh simulation. If it is assumed that

$$I_r = \ell_r^3 t_r = n^3 t_r,$$

where t_r defines the ratio of model-to-prototype tank wall thickness, the acceleration ratio becomes

$$a_r = E_r t_r / \rho_r n^2$$

A simulation chart in terms of the parameter $Q_r = E_r t_r / \rho_r$ is presented in Figure 6.9.

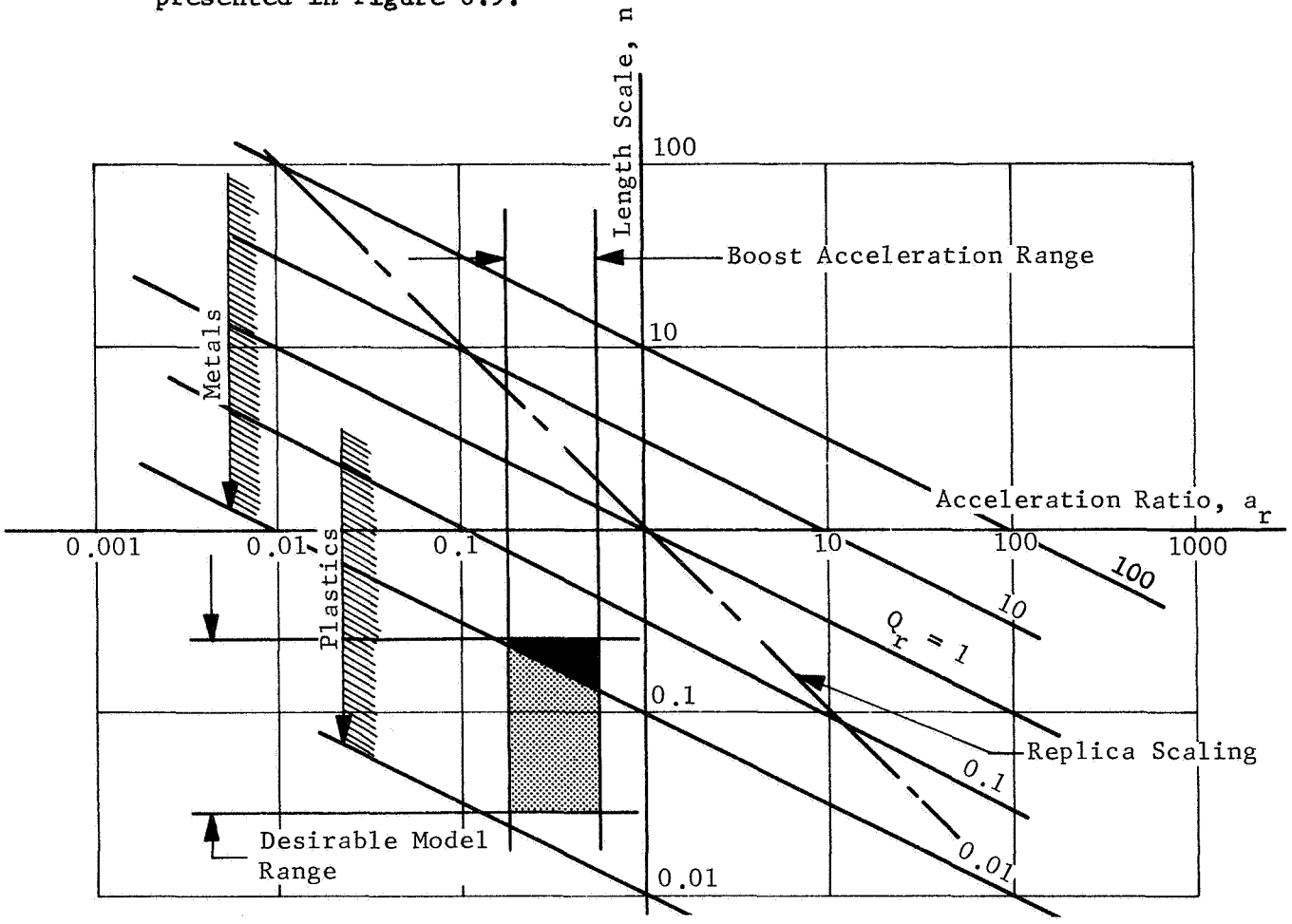

Figure 6.9 Simulation Chart: Elastic-Gravitational-Density Scaling

As typical model sizes and boost phase accelerations yield values of Q_r ranging from approximately 0.03 to 0.002, the applicability of metal models is limited. The liquid density ratio (unless mercury is used as the model liquid) cannot exceed about 2.0; the elastic modulus for aluminum prototype and magnesium model would be 0.6 and a thickness ratio of 0.1 would be required to achieve $Q_r = 0.03$. This ratio of tank wall thicknesses may create serious manufacturing, assembly and handling problems. To achieve lower values of Q_r requires the use of plastics in model construction and/or the use of mercury as the model liquid.

6.3 Simulation of Non-Linear Longitudinal Effects

The effect of longitudinal excitations upon liquids depends to a great extent upon the amplitude and the frequency of the excitations. At relatively low frequencies the free surface of the liquid may respond in a large amplitude standing wave with a frequency equal to one-half the excitation frequency. At high frequencies the liquid amplitude is diminished but the waves may disintegrate and generate a low frequency standing wave of large amplitude. At very high vibration input levels small vapor bubbles can become entrapped in the liquid. These bubbles can achieve negative buoyancy and sink to the tank bottom.

A historical survey and a summary of analyses and conclusions pertaining to these non-linear effects has been presented by Abramson (Ref 6.1).

6.3.1 Subharmonic, Superharmonic and Other Non-Linear Excitation

Free surface standing waves are generated when a cylindrical tank containing a liquid is forced to oscillate vertically. The primary liquid response occurs at one-half the excitation frequency and the liquid motion is usually identified as the one-half subharmonic response. Other response modes may occur at the excitation frequency as well as at superharmonic frequencies. This phenomenon is essentially non-linear and is a suitable area for simulation studies.

The functional relationship between liquid pressure and other independent variables in an assumed rigid tank is

$$P = f(g, \lambda, \rho, \omega, \ell)$$

where P = liquid pressure at depth d, F/L^2

g = steady state tank acceleration, L/T^2

λ = any length (e.g., excitation amplitude (x_o), radius of tank (R), liquid depth (d)), L

ρ = liquid density, FT^2/L^4

ω = excitation frequency, 1/T

ℓ = characteristic length, L.

Application of the principles of dimensional analysis yields three non-dimensional scaling relations. These relations are

$$\pi_1 = \omega^2\lambda/g, \qquad \pi_2 = P/\rho g \ell \quad \text{and} \quad \pi_3 = \lambda/\ell.$$

The first term, when written as

$$\pi_1^* = \omega^2 x_o/g$$

defines the dynamic-to-static acceleration ratio. π_2 may be expressed as

$$\pi_2^* = P/\rho g d$$

to define the dynamic-to-static pressure ratio. Complete geometric similarity is dictated by π_3.

6.3.2 Bubble Cluster Formation

Another non-linear phenomenon associated with vertical tank excitations is the formation of bubble clusters. These clusters arise due to the apparent negative buoyancy of small gas bubbles which, above some limiting oscillatory acceleration level, become trapped in the liquid. This phenomenon results in the periodic growth and destruction of gas bubble clusters below the liquid surface.

The functional relationship between liquid pressure and other variables is

$$P = f(g, \lambda, \rho, \omega, \ell, c, P_o)$$

where c = sonic velocity in liquid-bubble mixture, L/T

P_o = gas pressure, F/L^2

and the other variables are as defined in Section 6.3.1.

The five scaling relations developed from the above are

$$\pi_1 = \omega\lambda/c, \qquad \pi_2 = \lambda/\ell, \qquad \pi_3 = P_o/\rho g\ell,$$

$$\pi_4 = \omega^2\lambda/g \qquad \text{and} \qquad \pi_5 = P/\rho g\ell.$$

π_1, when expressed as

$$\pi_1^* = \omega d/c,$$

defines a dimensionless pressure wave length. π_3 can be written as

$$\pi_3^* = P_o/\rho gd$$

to define the gas-to-liquid static pressure ratio and π_5 as

$$\pi_5^* = P/\rho gd$$

to define liquid dynamic-to-static pressure ratio. The dynamic-to-static acceleration ratio follows from

$$\pi_4^* = \omega^2 x_o/g$$

and geometric similarity is dictated by π_2. The ratio of gas to liquid volumes

$$\pi_6 = V_g/V_\ell$$

follows from π_2.

7. DISTORTED SCALING OF LAUNCH VEHICLE STRUCTURES

Stiffened cylindrical and conical shells are typical of tank walls, interstage adapters and fairings. Proper simulation of their dynamic characteristics is required if accurate simulation of the overall launch vehicle dynamic characteristics is to be realized. Frequently, the thin skins that form a major portion of these structures preclude the use of replica scaling (Chapter 9). Replacement of the prototype shell structure with an equivalent distorted model is then necessary.

There are several approaches to the analysis of shell configurations. Classical solutions are available for most axisymmetric shell geometries (e.g., Ref 7.1) but many practical problems involve unsymmetrical or stiffened shells for which classical solutions are not readily available. Due to the complexity of the mathematical formulation, stiffened cylinders and cones are generally investigated through the use of finite element techniques. These techniques idealize the actual shell and stiffeners as structural systems of plates and beams having equivalent stiffness and mass. Application of these methods to symmetrically and unsymmetrically stiffened cylinders and to symmetrically stiffened cones is presented in Reference 7.2.

A somewhat analogous method of distorted shell modeling which appears to be applicable to typical launch vehicle structures is truss-ring modeling. This technique differs from that outlined in Reference 7.2 in that the shell is replaced by truss-ring modules consisting of transverse frames connected by a framework of axially loaded bars. Application of these methods to the dynamic modeling of shells is discussed in Section 7.1. Simulation of orthotropic cylinders using reinforced plastic models is discussed in Section 7.2.

7.1 Truss-Ring Modeling of Cylindrical Shells

The cylindrical shell considered here is a continuous three-dimensional skin structure. It is proposed that the shell be suitably divided into a number of units, each unit consisting of a number of segments. Therefore, the entire cylindrical shell can be considered as an assemblage of a finite number of segments.

The extremely thin skin gages which may result from replica scaling dictate that the cylindrical units be simulated with a distorted model. The model suggested to represent the continuous elastic properties of a typical cylindrical unit is defined as a "module." This module (Fig. 7.1) consists of an elastic ring and several axially stressed bars. The bars are equally spaced about the ring

circumference and are singly connected at each end by frictionless pin joints. These joints attach to the module ring on one side and to the ring of the adjacent module on the other side. Note that the geometrical arrangement of the truss bars must be symmetrical about any ring diameter.

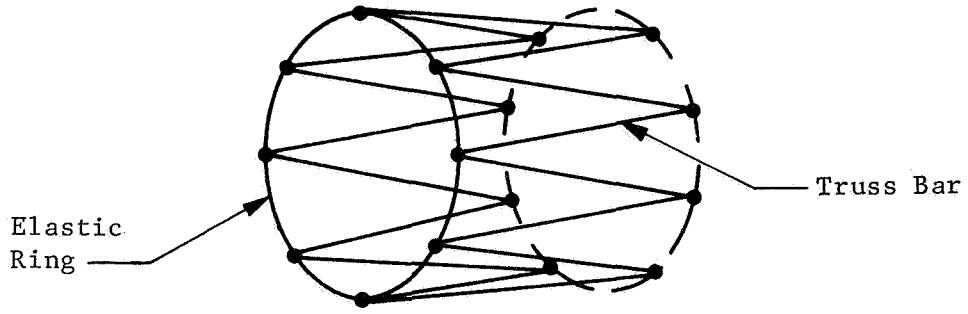

Figure 7.1 Truss-Ring Module

The proposed module must satisfy certain preassigned static and dynamic conditions. The elastic ring will simulate the radial effects while the bars are assumed to take only axial forces. The combination of truss and connecting ring provides the required overall simulation of longitudinal, lateral and torsional stiffnesses. The entire cylindrical shell may be simulated by a number of these modules. As the bars are pin-connected, the truss between adjacent rings forms a discrete system. Thus, the assemblage of the several modules is precisely an assemblage of discrete units and the entire truss-ring modeling analysis can be deemed to be analogous to a finite element approach.

The following sections detail the equivalent longitudinal, torsional, bending and lateral stiffnesses of a module. Buckling simulation is not considered in this analysis. The simulation of shell buckling characteristics is a logical extension to these analyses.

7.1.1 Geometry of Module Components

A typical module (Fig. 7.2) consists of an elastic ring and a number of pin-connected bars.

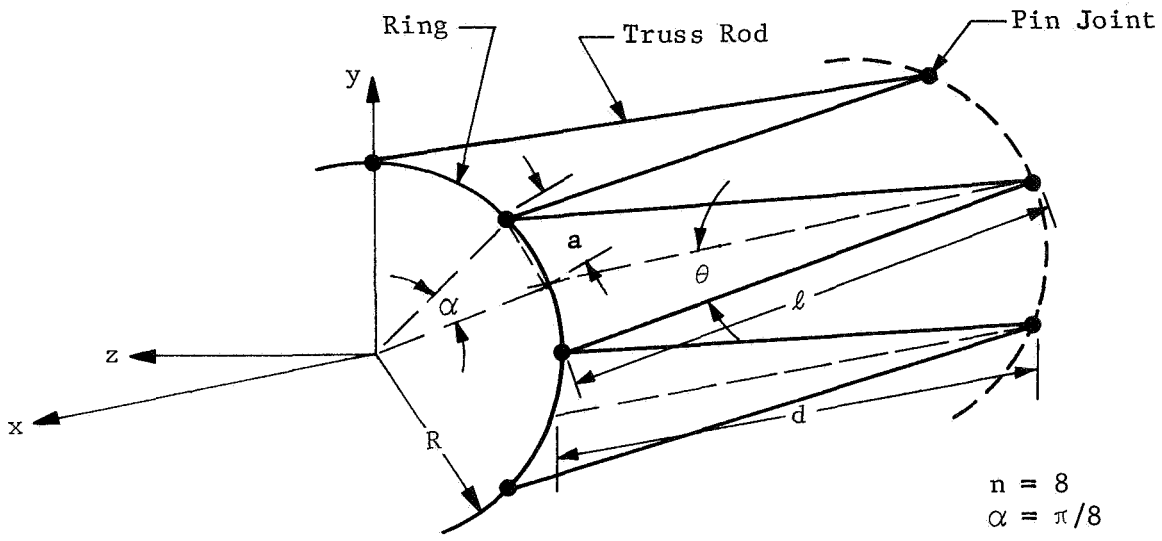

Figure 7.2 Geometry of Module Element

The number of joints attached to a ring is denoted by n and therefore the number of bars is equal to 2n. Geometrical symmetry dictates that all bars have identical length.

The notation used in the subsequent analyses of module stiffnesses is:

R = radius of ring centerline

n = number of joints on one side of ring,

d = longitudinal distance between ring centerlines,

ℓ = length of truss bar, $\ell^2 = a^2 + d^2$,

$\alpha = \pi/n$,

$\theta = \cos^{-1}(d/\ell)$,

$a = 2R \sin(\alpha/2)$.

A set of x, y, z axes are employed such that the x-axis defines the longitudinal module direction and the y and z axes define the lateral directions (Fig. 7.2). The axial bar force deviates from the module longitudinal axis by the angle θ and may therefore be decomposed into x, y and z components for the individual stiffness analyses.

7.1.2 Longitudinal Stiffness of a Module

The longitudinal module stiffness is defined as the longitudinal force required to produce unit longitudinal module deformation. The connecting rings are assumed rigid.

The length of a typical rod, expressed in terms of the module length d and chord distance between joints a, is

$$\ell^2 = d^2 + a^2. \tag{1}$$

The relationship between the variation in rod length $\delta\ell$ with change in module length δd can be obtained from the differentiation of Equation 1 and is

$$\delta\ell = (d/\ell)\ \delta d \tag{2}$$

The assumption of a rigid ring dictates that the dimension a remain constant. Assuming that the deformation is within the elastic range so that Hooke's Law is applicable allows the axial rod force to be expressed as

$$F_i = k(\delta\ell) = k(d/\ell)\ \delta d \tag{3}$$

where the axial stiffness of an individual rod is

$$k = AE/\ell. \tag{4}$$

It is to be noted that no subscript is used in Equation 4 as the rod area A, length ℓ and material elasticity E are assumed identical for all rods.

The longitudinal component F_{ix} of the axial rod force can be computed from Equation 3 and is

$$F_{ix} = F_i(d/\ell) = k(d/\ell)^2 \delta d. \quad (5)$$

Each module consists of 2n rods and the total longitudinal module force is

$$F_L = 2nF_{ix} = 2nk(d/\ell)^2 \delta d. \quad (6)$$

The longitudinal module stiffness, expressed in terms of the rod stiffness and the module geometry, is

$$k_L = F_L/\delta d = 2nk(d/\ell)^2. \quad (7)$$

In model analysis it is convenient to employ the concept of an equivalent elastic parameter. For longitudinal extension the equivalent longitudinal elasticity $\overline{AE}$ of a module can be defined as

$$\overline{AE} = k_L d = 2nAE(d/\ell)^3. \quad (8)$$

Note that no forces but the longitudinal resultant force of Equation 6 are required for unit longitudinal module deformation. This is a consequence of the assumptions of rigid ring and module symmetry. As the applied force and resulting deformation act in the same direction, the longitudinal stiffness is defined as a direct stiffness. The lateral components of the axial rod forces are mutually cancelled due to the symmetrical connections of truss loads to ring joints and no cross-stiffness terms exist.

7.1.3 Torsional Stiffness of a Module

The torsional module stiffness is provided by the axial tension and compression of the truss rods. Again it is assumed that the ring is rigid so that only a torque is required to produce twisting deformation. The torsional stiffness is defined as the torque required for unit twist angle and can be derived by rotating the rigid ring about the longitudinal axis through the angle $\delta\theta$. The pin-joint attached at the ring circumference will travel an arc distance δa (Fig. 7.3) where

$$\delta a = R(\delta\theta). \quad (9)$$

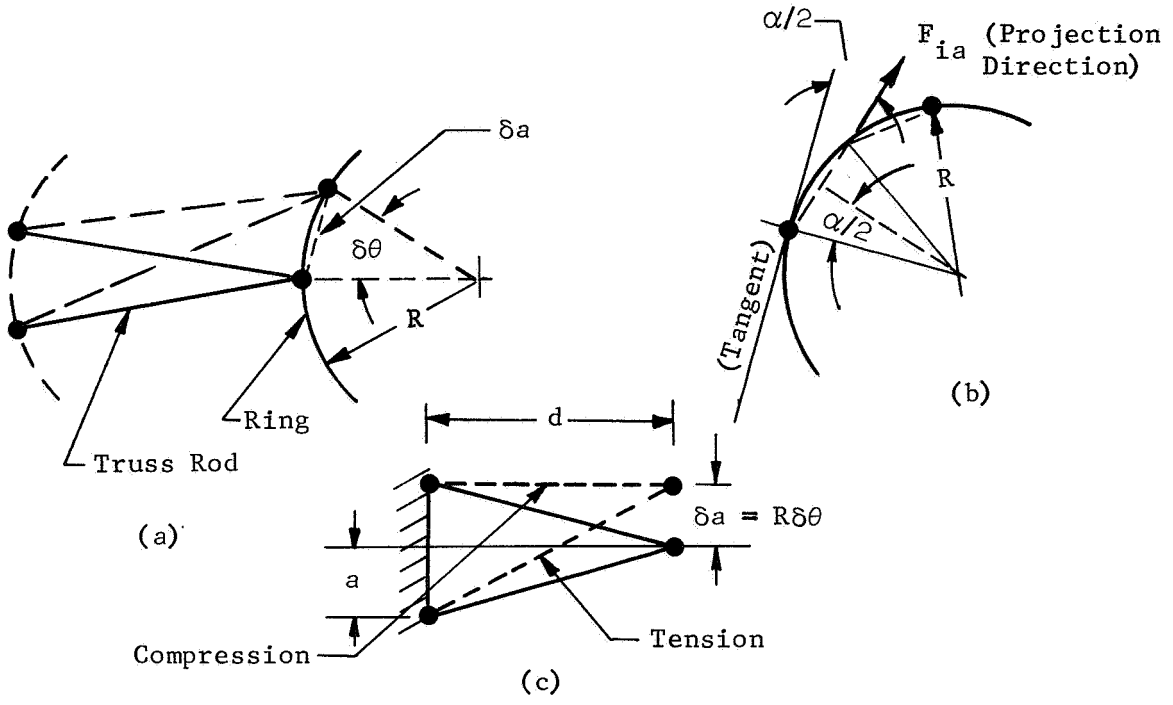

Figure 7.3 Torsional Displacement of Truss Triangle

Since the change in rod length $\delta\ell$ is a function of δa and the module length d is invarient, the differentiation of Equation 1 yields

$$\delta\ell = R(a/\ell)\ \delta\theta. \tag{10}$$

The axial rod force F_i, assuming that Hooke's Law is applicable, is

$$F_i = k(\delta\ell) = kR(a/\ell)\ \delta\theta \tag{11}$$

where k is as defined in Equation 4. This force can be decomposed into two components; one in the longitudinal direction and the other in the plane of the ring. The latter, which produces a twisting moment about the center of the ring (Fig. 7.3) can be expressed as

$$F_{ia} = F_i(a/\ell) = kR(a/\ell)^2\delta\theta. \tag{12}$$

The twisting moment T_i developed by this force is

$$T_i = F_{ia} R \cos(\alpha/2) = k(Ra/\ell)^2 \cos(\alpha/2)\delta\theta. \quad (13)$$

There are two rods associated with each pin joint; one in compression, the other in tension. The longitudinal components of the two rod forces are mutually cancelled but the in-plane components F_{ia} are equal in magnitude and act in the same projection direction. Hence, the total twisting moment T is

$$T = 2n\, T_i = 2nk(aR/\ell)^2 \cos(\alpha/2)\delta\theta. \quad (14)$$

and the torsional stiffness is

$$k_T = T/\delta\theta = 2nk(aR/\ell)^2 \cos(\alpha/2). \quad (15)$$

The equivalent torsional elasticity is

$$\overline{GJ} = k_T d = 2nAE(d/\ell)(aR/\ell)^2 \cos(\alpha/2). \quad (16)$$

The cancellation of the longitudinal rod force components at an individual joint implies that the torsional stiffness is independent of the longitudinal stiffness. Due to the assumed symmetry of the rods, the twisting force components provide neither sectional lateral shear or bending deformations. The torsional stiffness is therefore a direct stiffness.

7.1.4 Bending Stiffness of a Module

The bending stiffness is defined as the bending moment required to produce a unit ring rotation about a diametric axis (Fig. 7.4a). The ring is assumed to be rigid. The influence of rod forces will be discussed in a later section.

The truss rods are assumed to be arranged symmetrically about any diameter and it follows that two neutral axis positions must be considered. The bending neutral axis may either pass through the joints (Fig. 7.4b) or lie between the joints (Fig. 7.4c).

In order to establish the moment required to produce $\delta\phi$ it is necessary to consider the axial deformation of the truss rods. Let the joints be numbered counterclockwise as shown in Figure 7.4b. The initial joint is defined by the angle α_o and the angle between adjacent joints is 2α. The jth joint is then defined by the angle

$$\beta_j = 2j\alpha - \alpha_o \quad (17)$$

where $\alpha_o = 0$ if the neutral axis is as shown in Figure 7.4b and $\alpha_o = \alpha^o$ if the neutral axis is as shown in Figure 7.4c. The distance of the jth joint from the neutral axis is

$$y_j = R \sin \beta_j = R \sin (2j\alpha - \alpha_o) \tag{18}$$

and the longitudinal displacement x_j is

$$x_j = y_j \, \delta\phi. \tag{19}$$

It follows that the axial rod deformation at the jth joint is

$$\delta\ell_j = y_j (d/\ell) \delta\phi \tag{20}$$

and the axial rod force, assuming a linear elastic material, is

$$F_j = k \, \delta\ell_j = k y_j (d/\ell) \, \delta\phi \tag{21}$$

where k is as defined in Equation 4. The longitudinal component of F_j is

$$F_{jx} = F_j (d/\ell) = k y_j (d/\ell)^2 \, \delta\phi \tag{22}$$

and, as there are two identical components at the jth joint, the total longitudinal joint force is

$$2F_{jx} = 2k y_j (d/\ell)^2 \delta\phi. \tag{23}$$

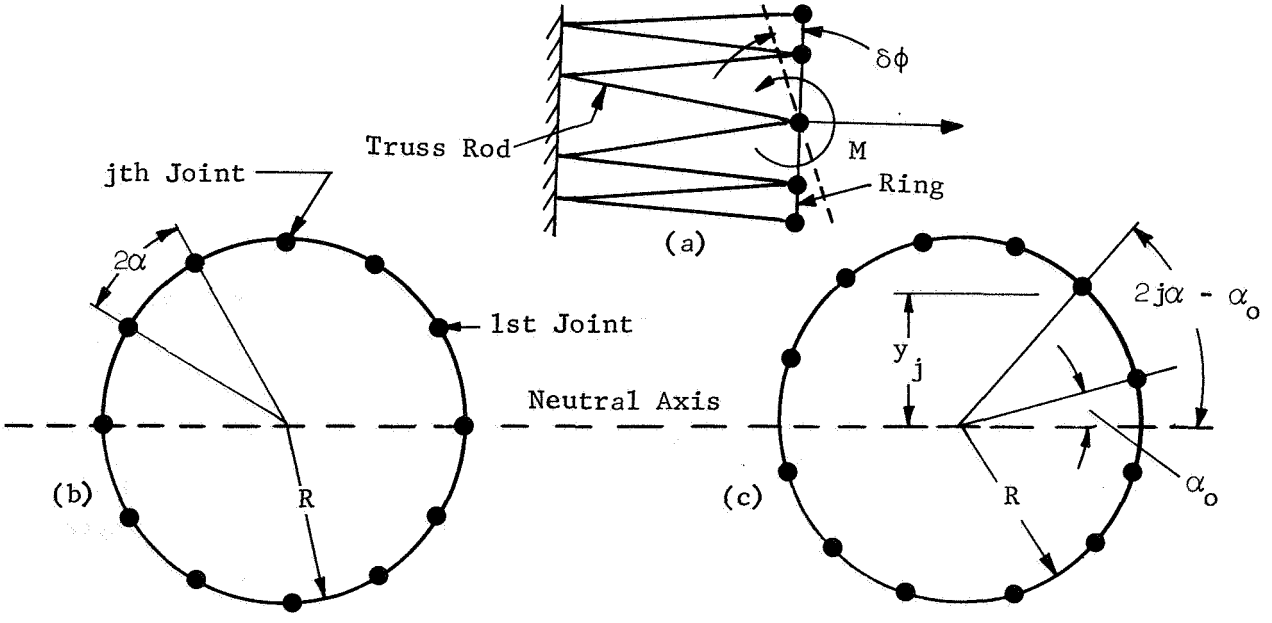

Figure 7.4 Bending Displacement of Truss-Ring Module

The bending moment about the neutral axis produced by the total joint force can be expressed as

$$M_j = 2F_{jx}y_j = 2k(y_j d/\ell)^2 \delta\phi \tag{24}$$

and the total moment is

$$M = \sum_{j=1}^{n} M_j = 2 \sum_{j=1}^{n/2} M_j = 4k(d/\ell)^2 \left[\sum_{j=1}^{n/2} y_j^2 \right] \delta\phi$$

$$= 4k(Rd/\ell)^2 \left[\sum_{j=1}^{n/2} \sin^2 (2j\alpha - \alpha_o) \right] \delta\phi. \tag{25}$$

The sum may be taken over half the circumference because the moments produced by the joint forces are symmetric about the neutral axis.

The bending stiffness is

$$k_B = M/\delta\phi = 4k(Rd/\ell)^2 \sum_{j=1}^{n/2} \sin^2(2j\alpha - \alpha_o) \tag{26}$$

and the equivalent bending elasticity can be expressed as

$$\overline{EI}_B = k_B d = 4AE(d/\ell)(Rd/\ell)^2 \sum_{j=1}^{n/2} \sin^2(2j\alpha - \alpha_o) \, . \tag{27}$$

The bending stiffness is a direct stiffness. However, it should be noted that this bending stiffness couples with a lateral cross-stiffness as a lateral force is required to prevent lateral ring displacement under the influence of the bending moment. The formulation of the lateral cross-stiffness is omitted.

7.1.5 Lateral Stiffness of a Module

The lateral stiffness is defined as the lateral ring force required to produce unit lateral displacement. All other displacements are zero and a rigid ring is assumed.

Consider the half circular ring and connecting joints shown in Figure 7.5.

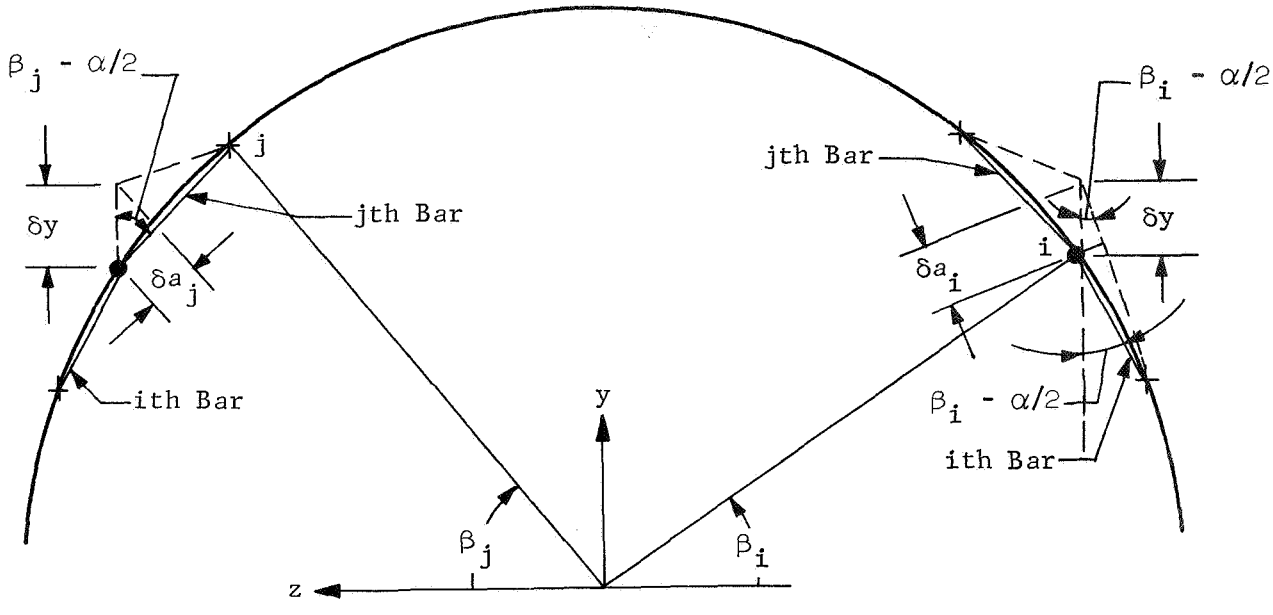

Figure 7.5 Lateral Displacement of Truss-Ring Module

The ith joint attaches to the ring and the jth joint attaches to the adjacent ring. It is evident that the elongation of the ith bar due to lateral displacement, δy, is

$$\delta a_i = \delta y \cos (\beta_i - \alpha/2) \tag{28}$$

and the compression of the jth bar is

$$\delta a_j = \delta y \cos (\beta_j - \alpha/2). \tag{29}$$

If the truss rods and joints are numbered as shown in Figure 7.5, either Equation 28 or Equation 29 may be used to express individual rod deformation provided that β is restricted to

$$0 \leq \beta \leq \pi/2 \tag{30}$$

The undeformed rod length has been given previously (Equation 1). As it is assumed that the module length d is held fixed, differentiation of Equation 1 yields

$$2\ell\delta\ell_i = 2a\delta a_i \quad \text{or} \quad \delta\ell_i = (a/\ell)\cos(\beta_i - \alpha/2)\delta y. \tag{31}$$

The axial bar force, assuming that the deformation is within the elastic range so that Hooke's Law is applicable, is

$$F_i = k\,\delta\ell_i = k(a/\ell)\cos(\beta_i - \alpha/2)\,\delta y \tag{32}$$

where k is as defined in Equation 4. This force can be decomposed into two components; one in the longitudinal direction and the other along the projection direction (Fig. 7.5). This latter component is

$$F_{ia} = F_i(a/\ell) = k(a/\ell)^2\cos(\beta_i - \alpha/2)\delta y. \tag{33}$$

The lateral component of F_{ia} is then

$$F_{iy} = F_{ia}\cos(\beta_i - \alpha/2) = k(a/\ell)^2\cos^2(\beta_i - \alpha/2)\delta y \tag{34}$$

and the total lateral force, determined by summing the rod forces over the quarter-circle defined by Equation 30, is

$$F_y = 4\sum_{i=1}^{n/2} F_{iy} = 4k(a/\ell)^2\left[\sum_{i=1}^{n/2}\cos^2(\beta_i - \alpha/2)\right]\delta y. \tag{35}$$

The lateral stiffness can now be expressed as

$$k_y = F_y/\delta y = 4k(a/\ell)^2\sum_{i=1}^{n/2}\cos^2(\beta_i - \alpha/2) \tag{36}$$

and the equivalent lateral elasticity as

$$\overline{EI}_L = k_y d = 4AE(d/\ell)(a/\ell)^2\sum_{i=1}^{n/2}\cos^2(\beta_i - \alpha/2)\ . \tag{37}$$

The lateral stiffness is a direct stiffness. However, it should be noted that this lateral stiffness couples with a bending cross-stiffness as a bending moment is required to prevent rotational

ring displacement under the influence of the lateral force. The formulation of the bending cross-stiffness is omitted.

7.1.6 Coupling Between Circumferential and Longitudinal Deformation

The analysis of module longitudinal stiffness (Section 7.1.2) is based upon the assumption that the truss rings are rigid. If the ring is considered to be elastic the effect of the axial rod force components which lie in the plane of a truss ring must be considered.

Consider a module subjected to a longitudinal force F. The longitudinal force component in an individual rod is

$$F_{ix} = F/2n \tag{38}$$

and the component along a chord projection in the ring plane is

$$F_{ia} = (F/2n)(a/d). \tag{39}$$

This force component can be further decomposed into two components. One of these components is tangential to the ring; the other is in the radial direction. The tangential components of two rods which connect at a single joint are mutually cancelled but the radial components introduce circumferential deformation (Figure 7.6a). The radial force component in a individual rod is

$$F_{ir} = F_{ia} \sin(\alpha/2) = (F/2n)(a/d) \sin(\alpha/2) \tag{40}$$

and it follows that the total radial force acting on the elastic ring can be expressed as

$$F_r = 2nF_{ir} = F(a/d) \sin(\alpha/2). \tag{41}$$

This resultant force can be approximated as a distributed compressive force acting about the circumference of the ring if the number of truss rods is large or the chord projection length is small. This approximate uniform force per unit length about the circumference is equal to

$$P_r = F_r/2\pi R = (F/2\pi R)(a/d) \sin(\alpha/2). \tag{42}$$

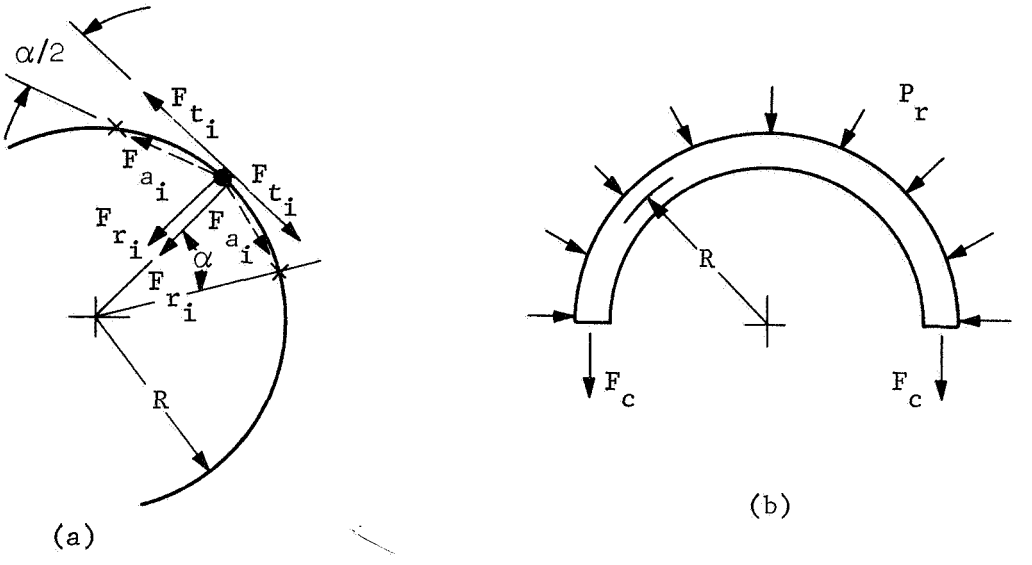

Figure 7.6 Circumferential-Longitudinal Coupling

For a uniform thin ring the circumferential force F_c (Fig. 7.6b) is obviously equal to

$$F_c = P_r R = (F/2\pi)(a/d) \sin (\alpha/2) \tag{43}$$

and the unit circumferential strain in the ring can be expressed as

$$\varepsilon_c = F_c/A_r E_r = (F/2\pi A_r E_r)(a/d) \sin (\alpha/2) \tag{44}$$

where E_r and A_r define the ring elasticity and cross-sectional area. This strain should be equivalent to the circumferential strain of the simulated shell.

The change in radius, ΔR, is equal to the total circumferential deformation divided by 2π, or

$$\Delta R = 2\pi R\varepsilon_c/2\pi = R\varepsilon_c. \tag{45}$$

Therefore, the unit radial strain (which is equal to ΔR divided by the undeformed radius) is

$$\varepsilon_r = \Delta R/R = \varepsilon_c . \tag{46}$$

The unit longitudinal module strain, based upon the equivalent longitudinal module elasticity (Section 7.1.2) can be expressed as

$$\varepsilon_x = F/\overline{AE} = F/[2n(d/\ell)^3 AE)] \tag{47}$$

where $\overline{AE}$ is defined in Equation 8 and AE defines the elasticity of an individual truss rod.

It should be noted that these results are based upon the assumption that there is a large number of truss bars so that the concentrated radial joint forces can be approximated by a uniformly distributed force. The concepts presented here are also applicable to other force components such as those which lead to bending and to lateral displacements. The extension of the analysis to include these effects is omitted here.

7.1.7 Circumferential Bending Stiffness

Proper simulation of the shell ring modes requires the simulation of circumferential bending stiffness. The bending stiffness of the rings can be expressed as

$$E_r I_r = dD_w \tag{48}$$

where d = longitudinal distance between ring centerlines, and

D_w = bending stiffness of a circumferential strip of width w for the prototype shell.

7.1.8 Computer Program

Appendix B presents the listing of a computer program, written in FORTRAN IV for the IBM 1130, to compute truss-ring module parameters from full-scale shell parameters.

7.2 Use of Reinforced and Stiffened Shells for Simulation of Orthotropic Cylinders

Although the structure to be modeled is a cylindrical shell, the following developments can be carried out with little regard to the shape of the structure. Flat plate elements are used and all materials involved are assumed to obey the generalized Hook's law. Bending and extensional rigidities for an orthotropic plate are found and the equivalent orthotropic properties are expressed in terms of the model shell geometry and constituent material properties.

7.2.1 Bending and Extensional Rigidities for an Orthotopic Plate

An orthotropic plate is one which has different material properties in two mutually perpendicular directions. In this section the two directions will be referred to as the longitudinal and transverse. Hooke's law for an orthotropic plate is:

$$\begin{aligned} \sigma_\ell &= C_{11}\,\varepsilon_\ell + C_{12}\varepsilon_t \\ \sigma_t &= C_{12}\,\varepsilon_\ell + C_{22}\varepsilon_t \\ \tau_{\ell t} &= C_{66}\,\gamma_{\ell t} \end{aligned} \tag{49}$$

By applying direct stresses in each of the two directions, the following set of relations can be obtained.

$$E_\ell = C_{11} - \frac{C_{12}^2}{C_{22}}$$

$$-\mu_{\ell_t} = -\frac{C_{12}}{C_{22}} = \frac{\varepsilon_t}{\varepsilon_\ell}$$

$$E_t = C_{22} - \frac{C_{12}^2}{C_{11}}$$

$$-\mu_{t\ell} = -\frac{C_{12}}{C_{11}} = \frac{\varepsilon_\ell}{\varepsilon t}$$

$$G = C_{66}$$

with $$\frac{C_{11}}{C_{22}} = \frac{E_\ell}{E_t} = \frac{\mu_{\ell t}}{\mu_{t\ell}} \tag{50}$$

Equations (49) can be rewritten to give strain instead of stress.

$$\varepsilon_\ell = \frac{1}{(C_{11}\, C_{22} - C_{12}^2)} (C_{22}\, \sigma_\ell - C_{12}\, \sigma_t)$$

$$\varepsilon_t = \frac{1}{(C_{11}\, C_{22} - C_{12}^2)} (-C_{12} + C_{11}\, \sigma_t)$$

$$\gamma_{\ell t} = \frac{1}{C_{66}}\, \tau_{\ell t}$$

or

$$\varepsilon_\ell = \frac{1}{E_\ell} (\sigma_\ell - \mu_{\ell t}\, \sigma_t)$$

$$\varepsilon_t = \frac{1}{E_t} (-\mu_{t\ell}\, \sigma_\ell + \sigma_t) \quad \text{and} \quad \gamma_{\ell t} = \frac{1}{G}\, \tau_{\ell t}$$

It can be seen that there are four independent material properties necessary to describe the behavior of an orthotropic plate. These properties are G and any three of the properties in Equation (50). The existence of Equation (50) dictates that G must be one of the independent properties.

Consider the bending of an orthotropic plate in the longitudinal direction. For small deflections the curvature can be expressed by

$$-\frac{\partial^2 \omega}{\partial \ell^2}$$

where ω is the lateral deflection. The unit elongation a distance a from the middle surface is

$$-z\, \frac{\partial^2 \omega}{\partial \ell^2}$$

In order to maintain continuity during bending the transverse strain must be zero. Therefore:

$$\varepsilon_\ell = \frac{1}{E_\ell} (\sigma_\ell - \mu_{\ell t}\, \sigma_t)$$

$$\varepsilon_t = \frac{1}{E_t} (-\mu_{t\ell}\sigma_\ell + \sigma_t) = 0, \quad \sigma_t = \mu_{t\ell}\, \sigma_\ell$$

Therefore:

$$\varepsilon_\ell = \frac{\sigma_\ell}{E_\ell} (1 - \mu_{\ell t} \mu_{t\ell})$$

and

$$\varepsilon_\ell = \frac{E_\ell \varepsilon_\ell}{(1 - \mu_{\ell t} \mu_{t\ell})} = \frac{E_{\ell z}}{(1 - \mu_{\ell t} \mu_{t\ell})} \frac{\partial^2 w}{\partial \ell^2}$$

The total bending moment can be obtained by integrating the bending stresses through the thickness of the plate

$$M = \int_{-h/2}^{h/2} \sigma_\ell z dz = 1 \int_{-h/2}^{h/2} \frac{E_\ell z^2}{(1 - \mu_{\ell t} \mu_{t\ell})} \frac{\partial^2 w}{\partial \ell^2} d_z = \frac{E_\ell h^3}{12(1-\mu_{\ell t}\mu_{t\ell})} \frac{\partial^2 w}{\partial \ell^2}$$

Therefore, the bending rigidity for longitudinal bending is:

$$D_\ell = \frac{E_\ell h^3}{12(1 - \mu_{\ell t}\mu_{t\ell})}$$

or

$$D_\ell = \frac{E^2_\ell h^3}{12(E_\ell - E_t \mu^2_{\ell t})}$$

A similar treatment for bending in the transverse direction yields:

$$D_t = \frac{E_\ell E_t h^3}{12(E_\ell - E_t \mu^2_{\ell t})}$$

Expressions for extensional rigidities in each of the two directions can be obtained in much the same manner.

$$K_\ell = \frac{E_\ell^2 h}{E_\ell - E_t \mu^2_{\ell t}}$$

$$K_t = \frac{E_\ell E_t h}{E_\ell - E_t \mu^2_{\ell t}}$$

7.2.2 Equivalent Properties in Terms of the Constituent Material Properties and Shell Geometry

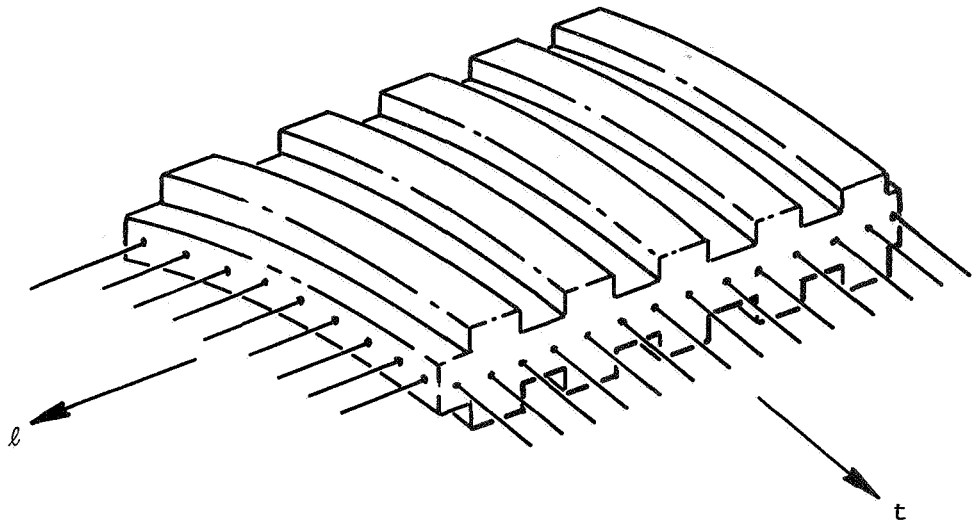

Fig. 7.7 Typical Model Section

Nomenclature:

μ_m	matrix Poisson's ratio
E_m, G_m	matrix moduli
E_f, G_f	fiber moduli
A_f	fiber cross-sectional area
h	thickness of unreinforced shell
t	depth of circumferential stiffeners
S_1	width of stiffeners
S_2	stiffener spacing
S_ℓ	longitudinal fiber spacing
S_t	transverse (circumferential) fiber spacing
R	middle surface radius

In order to derive an expression for the equivalent modulus in the longitudinal direction, a pseudo material is first developed.

This material consists of an unstiffened plate with fibers in the transverse direction only. The fibers are assumed to have a square cross-section with the same area as the actual fiber. This simplifying assumption allows one to assume a uniform strain distribution on a plane tangent to the fiber and perpendicular to the longitudinal axis. Equilibrium is enforced across this plane between adjacent elements with and without an encased fiber, see Fig. 7.8.

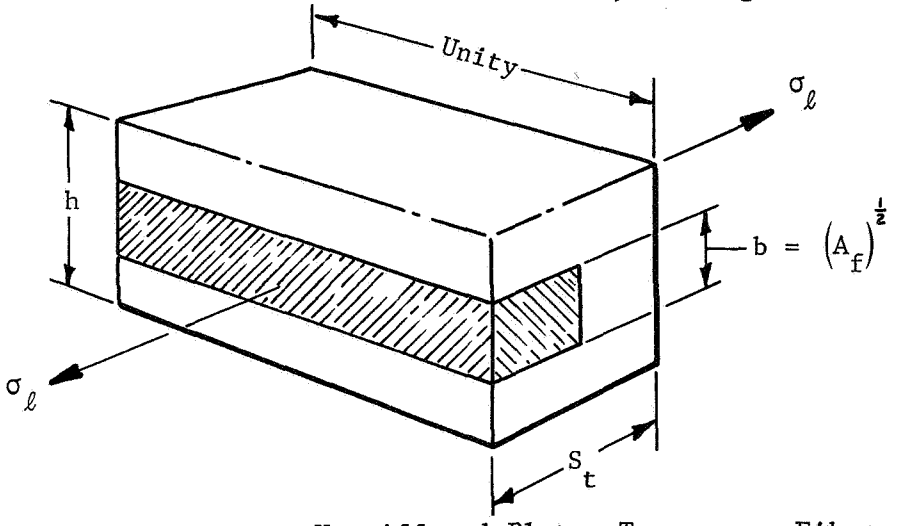

Figure 7.8 Unstiffened Plate, Transverse Fibers

The above conditions and assumptions lead to the following expression for the longitudinal modulus for a material with transverse fibers only.

$$E'_\ell = \frac{S_t E_m [\lambda E_f + (1-\lambda) E_m]}{bE_m + (S_t - b)[\lambda E_f + (1-\lambda) E_m]}$$

Where $\lambda = \frac{b}{h}$

Now, suppose that the stiffeners are included and that their presence is accounted for by allowing h to be replaced by an effective thickness $\bar{h}$, such that equilibrium is maintained between stiffened and unstiffened portions of the shell.

Then:
$$\bar{h} = \frac{h(S_1 + S_2)(h + 2t)}{h(S_1 + S_2) + 2tS_2}$$

and
$$\bar{E}_\ell = \frac{S_t E_m [\bar{\lambda} E_f + (1 - \bar{\lambda}) E_m]}{bE_m + (S_t - b)[\bar{\lambda} E_f + (1-\lambda) E_m]}$$

where $\bar{\lambda} = \frac{b}{\bar{h}}$

The total effective longitudinal modulus can now be obtained, using $\bar{E}_\ell$ as the matrix modulus for longitudinal extension. The total load in the ℓ direction will be the sum of the loads carried by the longitudinal fibers and the matrix. A uniform strain distribution is assumed.

$$P_\ell = \sigma_\ell \bar{A} = E_f \varepsilon_f A_f + \bar{E}_\ell \varepsilon_m \bar{A}_m$$

Therefore:

$$E_\ell = E_f \frac{A_f}{\bar{A}} + \bar{E}_\ell \frac{\bar{A}_m}{\bar{A}}$$

Let $$\alpha = \frac{A_{f_T}}{\bar{A}_T} = \frac{A_f}{S_\ell \bar{h}}$$, then

$$E_\ell = E_f \alpha + \bar{E}_\ell (1 - \alpha)$$

The derivation for the extensional modulus in the transverse direction is similar to the preceeding, however the effective thickness, $\bar{h}$, is replaced by h'. The new effective thickness is obtained by allowing the stiffeners to be "smeared" over the plate surface such that an equivalent area is offered to resist transverse loading.

$$h' = \frac{h(S_1 + S_2) + 2tS_1}{(S_1 + S_2)}$$

Then:

$$\bar{E}_t = \frac{S_\ell E_m [\lambda' E_f + (1-\lambda') E_m]}{bE_m + (S_\ell - b)[XE_f + (1-\lambda')E_m]}$$

and

$$E_t = E_f \beta + \bar{E}_t (1-\beta)$$

where $$\beta = \frac{A_{f_T}}{A_T} = \frac{A_f}{S_t h'}$$ and $$\lambda' = \frac{b}{h'}$$

It has been demonstrated that the extensional modulus in each of the orthogonal directions is a function of the fiber fraction. Each material contributes to the equivalent modulus according to its percent of volume present. However, an equivalent modulus derived from bending considerations depends upon the donation of each constituent material according to its percent of inertia present. For this reason, two different moduli result, depending on the mode of deflection; an extensional modulus and a bending modulus. In regard to the rigidities obtained in Section 7.2.1, when the product $E_f I_f/I$ is not a small quantity, the appropriate modulus must be used in each rigidity expression according to the implied deflection scheme.

In order to maintain consistency with the derivation of the longitudinal extensional modulus, the stiffeners are assumed to influence longitudinal bending in accordance with $\bar{h}$. Maintenance of compatible deflections and slopes of the fibers and matrix material during bending yields the following expression for the longitudinal bending modulus. Transverse fibers are assumed not to influence longitudinal bending.

$$E_{b\ell} = E_f \gamma_\ell + E_m (1-\gamma_\ell)$$

where $$\gamma_\ell = \frac{I_f}{I} = \frac{3A_f^2}{\pi S_\ell \bar{h}^3}$$

Transverse bending involves the inertia of the transverse fibers and stiffeners. The stiffeners are accounted for by using the equivalent thickness, h'. Longitudinal fibers are assumed ineffectual during transverse bending.

$$E_{bt} = E_f \gamma_f + E_m (1-\gamma_t)$$

where $$\gamma_t = \frac{I_f}{I} = \frac{3A_f^2}{\pi S_t h'^3}$$

Consider the following model, shown in Fig. 7.9.

For a load applied in the longitudinal direction, there will be a corresponding strain in the transverse direction, which is proportional to the longitudinal strain. The proportionality constant, or Poisson's ratio $\mu_{\ell t}$, can be obtained by enforcing transverse equilibrium between fiber and matrix material and assuming a unifrom strain distribution on a plane anywhere in the element, provided that it is normal to the transverse axis.

The derivation of $\mu_{\ell t}$ is as follows using Fig. 7.10.

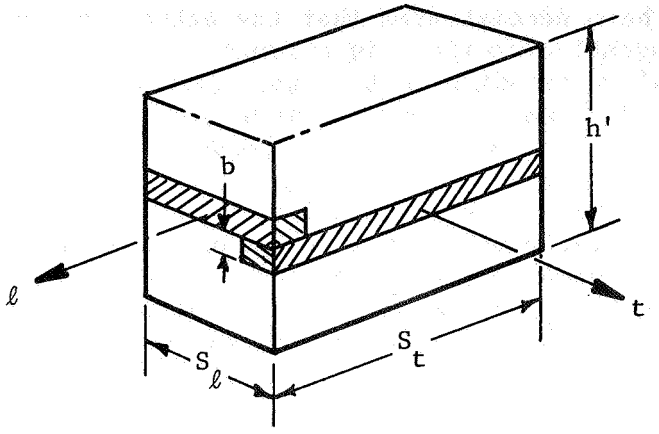

Fig. 7.9 Model of Element Reinforced in Two Directions

For transverse equilibrium,

$$\sigma_1 A_1 + \sigma_2 A_2 = \sigma_3 A_3 + \sigma_4 A_4$$

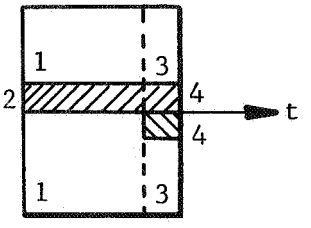

Fig. 7.10 Notation of an Element

where $A_1 = h'S_t - b^2$

$A_2 = b^2$

$A_3 = (h' - b)\, S_t - b^2$

$A_4 = b(S_t + b)$

The equilibrium equation becomes:

$$\varepsilon_1\{E_m(h'S_t - b^2) + E_f b^2\} = \varepsilon_3\{E_m[(h' - b^2] + E_f[b(S_t + b)]\}$$

With $e_1 + e_3 = e_t$

or, $$e_t = \varepsilon_t S_\ell = \varepsilon_1 (S_\ell - b) + \varepsilon_3 b$$

and $$\varepsilon_1 = \mu_m \varepsilon_\ell$$

Therefore:

$$\mu_{\ell t} = \frac{\mu_m}{S_\ell} (S_\ell - b) + b \frac{E_m (h' S_t - b^2) + E_f b^2}{E_m [(h' - b) S_t - b^2] + E_f [b(S_t + b)]}$$

The method for determining an expression for the equivalent shear modulus is analogous to that used for the equivalent extensional moduli . A pseudo material is developed for each orthogonal direction which includes the effects of resistance to shear in the direction of each fiber axis only. A uniform strain distribution is assumed on a plane tangent to the fiber and perpendicular to the plane, and equilibrium is enforced across this plane. For the total equivalent shear modulus the shear moduli of the pseudo materials are used as the matrix shear modulus in the appropriate direction. See Fig. 7.11 for notation.

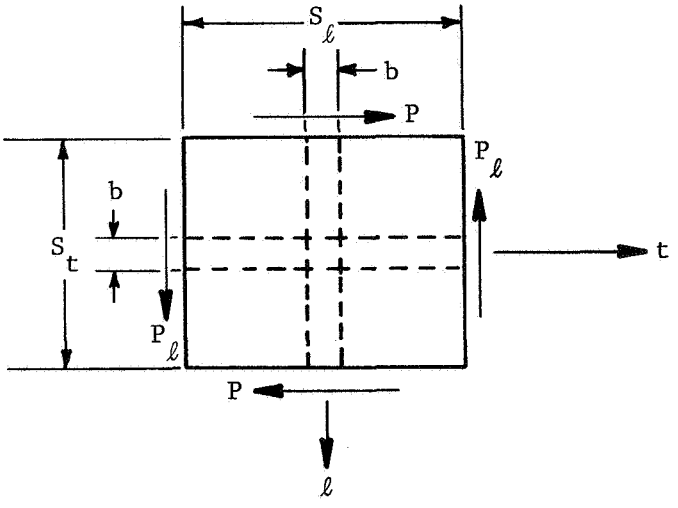

Fig. 7.11 Shears on an Element of Composite

For equilibrium,

$$P_t S_t = P_\ell S_\ell$$

with

$$P_t = \tau_t S_\ell h' \qquad \text{and} \qquad P_\ell = \tau_\ell S_t h'$$

Therefore,

$$\tau_t = \tau_\ell = \tau$$

Also,

$$P_t = G_f\gamma_t b^2 + G_t\gamma_t(S_\ell h' - b^2) = \tau_t S_\ell h'$$

$$P_\ell = G_f\gamma_\ell b^2 + G_\ell\gamma_\ell(S_t h' - b^2) = \tau_\ell S_t h'$$

The total shear strain is

$$\gamma = \frac{\gamma_t + \gamma_\ell}{2} = \frac{1}{2}\left(\frac{\tau_t}{G} + \frac{\tau_\ell}{G}\right) = \frac{\tau}{G}$$

Therefore,

$$G = \frac{2[G_f b^2 + G_t(S_\ell h' - b^2)][G_f b^2 + G_\ell(S_t h' - b^2)]}{S_\ell h'[G_f b^2 + G_\ell(S_t h' - b^2)] + S_t h'[G_f b^2 + G_t(S_\ell h' - b^2)]}$$

where,

$$G_t = \frac{S_t G_m[G_f\lambda'' + G_m(1-\lambda'')]}{bG_m + (S_t - b)[G_f\lambda'' + G_m(1-\lambda'')]}$$

$$G_\ell = \frac{S_\ell G_m[G_f\lambda'' + G_m(1-\lambda'')]}{bG_m + (S_\ell - b)[G_f\lambda'' + G_m(1-\lambda'')]}$$

and $$\lambda'' = \frac{b}{h'}$$

In retrospect, it should be mentioned that the preceeding analysis involves simplifying assumptions which should remain true for small displacements of thin plates (or shells). The intent of the analysis is to provide relatively simple, but meaningful expressions for the equivalent, orthotropic properties. Model geometry and constituent material properties are parameterized in order to reproduce prescribed equivalent properties.

8. APPLICATION TO SPACE STRUCTURES

The design and development of flexible orbital structures proposed for the future will require an accurate prediction of the structural deformations and dynamic loads encountered in a space environment. Some of the typical configurations that may be deployed during the next decade are:

a. Orbiting space stations such as the Apollo Applications Program (AAP) Orbital Workshop and the Manned Orbital Laboratory (MOL). The maximum dimension of such stations may be several hundred meters;

b. Dish antennas or radio telescopes with maximum dimensions of several hundred meters; very large radio telescopes with typical dimensions of several thousand meters.

The longest characteristic elastic periods of these structures may range from approximately 5 seconds for the manned space stations to values greater than 1000 seconds for the radio telescopes. The dynamic disturbances which influence these large artificial satellites are, in many instances, of a magnitude that is insignificant in the analysis of current, relatively stiff, space structures.

The dynamic behavior of AAP and MOL class space stations is characterized by the interaction between various dynamic disturbances including elastic deformations, rigid body motions and liquid motions. The dynamic behavior of large antennas or radio telescope structures, deployed and stabilized by centrifugal forces, can be affected by the interaction between the geomagnetic field and induced currents. Additionally, thermal distortions and distortions induced through photon pressure and the interaction of spin rate with the gravity gradient may produce appreciable elastic deformations.

An indicative (but not dimensionless) parameter that may be used to define the regimes of dynamic model simulation for vibration testing is the logarithm of the quotient of the characteristic maximum prototype dimension divided by the square of the fundamental prototype frequency, $\log (\ell/f^2)$. Table 8.1 shows approximate model simulation regimes. The characteristic dimension is measured in meters and the frequency in Hertz.

Table 8.1 Approximate Model Simulation Regimes for Vibration Testing

Scaling Parameter Log (ℓ/f^2)	Method of Dynamic Simulation	Configuration Applicability
-2	Predominately full-scale testing; some replica scale models	Small Launch Vehicles
0		
2	Direct geometric models; some distorted geometric models	AAP, MOL, etc.; Large Launch Vehicles
4	General geometric models (geometric simulation, distorted physical properties)	100-Meter Antenna, etc.
6		
8		
10	Completely distorted models	1500-Meter Radio Telescope, etc.

8.1 Scaling of Manned Orbital Configurations

The use of direct geometric scaling using similar materials is, in general, feasible for these configurations. This replica scaling will automatically satisfy structural scaling laws but, unfortunately is restricted by manufacturing and tolerance control limitations that arise in small scale models. Also, replica scaling cannot be used to simulate slosh effects. These limitations are discussed in Chapter 9. In those areas where direct replica scaling is not possible, equivalent distorted scaling techniques must be considered. Distorted scaling of shell-like structures is discussed in Chapter 7. The equivalent distorted scaling techniques must be carefully analyzed to ensure that the portion of the structure simulated by these techniques will deform in a manner similar to the prototype. Distorted scaling usually neglects some scaling parameters that are not important to the simulation of an individual phenomonon in order to preserve the more important parameters.

8.2 Scaling of Antennas and Radio Telescopes

The overall complexity and relatively small dimensions of the individual structural members of these configurations precludes the use of replica scaling. Adequate component strength for assembly and testing in the 1-g earth environment requires a much stiffer structure than would result from direct scaling. Frequencies of the model structures typically should exceed by one or two orders of magnitude the frequencies which result from direct scaling. Model masses may be two to four orders of magnitude higher than the equivalent directly scaled masses. In general, it should be possible to construct a limited distorted dynamic model that preserves the overall geometry but does not reproduce exactly the local geometries of the prototype.

Because the structural frequencies of large orbital structures are very low, the elastic vibration modes will couple with the gravity gradient induced mode (Ref 8.1). These modes will also respond to the excitation caused by local variations of the geocentric gravity field. In addition to gravity gradient effects, large structural deformations may be caused by periodic thermal expansion and by the incident solar wind.

MacNeal (Ref 8.2) discusses several of these effects in relation to a typical 1500-meter radio telescope and concludes that the maximum total photon pressure load is approximately 1/15 of the axial component of tension in the spiral fibers due to spin. Further, when it is assumed that the ratio of fiber stress to axial load is the same for the two conditions, the resulting reflector stresses are approximately ten times the stress due to the gravity gradient. A comprehensive investigation of gravity gradient-induced stresses in an axisymmetric body rotating about an axis perpendicular to the orbital plane can be found in Reference 8.3.

8.2.1 Simulation of Thermal Effects

The thermal modeling analysis of space structures is based upon the assumption that the structure is operating in a high vacuum environment. Therefore, the only thermal considerations are heat transfer by radiation and heat conduction within the structure.

The functional expression for the rate of internal heat production is

$$q = f(k, H, c, \sigma, \varepsilon, \alpha, \ell, t, \tau)$$

where q = rate of internal heat production/unit volume, Q/L^3T

k = thermal conductivity, Q/LTR

H = radiation intensity, Q/L^2T

c = heat capacity/unit volume, Q/L^3R

σ = Stefan-Boltzmann constant, Q/L^2TR^4

ε = emissivity,

α = absorptivity,

ℓ = characteristic length, L

t = time, T

τ = temperature, R.

The basic variable dimensions (Q, L, T, R) yield six independent scaling relations

$$\pi_1 = \varepsilon, \qquad \pi_2 = \alpha, \qquad \pi_3 = kt/c\ell^2,$$

$$\pi_4 = \sigma\tau^3\ell/k, \quad \pi_5 = H\ell/k\tau, \text{ and } \quad \pi_6 = q\ell^2/k\tau.$$

Other sets of non-dimensional groups might be obtained from the fundamental expression. This group is particularly convenient for dynamic scale modeling as each term, where possible, contains the characteristic length parameter (ℓ). Thus, it is possible to relate the several scaling parameters to the model-to-prototype scale factor.

Two methods of thermal simulation can be developed. These methods are:

a. Maintain identical temperature time histories for model (m) and prototype (p) with no material restrictions, or

b. Maintain identical materials for model (m) and prototype (p) and predict the temperature time histories.

The similitude requirements for the two cases, developed from π_1 through π_6, are presented in Table 8.2. The parameter n defines the length scale factor, $n = \ell_m/\ell_p$.

Table 8.2 Thermal Modeling Similitude Requirements

Temperature Time History Identical	Materials Identical
$\tau_m/\tau_p = 1$	$k_m/k_p = 1$
$H_m/H_p = 1$	$c_m/c_p = 1$
$k_m/k_p = 1$	$t_m/t_p = n^2$
$t_m/t_p = n(c_m/c_p)$	$\tau_m/\tau_p = n^{-1/3}$
$q_m/q_p = 1/n$	$q_m/q_p = n^{-7/3}$
	$H_m/H_p = n^{-4/3}$
$\varepsilon_m = \varepsilon_p$, $\alpha_m = \alpha_p$, $\sigma_m = \sigma_p$	

The concept of maintaining identical temperature time histories appears to be advantageous where steady state temperature conditions are involved. The advantage of either method is not obvious when transient thermal conditions are considered. A complete discussion of thermal similitude requirements for spacecraft models can be found in Reference 8.4.

8.2.2 Simulation of Gravity Gradient Effects

The necessity to scale the influence of the gravity gradient on large space structures depends upon the oscillatory period of the fundamental mode. When this period exceeds about 1000 seconds, the orbital structure cannot be regarded as an independent system. At higher structural frequencies there is sufficient frequency separation between elastic vibrations and gravity gradient-induced rigid-body oscillations and the coupling between these two types of modes can be disregarded.

Consider, for example, a beam-like space structure rotating about its center of mass (Fig. 8.1). A circular orbit is assumed.

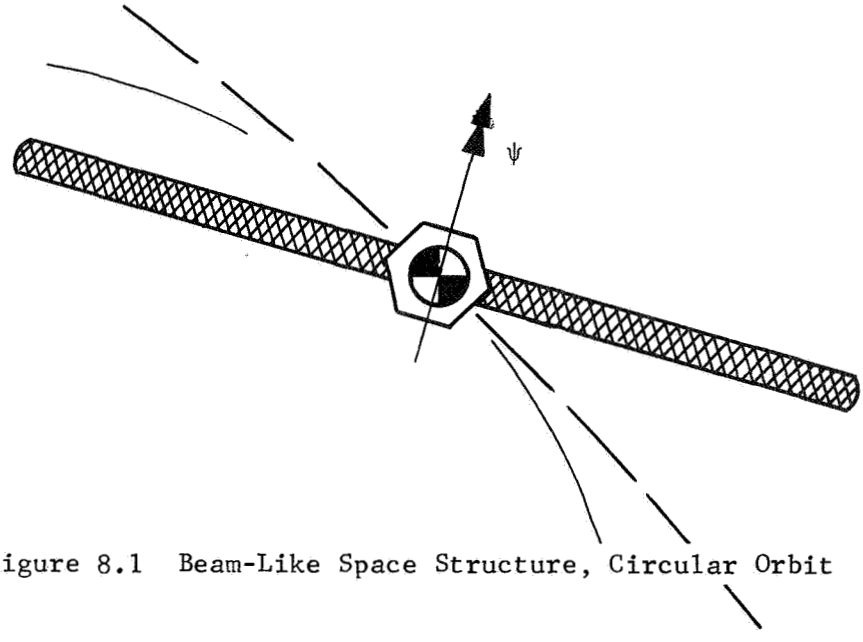

Figure 8.1 Beam-Like Space Structure, Circular Orbit

The longitudinal structural deformation can be expressed in functional form as

$$\delta = f(m, \ell, AE, \psi, \partial G/\partial R, \tau, t)$$

where δ = longitudinal deformation, L

ℓ = characteristic length, L

AE = extensional stiffness, F

ψ = beam rotation rate, 1/T

$\partial G/\partial R$ = gravity gradient, $1/T^2$

τ = orbital period, T

t = time, T.

The functional relationship contains eight variables in three basic dimensions. The principles of Chapter 3 indicate that five non-dimensional scaling relations exist. They are

$$\pi_1 = \delta/\ell, \qquad \pi_2 = m\ell^2\psi^2/AE, \qquad \pi_3 = t\psi,$$

$$\pi_4 = t/\tau \qquad \text{and} \qquad \pi_5 = (\partial G/\partial R)\tau^2.$$

The scaling relationships obtained from the above can be expressed in terms of the length scale ($n = \ell_m/\ell_p$) and the material properties as

$$\delta_m/\delta_p = n, \quad \psi_m/\psi_p = [m_p(AE)_m/m_m(AE)_p]^{1/2}/n,$$

$$t_m/t_p = \psi_p/\psi_m, \quad \tau_m/\tau_p = \psi_p/\psi_m,$$

$$\text{and} \quad (\partial G/\partial R)_m/(\partial G/\partial R)_p = (\psi_m/\psi_p)^2.$$

The use of a centrifuge for model simulation of the gravity gradient is considered to be feasible. A possible test configuration is shown schematically in Figure 8.2

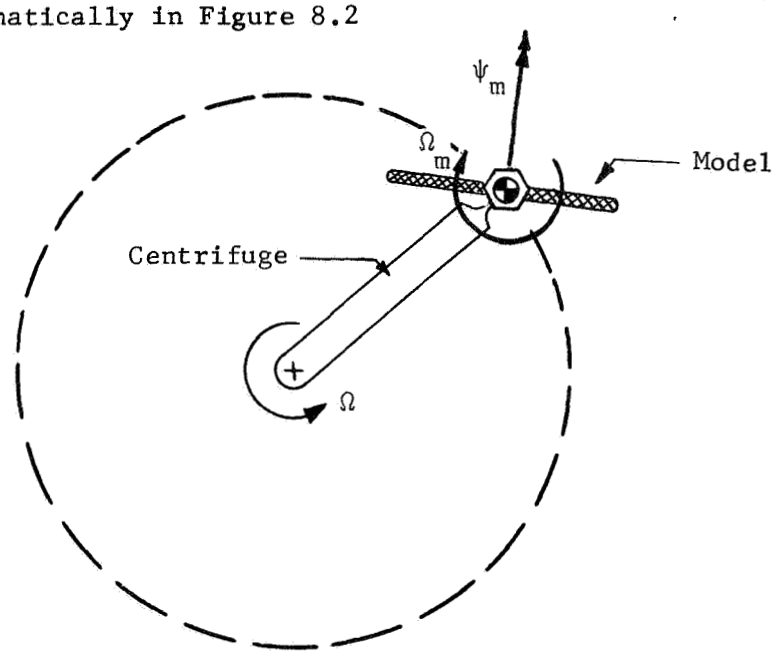

Figure 8.2 Centrifuge for Gravity Gradient Simulation

The desired model gravity gradient defines the required centrifuge velocity,

$$\Omega = (\partial G/\partial R)_m^{1/2}.$$

The period scaling, defined by the above expression and π_5, is

$$\tau_m/\tau_p = (\partial G/\partial R)_p^{1/2}/\Omega$$

and the velocity scaling is

$$\psi_m/\psi_p = \Omega/(\partial G/\partial R)_p^{1/2}.$$

The stiffness scaling, from π_2, is

$$(AE)_m/(AE)_p = n^2(m_m/m_p)\Omega^2/(\partial G/\partial R)_p.$$

An additional angular velocity, Ω_m, must be applied initially to the model to compensate for the relative motion between model and artificial gravity gradient vector. This velocity is

$$\Omega_m = \Omega + 1/\tau_m.$$

9. LIMITATIONS AND ECONOMICS OF DYNAMIC MODELS

The following sections define some of the major limitations associated with the simulation of full scale dynamic characteristics and the economic aspects of model design and construction.

9.1 Limitations

i) Manufacturing limitations--for very small scale factors it becomes very difficult to reproduce exactly the local geometry of the full scale configuration; errors due to material tolerances are increased.

ii) Non-linear structural effects--at certain loads conditions local skin buckling may occur.

iii) Aerodynamic effects--direct scaling of aerodynamic effects may not be possible under certain test conditions.

9.1.1 Manufacturing Limitations

The reproduction of launch vehicle configurations to small scale factors is restricted by the manufacturing limitations. Scale factors as low as 0.30 should cause no manufacturing problems for current launch vehicle configurations; at smaller scale it becomes increasingly more difficult to reproduce exactly the local geometry of stiffened shells, truss-like structures, and propellent tank walls. In addition, rivets and other fasteners become unreasonably small and the assembly of components by welding is no longer possible. An excellent example is found through examination of the prototype Saturn V vehicle. Typical second stage tank geometry and second-to-third stage adapter geometry (Ref 9.1) are shown in Figures 9.1 and 9.2. Note that at 10% scale factor skin thicknesses less than 0.005" would be realized in a model that is almost 40' high.

In order to keep model manufacturing costs within allowable limits, it is usually necessary to work with commercially available stock and thus eliminate costly manufacturing processes. Tolerances on available stock materials limit the accuracy of model calculations and the use of such stock introduces increasingly serious limitations as the proposed scale factor is diminished. The problem can be minimized by selective sizing of stock and by measuring the actual dimensions of the scaled structure.

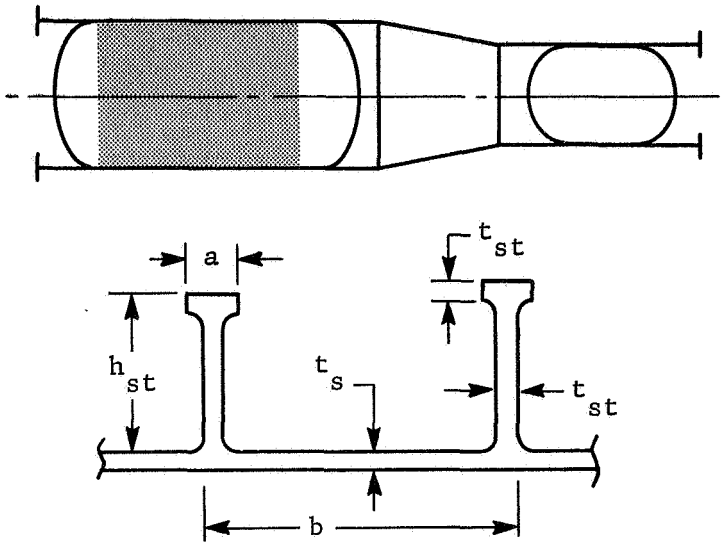

Prototype Dimensions, Inches	
b = 9.93	a = 0.365
t_s = 0.167	h_{st} = 1.21
t_{st} = 0.048	

Figure 9.1 Tank Wall Properties, Second Stage, Saturn V

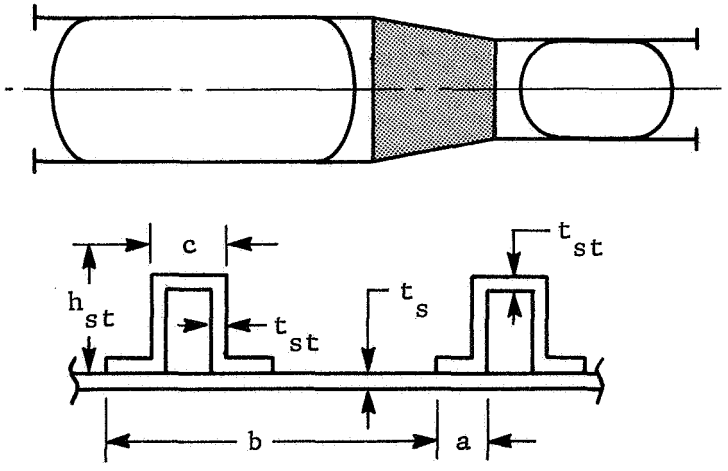

Prototype Dimensions, Inches	
b = 4.50	a = 0.816
t_s = 0.068	h_{st} = 1.360
t_{st} = 0.0714	c = 1.360

Figure 9.2 Adapter Properties, Second to Third Stage, Saturn V

9.1.2 Non-Linear Structural Effects

Several existing directly scaled models have exhibited a high degree of fidelity in their ability to reproduce accurately the dynamic characteristics of the prototype vehicle; the two best examples being the 10%-scale Saturn V (Ref 9.2) and the 20%-scale Titan III (Ref 9.3) models. However, while these models have exhibited excellent overall dynamic reproduction of their full-scale counterparts, in certain instances they have also exhibited certain of the limitations of the direct scaling approach. The necessity to reproduce the shell structure which comprises a major portion of this type of configuration requires that the model be relatively large. Nevertheless, in certain areas of the vehicle the resulting skin gages may still be inadequate to resist the assembly stresses caused by the integration of several components into the complete model. Imperfections of this type are inevitable when direct geometric scaling is employed and it may be necessary in the future to consider scaling techniques whereby direct scaling is applied to those areas of the vehicle where skin gage will permit and other, more critical areas employ distorted scaling.

9.1.3 Aerodynamic Effects

The direct scaling has only limited application in the area of aerodynamic testing due primarily to the restraints imposed by available tunnel facilities. The investigation of wind-induced oscillations on a Titan III model (Ref 9.4) illustrates this point. A 7.5% dynamically scaled model of the Titan III vehicle, transporter launch frame and umbilical mast was constructed in addition to a 7.5% geometrically scaled model of the umbilcal tower. The model simulated the mode shape and frequency characteristics of the full scale launch vehicle, umbilical mast and transporter.

The requirements for accurate dynamic scaling of this type of model are:

Matched Reynolds Number; $Re = \frac{\rho V \ell}{\mu}$,

Matched Strouhal Number; $S = \frac{\omega \ell}{V}$,

and matched model to air density ratio.

However, the tunnel imposed conditions (NASA Langley Research Center, 16-foot transonic tunnel) which arose due to the use of Freon 12 as the test medium were:

$$\rho_{TUNNEL}/\rho_{AIR} = 3.7$$

$$\mu_{TUNNEL}/\mu_{AIR} = 0.757$$

and it was therefore not possible to scale the stiffness of an unfueled vehicle without exceeding the scaled mass distribution. A compromise in the form of a mismatch in either Reynolds number or mass distribution was necessary and the former was selected as being the least severe. It is important to note that the Reynolds number of the model test in the tunnel will usually be much lower than the true flight condition (in the wind-induced oscillation test it was 45% of the full-scale value) but there is little that can be done to alleviate this problem. Test conditions should be chosen to make the Reynolds number as high as possible but the full-scale value will seldom be approached.

9.1.4 Structural Damping Effects

Structural damping is a phenomenon strongly dependent not only on the type of construction but on material finish, pressure in the joints caused by rivets or other fasteners (Ref 9.5), non-structural items mounted on primary structure, etc. Limited data is available on modal damping of models and for that reason no statistical evaluation is possible. However, a rather complete set of damping ratios was obtained during the Titan III model vibration test (Ref 2.3). Figure 2.8 (taken from Ref 2.3) shows the trend of damping ratios for lateral and longitudinal modes. No full scale corresponding values are available, consequently no conclusions can be drawn. The inability to assess the prototype model damping coefficient from model tests makes the use of dynamically similar models for design purposes somewhat questionable. This fact becomes even more so when unconventional structures are dealt with where no known previous damping data are available.

9.2 Economic Aspects

It does not seem logical to design and fabricate a model whose overall cost is greater than that of a prototype. On the other hand the manufacture of an inexpensive model may result in misleading and even incorrect data due to manufacturing simplifications which yield an incorrect dynamic simulation of the

full scale structure. It becomes essential to consider the overall optimization of the economic situation in order to achieve a realistic model test program - a program yielding results within prescribed tolerance levels and, at the same time, a program within allowable budgetary limits.

The study of the economics of dynamic model testing may, in a very general sense, be divided into four major categories:

i) Model design and construction

ii) Required test facilities, equipment and instrumentation

iii) Model testing

iv) Data acquisition and analysis.

Approximately 30 elastically scaled dynamic models of aircraft and launch vehicles were surveyed to establish dynamic modeling costs. Data collected included method of construction, total cost of model, estimated engineering cost, material cost, and a measure of simulation quality (the approximate number of modes simulated by the model). It was established that the method of construction and the approximate number of modes simulated, rather than model size or weight, defined model costs. The summary of the results of this survey is shown in Figure 9.3.

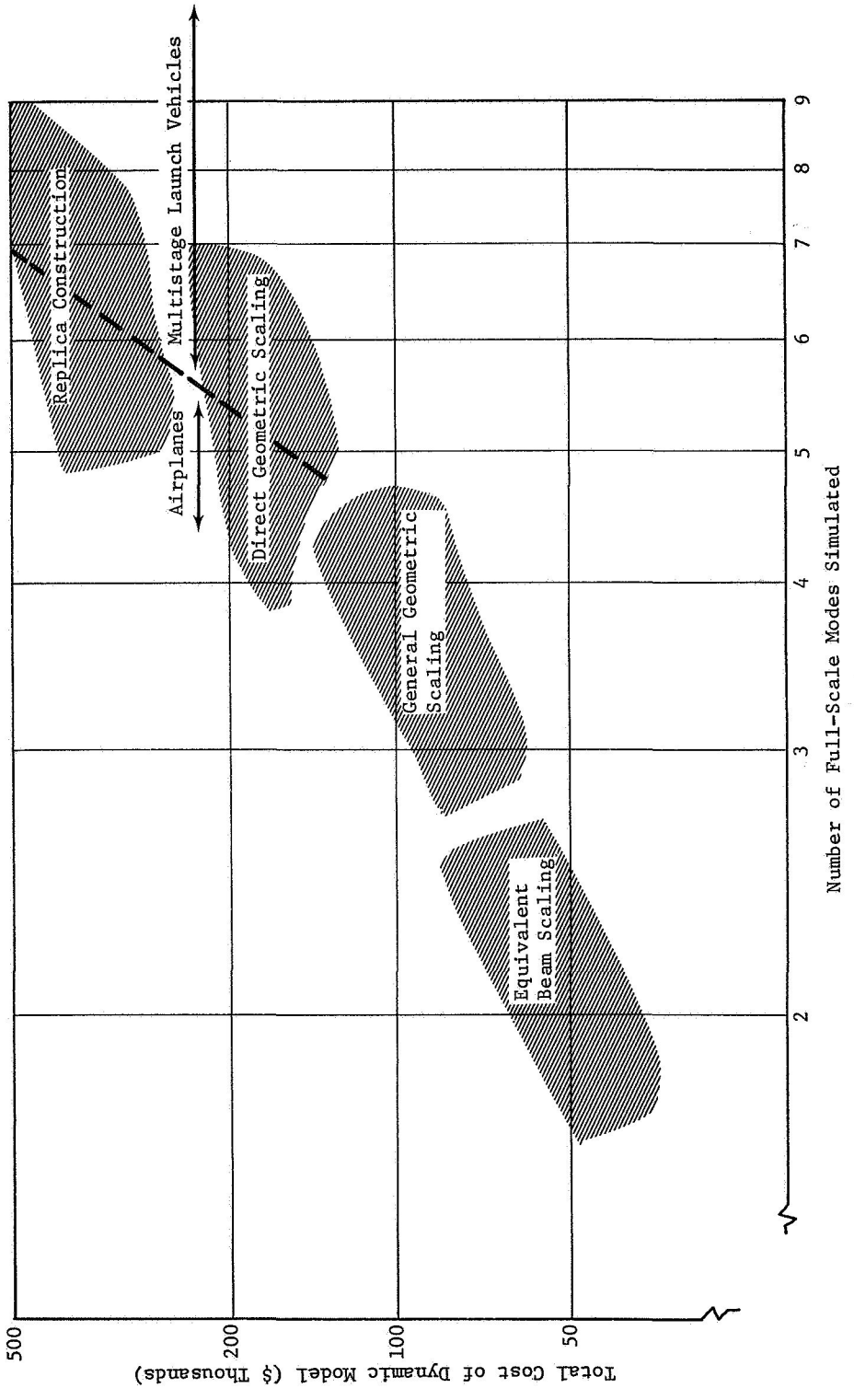

Figure 9.3 Dynamic Model Cost

10. CONCLUSIONS AND RECOMMENDATIONS

A comprehensive summary of the dynamic scaling laws applicable to current launch vehicle configurations is presented. Primary consideration is directed to the study of direct geometric scaling using similar materials (replica scaling) although, where applicable, certain distorted scaling techniques are considered.

A review of the current state-of-the-art regarding launch vehicle dynamic models indicates that the several vibration survey models used to either augment or replace the usual analytical investigation have exhibited faithful dynamic representation. Additionally, dynamic models used for aeroelastic investigations (e.g., wind-induced oscillations, buffet) have yielded satisfactory results in view of the limiting conditions imposed by available wind tunnels. A more extensive investigation of aerodynamic scaling and the restrictions imposed by the failure to exactly match all the required scaling parameters is recommended.

A simple matrix procedure which regularizes the derivation of scaling parameters to the extent that they can be developed through digital computer analysis is detailed. This procedure has no known previous application and is considered to be a substantial improvement over existing methods. Most of the scaling parameters presented here were developed using this procedure.

The scaling laws applicable to beam-like structures are summarized and the advantage of replica scaling, where possible, is emphasized. Simulation of uncoupled bending or torsional vibration is discussed and it is concluded that replica scaling is, where viscoelastic materials are concerned, impossible. An investigation of propellant slosh effects in beam-like tanks indicates the feasibility of simulating boost acceleration levels in a 1-g test environment through the proper adjustment of physical properties and time scale. A study of load and response scaling indicates that geometric similarity is not required to simulate these phenomena.

Simulation requirements for shell-like structures including isotropic and orthotropic cylindrical shells are summarized. This summary includes a study of coupled elastic-slosh modes and it is concluded that distorted scaling is required if small scale models are used to simulate the boost acceleration environment. The need for further investigation of possible construction techniques to simulate slosh-elastic coupling is clearly indicated. An experimental program to build and test such a model, possibly using plastics loaded with metal powder and heavy liquids as the simulated propellants is recommended.

Scaling laws applicable to the simulation of both uncoupled and elastically coupled lateral propellant sloshing are developed and it is concluded that an arbitrary prototype acceleration can be simulated with an appropriate adjustment of the time scale. The difficulty is maintaining exact similitude in all structural parameters, due primarily to manufacturing limitations imposed upon small scale models, is emphasized. Scaling requirements for simultaneous simulation of two or more liquid effects are presented.

The distorted shell simulation methods developed during this study (truss-ring modeling, reinforced plastic modeling) have had no previous practical application. An experimental program oriented toward verification of these methods is being performed. The results of this study will give a reasonable indication of the applicability of these distorted scaling techniques.

Only a limited investigation of modeling techniques applicable to large space structures has been conducted. A serious need exists for a detailed theoretical and experimental program to investigate the modeling techniques required for the simulation of such structures in the test laboratory. Simulation of gravity gradient effects, photon pressure effects, cyclic radiative thermal effects and interaction of induced currents with the Earth's magnetic field are possible areas of study. These effects, while insignificant to the "small" and rigid structures of the usual Earth environment (including launch vehicles), will couple with the structural dynamic deformations of large, and relatively light, orbital structures. The modeling techniques necessary to simulate these structures in a space environment will be established only through continued and intense research studies.

11. REFERENCES

2.1 S. A. Leadbetter and J. P. Raney: "Analytical and Experimental Studies of the Dynamics of Launch Vehicles." AIAA 1st Symposium on Structural Dynamics and Aeroelasticity, Boston, Mass., 1965.

2.2 H. L. Runyan: "Some Research Related to the Structural Dynamics of Launch Vehicles." Sixth International Symposium on Space Technology and Science, Tokyo, Japan, 1965.

2.3 I. J. Jaszlics and G. Morosow: "Dynamic Testing of a 20%-Scale Model of the Titan III." AIAA 1st Symposium on Structural Dynamics and Aeroelasticity, Boston, Mass., 1965.

2.4 I. J. Jaszlics: The Titan III Dynamic Model Test Program. 15. Raketen-und Raumfahrttagung, Bremen, Germany, 1966.

2.5 P. W. Hanson and R. V. Doggett: Aerodynamic Damping and Buffet Response of an Aeroelastic Model of the Saturn I, Block II Launch Vehicle. NASA TN D-2713, 1965.

2.6 P. W. Hanson and R. V. Doggett: Aerodynamic Damping of the 0.02 Scale SA-1 Model Vibrating in the First Free-Free Bending Mode. NASA TN D-1956, 1963.

2.7 R. V. Doggett and P. W. Hanson: An Aeroelastic Model Approach for the Prediction of Buffet Bending Loads on Launch Vehicles. NASA TN D-2022, 1963.

2.8 J. T. Uchiyama and F. W. Peters: "Buffet Response Measurements of a 7% Aeroelastically Scaled Model of Various Titan III Configuration." Thirty-Seventh Shock and Vibration Symposium, Orlando, Florida, 1967.

2.9 J. E. Robertson and T. R. Brice: Buffet Response of Aeroelastically Scaled Titan III Missile Configurations at Transonic Mach Numbers. TR-67-33. Arnold Engineering Development Center, Tullahoma, Tenn., 1967.

2.10 J. E. Robertson and T. R. Brice: Buffet Response and Aerodynamic Damping Characteristics of Aeroelastically Scaled Titan III/MOL Configurations at Transonic Speeds. TR-67-178. Arnold Engineering Development Center, Tullahoma, Tenn., 1967.

2.11 F. W. Peters: Phase II Titan III 7.5%-Scale Model Wind-Induced Oscillation Wind Tunnel Test, Final Data Analysis and Applications Report. SSD-CR-66-63. Martin Marietta Corporation, Denver, Colo., 1966.

2.12 Meeting on Ground Wind Load Problems in Relation to Launch Vehicles. Compilation of papers presented at the NASA Langley Research Center, 1966.

2.13 J. A. Cisneros: Modal Shape, Modal Deflection and Modal Frequency Tolerance Study for the Titan IIIC, Stage 0, Flight Plan VIII. Dynamics Memo 76. Martin Marietta Corporation, Denver, Colo., 1965.

2.14 G. Morosow: "Dynamic Characteristics of Titan III." Society of Automotive Engineers Aeronautics and Space Engineering and Manufacturing Meeting, Los Angeles, Calif., 1966.

3.1 E. Buckingham: "On Physically Similar Systems." Phys. Rev., Vol. 4, 1914, p. 345.

3.2 Rayleigh: "Stability of Flow of Fluids." Phil. Mag., Vol. 34, 1892, p. 59.

3.3 Rayleigh: "Investigations in Capillarity." Phil. Mag., Vol. 34, 1892, p. 59.

3.4 Rayleigh: "The Principle of Similitude." Nature, Vol. 95, 1915, p. 66.

3.5 G. Murphy: Similitude in Engineering. Ronald Press, New York, New York, 1950.

3.6 P. W. Bridgmon: Dimensional Analysis. Yale University Press, New Haven, Conn., 1931.

3.7 H.L. Langhaar: Dimensional Analysis and Theory of Models. John Wiley and Sons, New York, New York, 1951.

6.1 H. N. Abramson (Ed): The Dynamic Behavior of Liquids in Moving Containers. NASA SP-106, 1966.

6.2 H. F. Bauer: The Damping Factor Provided by Flat Annular Ring Baffles for Free Fluid Surface Oscillations. MTP-AERO-62-81, NASA Marshall Space Flight Center, 1962.

6.3 M. A. Silveira, D. G. Stephens and H. W. Leonard: An Experimental Investigation of the Damping of Liquid Oscillations in Cylindrical Tanks with Various Baffles. NASA TN D-715, 1961.

6.4 D. G. Stephens, H. W. Leonard and M. A. Silveira: An Experimental Investigation of the Damping of Liquid Oscillations in a Oblate Spheroidal Tank With and Without Baffles. NASA TN D-808, 1961.

6.5 J. W. Miles: "On the Sloshing of Liquid in a Flexible Tank." J. Appl. Mech, June 1958.

6.6 U. S. Lindholm, W. H. Chu, D. D. Kana and H. N. Abramson: "Bending Vibrations of a Circular Cylindrical Shell Containing an Internal Liquid with a Free Surface." AIAA Journal, Vol. 1, No. 9, Sept., 1963.

6.7 J. S. Mixson and R. W. Herr: An Investigation of the Vibration Characteristics of Pressurized Thin-Walled Circular Cylinders Partially Filled with Liquid. NASA TR R-145, 1962.

6.8 M. L. Baron and H. H. Bleich: The Dynamic Analysis of Empty and Partially Full Cylindrical Tanks, Part I. DASA No. 1123A. Defense Atomic Support Agency, 1959.

7.1 C. Gros and K. Forsberg: Vibrations of Thin Shells, A Partially Annoted Bibliography. SB-63-43. Lockheed Missiles and Space Co., Sunnyvale, Calif., 1963.

7.2 R. J. McGratten and E. L. North: Vibration Analysis of Shells Using Discrete Mass Techniques. ASCE Specialties Conference, Los Angeles, Calif., 1965.

8.1 H. Ashley: "Observations on the Dynamic Behavior of Large Flexible Bodies in Orbit." AIAA Journal, March, 1967.

8.2 R. H. MacNeal: Vibration Modes of an Orbiting Radio Telescope. ARC-R-242. Astro Research Corporation, Santa Barbara, Calif., 1967.

8.3 W. M. Robbins, Jr.: Some Preliminary Design Studies for a Very Large Radiotelescope. NASA CR-573, 1966.

8.4 S. Katzoff: Similitude in Thermal Models of Spacecraft. NASA TN D-1631, 1963.

9.1 G. W. Morgan: A Study of High Strength-to-Weight Ratio Structures as Applied to Dynamically Scaled Models of Second and Third Stages of the Saturn V Space Flight Vehicle. SID64-1331-1, North American Aviation, Inc., 1965.

9.2 S. A. Leadbetter: Design and Fabrication Considerations for 1/10 Scale Replica Model of the Apollo/Saturn V. NASA TN D-4138, 1967.

9.3 I. J. Jaszlics: Program 624A 20% Scale Dynamic Model Ground Vibration Survey, Final Test Report. SSD-CR-65-47, Martin Marietta Corporation, Denver Division, 1965.

9.4 D. W. Olson and F. W. Peters: Titan III 7.5% Scale Wind-Induced Oscillation Test, Phase II Final Report. SSD-CR-66-64, Martin Marietta Corporation, Denver Division, 1966.

9.5 B. R. Hanks and D. G. Stephens: Mechanisms and Scaling of Damping in a Practical Structural Joint. The Shock and Vibration Bulletin, January 1967.

APPENDIX A

BIBLIOGRAPHY

Literature Surveys

Structural Modeling. Literature Search 523, Jet Propulsion Laboratory, Pasadena, California, 1963. (119 References).

Dynamic Scaling Laws for Structures Parts I and II. NASA Literature Search 5221, NASA Scientific and Technical Information Facility, 1967. (34 References).

General Applications

Abramson, H. N. and G. E. Nevill: "Some Modern Developments in the Application of Scale Models in Dynamic Testing." Use of Models and Scaling in Shock and Vibration, ASME, 1963.

Crandall, S. H.: On Scaling Laws for Material Damping. NASA TN D-1467, 1962.

Ezra, A. A.: "Scaling Laws and Similitude Requirements for Valid Scale Model Work." Use of Models and Scaling in Shock and Vibration, ASME, 1963.

Goodier, J. N. and W. T. Thompson: Applicability of Similarity Principles to Structural Models. NACA TN-933 1944.

Gray, C. L.: Study in the Use of Structural Models for Sonic Fatigue. ASD-TR-61-547. Aeronautical Systems Division, U. S. Air Force, 1962.

Lee, R. H. and E. S. Levinsky: On the Non-Equilibrium Locally Similar Boundary Layer with Scaling Applications. ASD-TDR-63-160. Ballistic Systems Division, U. S. Air Force, 1963.

O'Sullivan, W. J.: Theory of Aircraft Structural Models Subject to Aerodynamic Heating and External Loads. NACA TN-4115, 1957.

Sedov, L. I.: Similarity and Dimensional Methods in Mechanics. Academic Press, New York, New York, 1959.

Soper, W. G.: "Dynamic Modeling with Similar Materials." Use of Models and Scaling in Shock and Vibration, ASME, 1963

Soper, W. G.: "Scale Modeling." International Science and Technology, February, 1967.

White, R. W., K. E. Eldred and W. H. Roberts: Investigation of a Method for the Prediction of Vibratory Response and Stress in Typical Flight Vehicle Structures, ASD-TDR-62-801. Aeronautical Systems Division, U. S. Air Force, 1963.

Proceedings of Symposium on Aeroelastic and Dynamic Modeling Technology. RTD-TDR-63-4197. Research and Technology Division, U. S. Air Force, 1963.

Applications to Launch Vehicles

Arcilesi, C. J. and C. R. Bruck: "Investigation of Dynamic Characteristics of a 1/20-Scale Model of the Launch Phase Simulator." The Shock and Vibration Bulletin, Bulletin 35, Part 3, 1966.

Kelly, T. C.: Effects of Model Geometric Accuracy on Comparison of Wind Tunnel and Flight Pressure Measurements on a Launch Vehicle. NASA TN D-3276, 1966.

McCoy, M. E., et al: "Application of the Direct Stiffness Method to the Elastic Mathematical Modeling of the Saturn S-IB." The Shock and Vibration Bulletin, Bulletin 35, Part 3, 1966.

Mixson, J. S.: Experimental Lateral Vibration Characteristics of a 1/5-Scale Model of Saturn SA-1 with an Eight Cable Suspension System. NASA TN D-2214, 1964.

Reed, W. H.: Models for Obtaining Effects of Ground Winds on Space Vehicles Erected on the Launch Pad. Conference on the Role of Simulation in Space Technology, VPI, Blacksburg, Va., 1964.

Regier, A. A.: "The Use of Scaled Dynamic Models In Several Aerospace Vehicle Studies." Use of Models and Scaling in Shock and Vibration, ASME, 1963.

Roberts, W. H., K. M. Eldred and R. W. White: "Utilization of Dynamically Similar Structural Models in Predicting Vibration Response of Flight Vehicles." Shock, Vibration and Associated Environments, Bulletin 31, 1963.

Runyan, H. L., H. G. Morgan and J. S. Mixson: "Role of Dynamic Models in Launch Vehicle Development." Experimental Techniques in Shock and Vibration, ASME, 1963.

Sandorff, P. E.: Principles of Design of Dynamically Similar Models for Large Propellant Tanks. NASA TN D-99, 1960.

Thompson, W. M.: An Investigation of the Response of a Scaled Model of a Liquid Propellant Multistage Launch Vehicle to Longitudinal Excitation. NASA TN D-3975, 1967.

Umsen, G. N. and R. J. Schramm: A Study of the Feasibility of Fabricating and Testing a Scaled Model of the Titan III-Four Segment Solid Booster Configuration with Payload. The Martin Company, Denver, Colorado, 1962.

Applications to Space Structures

Brewer, W. N. and N. L. Jeppeson: "Methods of Evaluation of Inflatable Structures for Space Applications." AIAA 5th Annual Structures and Materials Conference, Palm Springs, California, 1964.

Brooks, G. W.: "Techniques for Simulation and Analysis of Shock and Vibration Environments of Space Flight Systems." Experimental Techniques in Shock and Vibration, ASME, 1962.

Fowle, A. A., F. Gabron and J. M. F. Vickers: "Thermal Scale Modeling of Spacecraft: An Experimental Investigation." J. Spacecraft Rockets, Vol. 3, No. 4, 1966.

Greenspon, J. E.: Modeling of Spacecraft Under Random Loading. NASA CR-132, 1964.

Hassell, J. L.: Investigation of the Low-Subsonic Stability and Central Characteristics of a 0.34-Scale Free-Flying Model of a Modified Half-Cone Re-Entry Vehicle. NASA TM X-665, 1962.

Morgan, G. W.: "Scaling Techniques for Orthotropic Cylindrical Aerospace Structures." AIAA 5th Annual Structures and Materials Conference, Palm Springs, California, 1964.

Nevill, G. E.: Similitude Studies of Re-Entry Vehicle Response to Impulsive Loading. AFSWC-TDR-63-1. Air Force Special Weapons Center, U. S. Air Force, 1963.

Yu, S. Y. and J. E. Taber: "Steady State Dynamics of Large Spinning Net Configuration Structures." AIAA/ASME 8th Structures, Structural Dynamics and Materials Conference, Palm Springs, California, 1967.

APPENDIX B

B.1 ORTHOTROPIC SHELL SIMULATION USING TRUSS-RING MODULE

The scaling parameters for simulation of orthotropic cylindrical shells are

$$\pi_1 = d_s\lambda^2\omega^2/K_{xx}, \quad \pi_2 = K_{xy}/K_{xx}, \quad \pi_3 = K_{yy}/K_{xx},$$

$$\pi_4 = D_{xx}/K_{xx}\lambda^2, \quad \pi_5 = D_{xy}/K_{xx}\lambda^2, \quad \pi_6 = D_{yy}/K_{xx}\lambda^2,$$

$$\pi_7 = B_{xy}/K_{xx}, \quad \pi_8 = B_{xz}/K_{xx}, \quad \pi_9 = B_{yz}/K_{xx}$$

$$\text{and} \quad \pi_{10} = \lambda/\ell$$

where ω = frequency, $1/T$

d_s = surface mass density, FT^2/L^3

K_{xx}, K_{xy}, L_{yy} = extensional rigidities, F/L

D_{xx}, D_{xy}, D_{yy} = bending rigidities, FL

B_{xy} = in-plane shear rigidity, F/L

B_{xz}, B_{yz} = transverse shear rigidities, F/L

ℓ = characteristic length, L

λ = any length.

The relations between orthotropic shell parameters and truss ring module parameters (Section 7.1.6) are

Orthotropic Shell	Truss-Ring Module
K_{xx}	$(n/\pi)(AE/R)(d/\ell)^3$
K_{yy}	A_rE_r/d
D_{yy}	E_rI_r/d
B_{xy}	$(n/\pi)(AE/R)(d/\ell)(a/\ell)^2\cos(\alpha/2)$

Orthotropic Shell	Truss-Ring Module
K_{yx}	$(n/\pi)(AE/2R)(d/\ell)(a/\ell)^2$
ν_e	$(n/\pi)(E/E_r)(A/A_r)(a/d)(d/\ell)^3(a/2R)$

where n = number of joints on one side of ring,

R = radius of ring centerline,

d = longitudinal distance between ring centerlines,

ℓ = length of truss bar, $\ell^2 = a^2 + d^2$,

$\alpha = \pi/n$,

$a = 2R \sin(\alpha/2)$,

A = area of truss bar,

E = modulus of elasticity of truss bar,

A_r = area of ring,

E_r = modulus of elasticity of ring,

I_r = area moment of inertia of ring.

and ν_e is the equivalent Poisson's ratio.

The computational procedure for truss-ring module design is based upon knowledge of the prototype rigidities.

$$K_{xx_p}, K_{yy_p}, D_{yy_p} \text{ and } B_{xy_p}$$

and specified values of the model-to-prototype ratios

$$d_{s_m}/d_{s_p}, \lambda_m/\lambda_p \text{ and } \omega_m/\omega_p.$$

If values for n, R, E and E_r are selected, the unknown model parameters can be established. The truss rod spacing is

$$a = 2R \sin(\alpha/2) \qquad \text{(B.1-1)}$$

where $\alpha = \pi/n$. The truss ring spacing can be established from the scaling relation

$$B_{xy_m}/K_{xx_m} = \pi_7 = B_{xy_p}/K_{xx_p} = (a/d)^2 \cos(\alpha/2)$$

and is

$$d = a[\cos(\alpha/2)K_{xx_p}/B_{xy_p}]^{1/2}. \qquad (B.1\text{-}2)$$

The truss rod length is then

$$\ell = [a^2 + d^2]^{1/2}. \qquad (B.1\text{-}3)$$

The truss rod cross-sectional area can be established from the similitude requirement

$$d_{s_m}\lambda_m^2\omega_m^2/K_{xx_m} = \pi_1 = d_{s_p}\lambda^2{}_p\omega^2{}_p/K_{xx_p}$$

and the scaling relation

$$K_{xx_m} = (n/\pi)(AE/R)(d/\ell)^3$$

and is

$$A = (R/E)(\pi/n)(\ell/d)^3 K_{xx_m} \qquad (B.1\text{-}4)$$

The truss ring cross-sectional area, established by the similitude requirement

$$K_{yy_p}/K_{xx_p} = \pi_3 = K_{yy_m}/K_{xx_m}$$

and the scaling relation

$$K_{yy_m} = A_r E_r/d,$$

is

$$A_r = (d/E_r)(K_{yy_p}/K_{xx_p})K_{xx_m} \qquad (B.1\text{-}5)$$

Likewise, the truss ring cross-sectional area, established by the similitude requirement

$$D_{yy_p}/K_{xx_p}\lambda^2_p = \pi_6 = D_{yy_m}/K_{xx_m}\lambda^2_m$$

and the scaling relation

$$D_{yy_m} = E_r I_r/d,$$

is

$$I_r = (d/E_r)(\lambda_m/\lambda_p)^2(D_{yy_p}/K_{xx_p})K_{xx_m} \qquad \text{(B.1-6)}$$

The equivalent Poisson ratio

$$\nu_e = (n/\pi)(E/E_r)(A/A_r)(a/d)(d/\ell)^3(a/2R)$$

may be written

$$\nu_e = [(n/\pi)(AE/R)(d/\ell)^3][(d/A_rE_r)(a/d)^2]/2$$

$$\nu_e = (a/d)^2(K_{xx_m}/K_{yy_m})/2$$

$$\nu_e = (a/d)^2(K_{xx_p}/K_{yy_p})/2 \qquad \text{(B.1-7)}$$

This procedure gives exact representation of the similitude requirements dictated by π_1, π_3, π_6 and π_7. Close simulation of π_2 will be achieved for realistic structures.

```
*IOCS(CARD,TYPEWRITER,KEYBOARD,1132 PRINTER,DISK)
C
C SCALING PROGRAM FOR SHELL SIMULATION
C INPUT PARAMETERS
C
C   SL = MODEL LENGTH / FULL-SCALE LENGTH
C   SF = MODEL FREQUENCY / FULL-SCALE FREQUENCY
C   SM = MODEL SURFACE MASS DENSITY / FULL-SCALE SURFACE MASS DENSITY
C   SXX = KXX FOR FULL-SCALE AT THIS SECTION (SECTION 5.2)
C   SYY = KYY FOR FULL-SCALE AT THIS SECTION (SECTION 5.2)
C   DYY = DYY FOR FULL-SCALE AT THIS SECTION (SECTION 5.2)
C   BXY = BXY FOR FULL-SCALE AT THIS SECTION (SECTION 5.2)
C
C REPEAT INPUT DATA FOR EACH CHANGE OF SECTION PROPERTIES
C STOP WITH BLANK CARD
C
    1 READ(2,100) SL,SF,SM,SXX,SYY,DYY,BXY
  100 FORMAT(7F10.0)
C
      IF(SL) 500,500,2
C
    2 CALL BASK(SL,SF,SM,SXX,SYY,DYY,BXY)
C
      GO TO 1
C
  500 STOP
      END



      SUBROUTINE BASK(SL,SF,SM,SXX,SYY,DYY,BXY)
C
C INPUT PARAMETERS
C    N = NUMBER OF JOINTS (N.GT.2)
C    R = RADIUS OF SHELL
C    E = TRUSS MODULUS OF ELASTICITY
C   ER = RING MODULUS OF ELASTICITY
C
      READ(2,100)N,R,E,ER
  100 FORMAT(I10,3F10.0)
C
      IF(N-2)5,10,10
    5 WRITE(3,200)
  200 FORMAT(40H NOT ENOUGH JOINTS SPECIFIED-ABORT CYCLE)
      GO TO 500
C
   10 CN=N
      ALFA=3.141593/CN
      A=2.*R*SIN(ALFA/2.)
      D=A*SQRT(COS(ALFA/2.)*SXX/BXY)
      XL=SQRT(A**2+D**2)
      SXXM=SXX*SM*SL**2*SF**2
      AROD=(R*3.141593*XL**3/(E*CN*D**3))*SXXM
      ARING=D*SYY*SXXM/(ER*SXX)
      XIRIN =D*SL**2*DYY*SXXM/(ER*SXX)
      SYYM=SXXM*SYY/SXX
      POIS=0.5*A**2*SXXM/(SYYM*D**2)
C
      WRITE(3,210)
  210 FORMAT(42H  SHELL SIMULATION USING TRUSS-RING MODULE///)
```

```
      WRITE(3,201)SL,SF,SM,SXX,SYY,DYY,BXY
  201 FORMAT(27H  MODEL-TO-PROTOTYPE RATIOS//6H  SL =,F7.3/6H  SF =,F7.3
     1/6H  SM =,F7.3//22H  PROTOTYPE RIGIDITIES//7H  KXX =,E14.6/
     27H  KYY =,E14.6/ 7H  DYY =,E14.6/7H  BXY =,E14.6///)
      WRITE(3,202)N,R,E,ER
  202 FORMAT(36H  TRUSS-RING MODULE INPUT PARAMETERS//20H  NUMBER OF JOI
     1NTS =,I4/10H  RADIUS =,F6.3/31H  TRUSS MODULUS OF ELASTICITY =,
     2E14.6/30H  RING MODULUS OF ELASTICITY =,E14.6///)
      WRITE(3,203)A,D,XL,AROD,ARING,XIRIN
  203 FORMAT(37H  TRUSS-RING MODULE OUTPUT PARAMETERS//5H  A =,E14.6/
     15H  D =,E14.6/5H  L =,E14.6/18H  TRUSS ROD AREA =,E14.6/19H  TRUSS
     2 RING AREA =,E14.6/37H  TRUSS RING AREA MOMENT OF INERTIA =,E14.6/
     3//)
      WRITE(3,204)POIS
  204 FORMAT(28H  EQUIVALENT POISSON RATIO =,E14.6///)
      WRITE(3,205)
  205 FORMAT(51H  SCALING TERMS SATISFIED = PI(1),PI(3),PI(6),PI(7)//
     162H  SCALING TERMS NOT SATISFIED = PI(4),PI(5),PI(8),PI(9),PI(10)/
     2/39H  SCALING TERM APPROX SATISFIED = PI(2))
C
  500 CONTINUE
      RETURN
      END
```

B.2 ORTHOTROPIC SHELL SIMULATION USING REINFORCED PLASTIC MODEL

The computational procedure to determine the reinforced shell model properties is based upon the physical model shown in Figure 7.7 and described in detail in Section 7.2. The notation is that of Section 7.2.

The approximate wall thickness, fiber area and fiber spacing are determined in the longitudinal direction (perpendicular to the ridges) from the simplified rigidity expressions

$$K_\ell = E_m h + A_f(E_f - E_m)/S_\ell \tag{B.2-1}$$

and

$$12D_\ell = E_m h^3 + A_f^2(E_f - E_m)/S_\ell. \tag{B.2-2}$$

For assumed square fibers, the fiber width is $d = A_f^{1/2}$ and, if the fiber spacing is specified as $S_\ell = nd$, Equations B.2-1 and B.2-2 become

$$K_\ell = E_m h + d(E_f - E_m)/n \tag{B.2-3}$$

and

$$12D_\ell = E_m h^3 + d^3(E_f - E_m)/n. \tag{B.2-4}$$

Similarly, the matrix thickness may be expressed as $h=kd$ and it is seen that the constants n and k are restricted to $N \geq 1$ and $k \geq 1$; the minimum values (n=1, k=1) specify a solid sheet of the fiber material.

Rewriting Equations B.2-3 and B.2-4 in terms of d, k and n yields

$$K = d(kE_m + (E_f - E_m)/n) \tag{B.2-5}$$

and

$$12D_\ell = d^3(k^3E_m + (E_f - E_m)/n). \tag{B.2-6}$$

Figure B-1 shows the physical limitations on d as a function h. Parametric lines of k=const and N=const for given values of K_ℓ and D_ℓ are indicated.

If k is set at a constant value and d is eliminated from Equations B.2-5 and B.2-6, a cubic equation in n can be obtained. This equation is

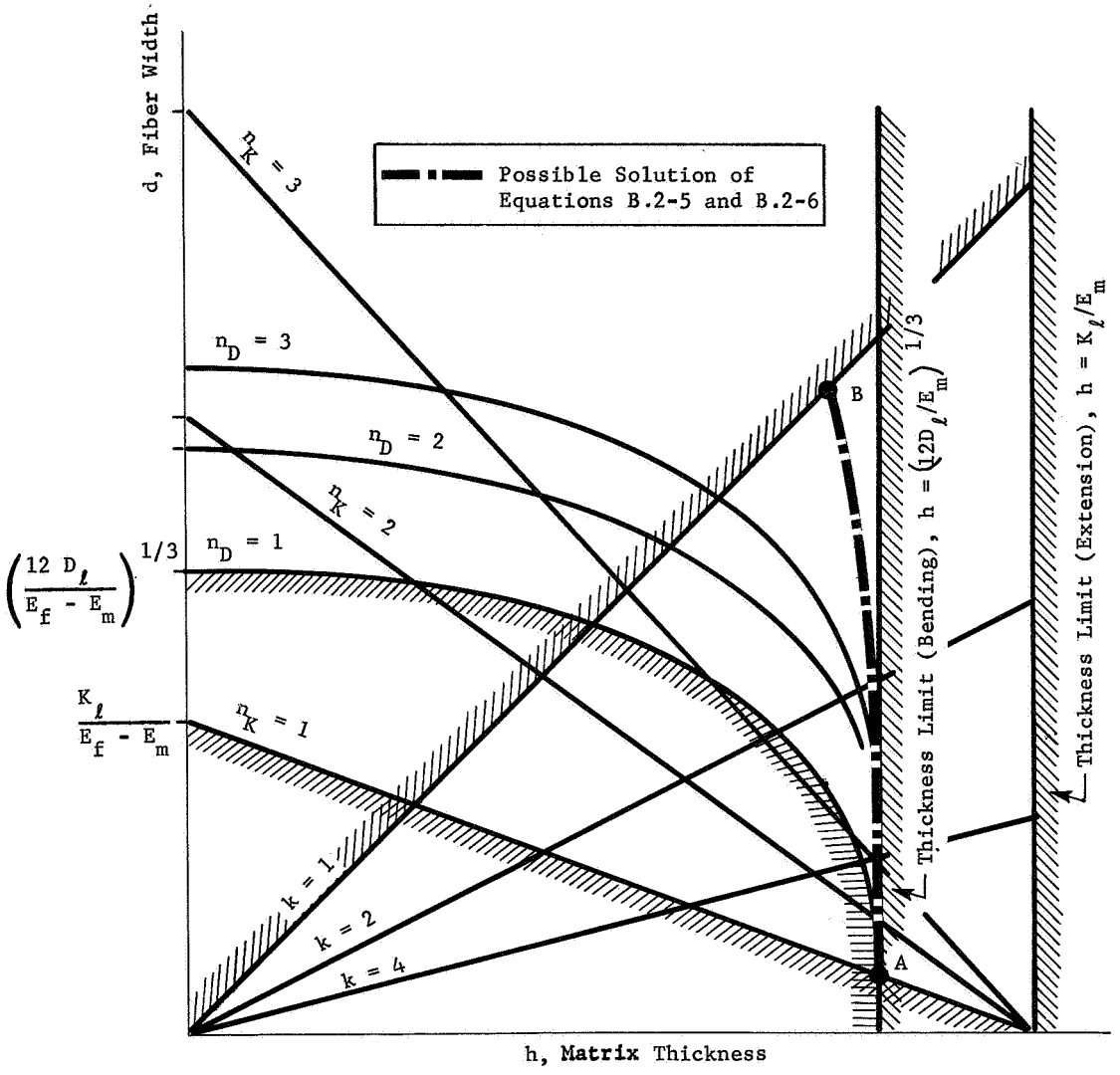

Figure B-1. Fiber Width versus Matrix Thickness

$$A_3 n^3 + A_2 n^2 + A_1 n + A_o = 0 \qquad \text{(B.2-7)}$$

where

$$\begin{aligned} A_3 &= k^3 E_m (12 D_\ell E_m^2 - K_\ell^3) \\ A_2 &= (E_f - E_m)(36 D_\ell k^2 E_m^2 - K_\ell^3) \\ A_1 &= 36 D_\ell k E_m (E_f - E_m)^2 \\ A_0 &= 12 D_\ell (E_f - E_m)^3 . \end{aligned} \qquad \text{(B.2-8)}$$

Physically realistic solutions are limited to $k \geq 1$. If the value of n obtained for k=1 is less than unity, there exists no physical solution for the given values of E_m and E_f and the specified values of K_ℓ and D_ℓ. Realistic values of n and k may be obtained by increasing E_f. A value of $n \geq 1$ obtained for $k \geq 1$ represents a physically possible reinforced shell model. Further increasing the value of k will result in a decrease in the value of n. The algorithm for the optimization of n and k in the initial parameter selection maximizes the product (n-1)(k-1).

When n and k have been established, Equation B.2-5 can be used to compute the fiber width. This parameter is

$$d = nK_\ell / [(nk-1)E_m + E_f] \qquad \text{(B.2-9)}$$

and it follows that the matrix thickness and longitudinal fiber spacing are h = kd and S_ℓ = nd. Note that Equation B.2-9 will yield only an approximate value for d as Equations B.2-1 and B.2-2 are themselves only approximations. After the approximate parameters are determined for the transverse direction, these longitudinal parameters can be modified by an iteration process.

The approximate matrix parameters in the transverse direction (direction of the ridges) from the simplified rigidity expressions

$$K_t = E_m h + 2E_m Q t + A_f (E_f - E_m)/S_t \qquad \text{(B.2-10)}$$

and

$$12 D_t = (1 - Q) E_m h^3 + Q(h + 2t)^3 E_m + A_f^2 (E_f - E_m)/S_t \qquad \text{(B.2-11)}$$

where

S_t = width of "ridges" used for bending reinforcement (Fig. 7.7),
T = width of "valleys" and Q = S/(S+T).

The ridge height is t. If it is assumed that A_f is the same in both the longitudinal and the transverse directions and if the transverse fiber sapcing is written as a multiple of the longitudinal fiber spacing, Equations B.2-10 and B.2-11 can be rewritten as

$$K_t = E_m h + 2E_m Qt + d(E_f - E_m)/(nj) \qquad (B.2\text{-}12)$$

and

$$12D_t = (1-Q)E_m h^3 + Q(h+2t)^3 E_m + d^3(E_f - E_m)/(nj) \qquad (B.2\text{-}13)$$

with the restrictions that

$$nj \geqslant 1, \qquad 0 \leqslant Q \leqslant 1 \qquad \text{and} \qquad t \geqslant 0. \qquad (B.2\text{-}14)$$

The initial data computation algorithm proceeds by arbitrarily setting Q = 0.4. Elimination of the product nj from Equations B.2-12 and B.2-13 yields a cubic equation for t

$$B_3 t^3 + B_2 t^2 + B_1 t + B_0 = 0 \qquad (B.2\text{-}15)$$

where

$$B_3 = 8QE_m$$

$$B_2 = 12QE_m h$$

$$B_1 = 2QE_m(3h^2 - d^2)$$

$$B_0 = d^2(K_t - E_m h) - 12D_t + E_m h^3.$$

If no positive real root exists, the longitudinal and transverse directions should be interchanged. If one positive real root exists,

$$j = d(E_f - E_m)/(nK_t - nE_m h - 2nE_m Qt) \qquad (B.2\text{-}17)$$

If more than one positive real root exists, the resulting values of j can be computed from Equation B.2-17. No physical solution exists for $jn \leqslant 1$.

At this point the computer program presents a choice to the operator. The current values of j, jn, t, t/h and Q are printed. If more than one set of these variables is available the operator may select the most desirable solution or he may elect to change the value of Q. If this is done, Equation B.2-15 is recycled and new solutions are formulated. Once a "desirable" value of j is attained, the transverse fiber spacing ($S_t = jS_\ell$) is computed and the preliminary computation of the shell model parameters is complete.

The equations of Section 7.2 are then used to compute the actual values of D , K , D_t and K_t and the equivalent shear modulus, G. The ratios of desired to actual shell rigidities are determined for the four controlling rigidities and if these ratios are satisfactory, the program is terminated. If the ratios are not satisfactory, a operator-controlled iteration process is initiated and used until the ratios of desired rigidities to actual rigidities are computed to within an allowable unit.

```
*IOCS(CARD,TYPEWRITER,KEYBOARD,1132 PRINTER,DISK)
C  1130 PROGRAM TO COMPUTE REINFORCED SHELL PROPERTIES
      DIMENSION XCOF(4),COF(4),ROOTR(3),ROOTI(3)
    1 CONTINUE
C READ DATA
      READ(2,999) EM, EF, XMU, GM, GF
      READ(2,999) SXX, SYY, DXX, DYY
  999 FORMAT(8F10.0)
      WRITE(1,998) EM, EF, XMU, GM, GF
      WRITE(1,998) SXX, SYY, DXX, DYY
  998 FORMAT(/,10X, 5E15.3)
    8 WRITE(1,99)
   99 FORMAT(' DETERMINE H,D, AND SL')
C ASSIGN SUBSCRIPT T TO LARGER ONE OF BENDING RIGIDITIES AND THE
C EXTENSIONAL RIGIDITY ASSOCIATED WITH IT
      IF(DXX-DYY)10,10,12
   10 DL=DXX
      SL=SXX
      DT=DYY
      ST=SYY
       GO TO 14
   12 DL=DYY
      DT=DXX
      SL=SYY
      ST=SXX
C START COMPUTATION LOOP ON INDEX L
C FIRST MMC(=MAN-MACHINE COMMUNICATION EXCHANGE)
C MMC = WHAT K DESIRED
   14 WRITE(1,100)
  100 FORMAT(' TYPE VALUE OF K DESIRED IN FORMAT F10.0')
      READ(6,101)XK
  101 FORMAT(F10.0)
C COMPUTE POLYNOMIAL COEFFICIENTS TO GET N
      XCOF(4)=XK**3*EM*(12.*DL*EM**2-SL**3)
      XCOF(3)=(EF-EM)*(36.*DL*XK**2*EM**2-SL**3)
      XCOF(2)=(EF-EM)**2*36.*DL*XK*EM
      XCOF(1)=12.*DL*(EF-EM)**3
      XCOF(3)=XCOF(3)/XCOF(4)
      XCOF(2)=XCOF(2)/XCOF(4)
      XCOF(1)=XCOF(1)/XCOF(4)
      XCOF(4)=1.
C POLYNOMIAL ROOTS
      CALL POLRT(XCOF,COF,3,ROOTR,ROOTI,IER)
      IF(IER)16,18,16
C MMC = ERROR PROCEDURE (IF ANY, MAY QUIT, OR START WITH NEW K)
   16 WRITE(1,102)IER
  102 FORMAT(' IER=',I3,' TYPE 1.0 FOR NEW K,2.0 FOR STOP')
      READ(6,101)CHECK
      IF(CHECK-1.0)17,14,17
   17 STOP
C ROOTS OF THE POLYNOMIAL
C THESE ARE POSSIBLE VALUES OF N
   18 WRITE(1,103)
  103 FORMAT(' ROOTS OF THE POLYNOMIAL( N ) ARE')
      DO 20 I=1,3
   20 WRITE(1,104)ROOTR(I),ROOTI(I)
  104 FORMAT(/2X,E15.7,' + ',E15.7,' I')
C OPTION TO TRY NEW K, OR PROCEED
      WRITE(1,105)
  105 FORMAT(' IF THIS IS NOT SATISFACTORY TYPE 2., IF YES, 1.')
```

```
      READ(6,101)CHECK
      IF(CHECK-1.)14,22,14
C MMC = VALUE OF K PREFERRED, VALUE OF COMPATIBLE REAL N
   22 WRITE(1,106)
  106 FORMAT(' TYPE IN DESIRED K IN F10.0')
      READ(6,101)XK
      WRITE(1,108)
  108 FORMAT(' TYPE IN DESIRED VALUE OF N IN F 10.0')
      READ(6,101)XN
C COMPUTE AND DISPLAY D,H,S1
      D=(XN*SL)/((XN*XK-1.)*EM+EF)
      H=XK*D
      S1=XN*D
      WRITE(1,110)D,H,S1
  110 FORMAT(' D = ',E15.7,' H = ',E15.7,' S1 = ',E15.7)
      WRITE(1,111)
  111 FORMAT(' THESE ARE THE INITIAL VALUES ')
C END LOOP ON INDEX L
C START INDEX T COMPUTATION LOOP
   25 WRITE(1,112)
  112 FORMAT(' COMPUTE T, S2, AND Q')
C  MMC = WHAT IS DESIRED Q
      WRITE(1,113)
  113 FORMAT(' SPECIFY INITIAL VALUE OF Q BETWEEN 0 AND 1.')
      READ(6,101)Q
C COMPUTE POLYNOMIAL COEFFICIENTS
      XCOF(4)=8.*Q*EM
      XCOF(3) = 12.*Q*EM*H
      XCOF(2)=6*Q*EM*H**2-2.*D**2*Q*EM
      XCOF(1)=D**2*(ST-EM*H)-12.*DT*  EM*H**3
      XCOF(1)=XCOF(1)/XCOF(4)
      XCOF(2)=XCOF(2)/XCOF(4)
      XCOF(3)=XCOF(3)/XCOF(4)
      XCOF(4)=1.
C ERROR PROCEDURE
      CALL POLRT(XCOF,COF,3,ROOTR,ROOTI,IER)
C IF IER N.E. 0, TRY NEW Q
C  MMC= MAY QUIT ON ERROR, OR TRY NEW Q
      IF(IER)28,30,28
   28 WRITE(1,115)IER
  115 FORMAT(' IER=',I3,' TYPE 1. FOR NEW Q, 2. FOR STOP')
      READ(6,101)CHECK
      IF(CHECK-1.)29,25,29
   29 STOP
   30 CONTINUE
C POLYNOMIAL ROOTS
C POSSIBLE VALUES OF T
      WRITE(1,203)
  203 FORMAT(' ROOTS OF THE POLYNOMIAL (T) ARE')
      DO 31 I=1,3
   31 WRITE(1,104)ROOTR(I),ROOTI(I)
C MMC = OPTION TO TRY NEW Q, OR PROCEED
      WRITE(1,105)
      READ(6,101)CHECK
      IF(CHECK-1.)25,32,25
C    MMC = ENTER COMPATIBLE PAIR OF T AND Q
   32 WRITE(1,117)
  117 FORMAT(' TYPE IN VALUE OF Q ')
      READ(6,101)Q
      WRITE(1,118)
  118 FORMAT(' TYPE IN VALUE OF T')
```

```
      READ(6,101)T
      XJ=D*(EF-EM)/(XN*ST-XN*EM*H-2.*XN*Q*EM*T)
C  DISPLAY VALUE OF J AND NJ
      WRITE(1,119)XJ
  119 FORMAT(' THE VALUE OF J IS',E14.7)
      SAM=XJ*XN
      WRITE(1,120)SAM
  120 FORMAT(' THE PRODUCT J*N IS ',F10.4)
      S2=S1*XJ
C  MC CHOICE TO START T LOOP AGAIN, OR PROCEED
      WRITE(1,121)
  121 FORMAT(' IF THIS IS OK, TYPE 1., IF NOT 2.')
      READ(6,101)CHECK
      IF(CHECK-1.)25,35,25
C DISPLAY SUMMARY OF DATA OBTAINED THUS FAR
  700 WRITE(1,150)
  150 FORMAT(' FOR RERUN SPECIFY DESIRED H,D,S1,S2,Q,T IN F10.0')
      READ(6,101)H
      READ(6,101)D
      READ(6,101)S1
      READ(6,101)S2
      READ(6,101)Q
      READ(6,101)T
   35 WRITE(1,124)H,D,S1,S2,Q,T
  124 FORMAT(' SUMMARY OF MATRIX DATA'/' H=',E14.7/' D =',E14.7/' S1=',E
     114.7,' S2=',E14.7/' Q =',E14.7,' T =',E14.7)
C SHOW RATIOS OF DESIRED AND ACTUAL RIGIDITIES
      WRITE(1,125)
  125 FORMAT(' SUMMARY OF BASIC RIGIDITY PARAMETERS AND RATIOS TO DESIRE
     1D VALUES'/)
      HBAR=1./(H+2.*T)+2.*T*(1.-Q)/(H*(H+2.*T))
      XLAM=D*HBAR
      ELB=(S2*EM*(XLAM*EF+(1.-XLAM)*EM))/(D*EM+(S2-D)*(XLAM*EF+(1.-XLAM)
     1*EM))
      ALF=D**2*HBAR/S1
      EL=EF*ALF+ELB*(1.-ALF)
      HPR=1./(H+2.*T*Q)
      XLP=D*HPR
       ETB=S1*EM*(XLP*EF+(1.-XLP)*EM)/(D*EM+(S1-D)*(XLP*EF+(1.-XLP)*EM))
      BET=D**2*HPR/S2
      ET=EF*BET+ETB*(1.-BET)
      XMULT=(XMU/S1)*(S1-D)+D*(EM*(S2/HPR-D**2)+EF*D**2)/(EM*((1./HPR-D)
     1*S2-D**2)+EF*(D*(S2+D)))
      CSL=EL**2*H/(EL-ET*XMULT**2)
      CSL=CSL/(H*HBAR)
      CST=EL*ET*H/(EL-ET*XMULT**2)
      CST=CST/(H*HPR)
      GAML=3.*D**4*HBAR**3/(S1*3.1416)
      GAMT=3.*D**4*HPR**3/(S2*3.1416)
      EBL=EF*GAML+EM*(1.-GAML)
      EBT=EF*GAMT+EM*(1.-GAMT)
      CDL=EBL**2*H**3/(12.*(EBL-EBT*XMULT**2))
      CDL=CDL/(H**3*HBAR**3)
      CDT=EBL*EBT*H**3/(12.*(EBL-EBT*XMULT**2))
      CDT=CDT/(H**3*HPR**3)
      AF=D**2
C  TEMPORARY CHECK SECTION
      CALL DATSW(3,JJ)
      IF(JJ-2)670,667,670
  667 WRITE(1,175)
  175 FORMAT(' SIMPLIFIED PROPERTY CALCULATION')
```

```
      CSL=AF*(EF-EM)/S1+H*(H+2.*T)*EM/((H+2.*T)*(1.-Q)+H*Q)
      CST=AF*(EF-EM)/S2+(H+2*Q*T)*EM
      C
     1DL=D**4*(EF-EM)/(12.*S1)+H**3*(H+2.*T)**3*EM/(12.*Q*H**3+12.*(1.-Q
     1)*(H+2.*T)**3)
      CDT=D**4*(EF-EM)/(12*S2)+Q*EM*(H+2*T)**3/12+(1-Q)*H**3*EM/12
  670 CONTINUE
C   TEMPORARY CHECK SECTION          ENDS HERE
      XSL=CSL/SL
      XST=CST/ST
      XDL=CDL/DL
      XDT=CDT/DT
      WRITE(1,126)CSL,SL,XSL
      WRITE(1,127)CST,ST,XST
      WRITE(1,128)CDL,DL,XDL
      WRITE(1,129)CDT,DT,XDT
  126 FORMAT(' CSL =',E14.7,' SL =',E14.7,' RATIO =',F10.4)
  127 FORMAT(' CST =',E14.7,' ST =',E14.7,' RATIO =',F10.4)
  128 FORMAT(' CDL =',E14.7,' DL =',E14.7,' RATIO =',F10.4)
  129 FORMAT(' CDT =',E14.7,' DT =',E14.7,' RATIO =',F10.4)
C MMC = MAY PROCEED, OR RETURN TO T LOOP, OR RETURN TO START
      WRITE(1,130)
  130 FORMAT(' IF OK, TYPE 0., IF RESTART, TYPE 1., IF RESTART 0, 2.')
      READ(6,101)CHECK
      IF(CHECK-1.)50,8,25
C COMPUTE SHEAR RIGIDITY
   50 G=2.*(GF*D**2+GM*(S1/HPR-D**2))
      G=G*(GF*D**2+GM*(S2/HPR-D**2))
      G=G/(S1/HPR*(GF*D**2+GM*(S2/HPR-D**2))+S2/HPR*(GF*D**2+GM*(S1/HPR-
     1D**2)))
      CSS=G/HPR
      CSLT=CST*XMULT
      CSTL=CSLT*HPR/HBAR
      CDTL=CDT*XMULT
      CDLT=CDTL*(HPR/HBAR)**3
      WRITE(1,131)
      WRITE(1,132)
      WRITE(1,133)CSS,CSLT,CSTL,CDTL,CDLT
  131 FORMAT(' SUMMARY OF THE OTHER RIGIDITIES')
  132 FORMAT('      CSS            CSLT           CSTL           CDTL
     1   CDLT'/)
  133 FORMAT(5E17.8)
      WRITE(1,130)
      READ(6,101)CHECK
      IF(CHECK-1.)500,8,25
  500 CONTINUE
      WRITE(1,301)
  301 FORMAT(' TYPE 0 FOR ARBITRARY INPUT,1. FOR RESTART,2 TO STOP')
      READ(6,101)CHECK
      IF(CHECK-1.)700,1,501
  501 STOP



      SUBROUTINE POLRT(XCOF,COF,M,ROOTR,ROOTI,IER)
      DIMENSION XCOF(1),COF(1),ROOTR(1),ROOTI(1)
      IFIT=0
      N=M
      IER=0
      IF(XCOF(N+1)) 10,25,10
   10 IF(N) 15,15,32
```

```
C        SET ERROR CODE TO 1
   15 IER=1
   20 RETURN
C        SET ERROR CODE TO 4
   25 IER=4
      GO TO 20
C        SET ERROR CODE TO 2
   30 IER=2
      GO TO 20
   32 IF(N-36) 35,35,30
   35 NX=N
      NXX=N+1
      N2=1
      KJ1 = N+1
      DO 40 L=1,KJ1
      MT=KJ1-L+1
   40 COF(MT)=XCOF(L)
C        SET INITIAL VALUES
   45 XO=.00500101
      YO=0.01000101
C        ZERO INITIAL VALUE COUNTER
      IN=0
   50 X=XO
C        INCREMENT INITIAL VALUES AND COUNTER
      XO=-10.0*YO
      YO=-10.0*X
C        SET X AND Y TO CURRENT VALUE
      X=XO
      Y=YO
      IN=IN+1
      GO TO 59
   55 IFIT=1
      XPR=X
      YPR=Y
C        EVALUATE POLYNOMIAL AND DERIVATIVES
   59 ICT=0
   60 UX=0.0
      UY=0.0
      V =0.0
      YT=0.0
      XT=1.0
      U=COF(N+1)
      IF(U) 65,130,65
   65 DO 70 I=1,N
      L =N-I+1
      XT2=X*XT-Y*YT
      YT2=X*YT+Y*XT
      U=U+COF(L )*XT2
      V=V+COF(L )*YT2
      FI=I
      UX=UX+FI*XT*COF(L )
      UY=UY-FI*YT*COF(L )
      XT=XT2
   70 YT=YT2
      SUMSQ=UX*UX+UY*UY
      IF(SUMSQ) 75,110,75
   75 DX=(V*UY-U*UX)/SUMSQ
      X=X+DX
      DY=-(U*UY+V*UX)/SUMSQ
      Y=Y+DY
   78 IF( ABS(DY)+ ABS(DX)-1.0E-05) 100,80,80
```

```
C         STEP ITERATION COUNTER
   80 ICT=ICT+1
      IF(ICT-500) 60,85,85
   85 IF(IFIT) 100,90,100
   90 IF(IN-5) 50,95,95
C         SET ERROR CODE TO 3
   95 IER=3
      GO TO 20
  100 DO 105 L=1,NXX
      MT=KJ1-L+1
      TEMP=XCOF(MT)
      XCOF(MT)=COF(L)
  105 COF(L)=TEMP
      ITEMP=N
      N=NX
      NX=ITEMP
      IF(IFIT) 120,55,120
  110 IF(IFIT) 115,50,115
  115 X=XPR
      Y=YPR
  120 IFIT=0
  122 IF( ABS(Y/X)-1.0E-04) 135,125,125
  125 ALPHA=X+X
      SUMSQ=X*X+Y*Y
      N=N-2
      GO TO 140
  130 X=0.0
      NX=NX-1
      NXX=NXX-1
  135 Y=0.0
      SUMSQ=0.0
      ALPHA=X
      N=N-1
  140 COF(2)=COF(2)+ALPHA*COF(1)
  145 DO 150 L=2,N
  150 COF(L+1)=COF(L+1)+ALPHA*COF(L)-SUMSQ*COF(L-1)
  155 ROOTI(N2)=Y
      ROOTR(N2)=X
      N2=N2+1
      IF(SUMSQ) 160,165,160
  160 Y=-Y
      SUMSQ=0.0
      GO TO 155
  165 IF(N) 20,20,45
      END
```

APPENDIX C

Table C-1 Properties of Maraging Steel

FORM	SIZES (INCHES)	FABRICABILITY
Castings	Not Available	
Sheet	Thickness from 0.050 to 0.249, width to 48.0, length to 144; larger sizes on special order.	Machinability of all grades equivalent to 4340 at same hardness. Heat treatable, high efficiency welds. Good formability in annealed condition.
Plate	Thickness from 0.250 to 1.50, width to 120, length to 240. Larger sizes on special order.	Same as sheet.
Forgings	Have been made in limited sizes. Limitations not established.	Same as sheet. Remove surface scale after forging.
Wire	Diameter from 0.020 to 0.625.	Same as sheet.
Tubing	Seamless on special order.	Same as sheet.
Bar	Round, hexagon, square and flat from 0.25 to 2.5.	Same as sheet.
Note: 18% Ni (200, 250, and 300 grades).		

C-2

Table C-2 Properties of Aluminum

ALLOY	F_{tu}, KSI
1100, 3003	15-20
2014, 2024	67
5456	50
6061	45
7075, 7178	75

FABRICABILITY			
WELDABILITY		HEAT TREATABILITY	
1100, 3003, 5456, 6061	Good	1100, 3003, 5456	Not Hardenable
2014	Fair	2014, 2024, 6061	Hardenable
2024	Poor	7075, 7178	
7075, 7178	No		

FORM	SIZE, INCHES UNLESS SPECIFIED			
FORGINGS		MINIMUM		MAXIMUM
	THICKNESS	0.100		12.0
	WIDTH			12.0 +0.063, -0.125
	LENGTH	As specified ±0.125		50.0 ±1.0
ROLLED, DRAWN BAR		ROD		BAR
		MIN	MAX	MIN	MAX
	THICKNESS	0.375 ± 0.0015	8.0 ± 0.031	0.375 ± 0.002	4.0 ± 0.020
	WIDTH			0.375 ± 0.002	10.0 ± 0.062
	LENGTH	12.0 ± 0.125	50.0 ± 1.0	12.0 ± 0.125	50.0 ± 1.0
SHEET, PLATE		SHEET		PLATE	
		MIN	MAX	MIN	MAX
	THICKNESS	0.006 ± 0.0015	0.249 ± 0.011	0.250 ± 0.0025	6.0 ± 0.180
	WIDTH	12.0 ± 0.062	168.0 ± 0.25	12.0 ± 0.375	168.0 ± 0.75
	LENGTH		600.0 ± 1.0		600 ± 1.0
WIRE		MIN		MAX	
	THICKNESS	0.010 ± 0.0005		0.375 ± 0.0015	
	LENGTH	As Specified ± 0.125		5000 ft ± 1.0	
EXTRUSIONS(1)		MIN		MAX	
	THICKNESS	0.050 ± 0.006		7.0 ± 0.081	
	RADII	0.125			
	AREA	0.250		60.0	
	WIDTH			30.0 ± 0.081	
	LENGTH			500 ft ± 100 ft	
TUBING, PIPE		MIN		MAX	
	THICKNESS (WALL)	0.010 ± 0.002		0.500 ± 0.020	
	DIAMETER (O.D.)	0.125 ± 0.003		12.0 ± 0.025	
	LENGTH			500.0 ± 100.0	

(1) Must be grain size controlled for better weldability.

Table C-3 Properties of Titanium

FORM	ALLOYS	SIZES, INCHES UNLESS SPECIFIED	FABRICABILITY
FORGINGS	COMM. PURE Ti-6Aℓ-4V Ti-5Aℓ-2.5Sn OTHERS	CONVENTIONAL FORGING LARGE: THICKNESS TOL. +0.25 -0.03; LENGTH TOL. ±0.03; MIN. FILLET RADIUS 1.0; MIN. WEB THICK 0.62 SMALL: +0.09 -0.03; ±0.03; 0.75; 0.25	MACHINABLE(2) REQUIRES SCALE REMOVAL WELDABLE FORMABLE CHEM. MILLABLE HEAT TREATABLE
ROLLED OR DRAWN BAR	ALL(1)	MIN / MAX THICKNESS (ROUNDS) 0.3125 ± 0.005 THICKNESS (SQUARE, HEX) 0.3125 – 4.50 THICKNESS (RECT) 0.200 – 10.0 LENGTH – 50 ft	MACHINABLE(2) WELDABLE FORMABLE HEAT TREATABLE CHEM. MILLABLE
SHEET	ALL(1)	MIN / MAX THICKNESS 0.008 ± 0.002 / 0.1875 ± 0.014 WIDTH 24.0 ± 0.062 / 100.0 ± 0.125 LENGTH – / 600.0 ± 0.50	SAME AS ROLLED OR DRAWN BAR
PLATE	ALL(1)	MIN / MAX THICKNESS 0.1875 ± 0.046 / 3.0 ± 0.10 WIDTH 10.0 ± 0.125 / 150.0 ± 0.25 – / 600.0 ± 0.25	SAME AS ROLLED OR DRAWN BAR
WIRE	ALL(1)	THICKNESS 0.009 (MIN. DIAMETER) LENGTH 500 ft	SAME AS ROLLED OR DRAWN BAR
EXTRUSIONS	COMM. PURE Ti-6Aℓ-4V Ti-6Aℓ-6V-2Sn Ti-5Aℓ-2.5Sn Ti-8Aℓ-1Mo-1V Ti-13V-11Cr-3Aℓ	MIN / MAX THICKNESS 0.125 / 1.25 FINISH MACHINED 0.060 ± 0.005 LENGTH – / 40 ft FILLET RADII 0.062 LENGTH/THICKNESS – / 14	SAME AS ROLLED OR DRAWN BAR, BUT MUST BE DESCALED
TUBING, PIPE	COMM. PURE Ti-6Aℓ-4V Ti-5Aℓ-2.5Sn Ti-13V-11Cr-3Aℓ Ti-8Aℓ-1Mo-1V Ti-5Aℓ-5Sn-5Zr	MIN / MAX WALL THICKNESS 0.004 ± 0.004 / 0.250 ± 0.0250 DIAMETER(O.D.) 0.250 +0.015 -0.030 / 12.0 +0.090 -0.030	SAME AS ROLLED OR DRAWN BAR

(1) Unalloyed (Comm. Pure): Ti-0.2Pd, Ti-5Aℓ-2.5Sn, Ti-7Aℓ-2Cb-1Ta, Ti-8Aℓ-1Mo-1V, Ti-6Aℓ-4V, and Ti-6Aℓ-6V-2Sn.

(2) Approximately 20 (AISI B1112 Steel = 100).

C-4

Table C-4 Properties of Nickel

FORM	ALLOYS	SIZES, INCHES UNLESS SPECIFIED		
FORGINGS	INCONEL 600, 700, 718 x 750, 901; UDIMET 500, 700; OTHERS		MIN	MAX
		THICKNESS	0.125 ± 0.005	4.00
		DRAFT ANGLE	2.0 deg	3.0 deg
ROLLED, OR DRAWN BAR	INCONEL 600-702, 718 x 750, 901; HASTELLOY C, R-235; OTHERS		MIN	MAX
		THICKNESS (ROUNDS)	0.312 - 0.002	3.00 - 0.005
		THICKNESS (HEX, SQUARE, OCT.)	0.312 - 0.002	3.00 - 0.007
		LENGTH	As Specified ±0.125	Spec. ±0.025
SHEET	ALL ABOVE PLUS WASPALLOY, RENE 41 NEMONIC 80A, 90; OTHERS		MIN	MAX
		THICKNESS	0.008 ± 0.002	0.1875 ± 0.014
		WIDTH	24.0 ± 0.062	100.0 ± 0.25
		LENGTH		600.0 ± 0.50
PLATE	ALL ABOVE PLUS WASPALLOY, RENE 41 NEMONIC 80A, 90; OTHERS		MIN	MAX
		THICKNESS	0.1875 ± 0.046	3.0 ± 0.1
		WIDTH	10.0 ± 0.25	150.0 ± 0.25
		LENGTH		600.0 ± 0.25
WIRE	ALL ABOVE		MIN	MAX
		DIAMETER	0.062 ± 0.0007	0.500 ± 0.0015
		LENGTH	As Specified	As Specified
EXTRUSIONS	ALL ABOVE		MIN	MAX
		CIRCUMSCRIBED CIRCLE		4.50
		LENGTH		60 ft
		CROSS SECTION	0.50 $in.^2$	
		THICKNESS	0.156	
		RADII, CORNER	0.062	
		RADII, FILLET	0.250 ± 0.062	
TUBING, PIPE	ALL ABOVE		MIN	MAX
		WALL THICKNESS	0.0015 ± 0.00015	0.625 ± 0.0625
		DIAMETER (O.D.)	0.012 ± 0.002	6.00 ± 0.005
		LENGTH	As Specified	100 ft ± 0.25